Wissenschaftszentrum Weihenstephan für Ernährung, Landnutzung und Umwelt

Lehrstuhl für Ökophysiologie der Pflanzen

Hydraulics of European beech and Norway spruce under experimental drought

Martina Tomasella

Vollständiger Abdruck der von der Fakultät Wissenschaftszentrum Weihenstephan für Ernährung, Landnutzung und Umwelt der Technischen Universität München zur Erlangung des akademischen Grades eines

Doktors der Naturwissenschaften (Dr. rer. nat.)

genehmigten Dissertation.

Vorsitzender: Prof. Dr. Johannes Kollmann

Prüfer der Dissertation:
1. apl. Prof. Dr. Thorsten Grams
2. Prof. Dr. Stefan Mayr
3. Prof. Dr. Urs Schmidhalter

Die Dissertation wurde am 09.11.2017 bei der Technischen Universität München eingereicht und durch die Fakultät Wissenschaftszentrum Weihenstephan für Ernährung, Landnutzung und Umwelt am 24.01.2018 angenommen.

Table of contents

List of Figures

List of Tables

List of Publications

Parts of this thesis (Part I and Part IIA) have been published in peer re-reviewed international journals:

- Tomasella M., Beikircher B., Häberle K.-H., Hesse B., Kallenbach C., Matyssek R., Mayr S. (2017a) Acclimation of branch and leaf hydraulics in adult *Fagus sylvatica* and *Picea abies* in a forest through-fall exclusion experiment. Tree Physiology, DOI: 10.1093/treephys/tpx140.
- Tomasella M., Häberle K.-H., Nardini A., Hesse B., Machlet A., Matyssek R. (2017b) Post-drought hydraulic recovery is accompanied by non-structural carbohydrate depletion in the stem wood of Norway spruce saplings. Scientific reports 7, 14308; DOI: 10.1038/s41598-017-14645-w.

Other publications with doctoral candidate's co-authorship published during the doctoral period:

- Hafner B.D., Tomasella M., Häberle K.-H., Goebel M., Matyssek R., Grams T.E.E. (2017) Hydraulic redistribution under moderate drought among English oak, European beech and Norway spruce determined by deuterium isotope labeling in a split-root experiment. Tree Physiology 37, 950-960.
- Casolo V., Tomasella M., De Col V., Braidot E., Savi T., Nardini A. (2015) Water relations of an invasive halophyte (*Spartina patens*): osmoregulation and ionic effects on xylem hydraulics. Functional Plant Biology 42, 264-273.

Summary

Two central prerequisites for survival of trees are the maintenance of sufficient water transport from roots to leaves and the availability of carbon for respiration, growth, defence and repair mechanisms. Drought constrains both aspects because high xylem tensions can induce xylem embolism resulting in partial or substantial loss of xylem hydraulic conductivity (hydraulic failure). Moreover, carbohydrates may be depleted to critical levels (carbon starvation) or be not available/transportable to the sinks (phloem transport failure).

Considering the current climate change scenarios, drought responses, hydraulic acclimation and embolism repair potential of European beech (*Fagus sylvatica* L.) and Norway spruce (*Picea abies* (L.) Karst) were investigated. These tree species, currently dominating Central European forests and representing a relevant ecological and silvicultural resource, are currently threatened by drought.

The first question addressed in part I of this study is whether and to which extent beech and spruce are able to hydraulically acclimate to long-lasting, i.e. chronic, droughts, as acclimation of hydraulic traits would reduce the risks of hydraulic dysfunction. This aspect was studied in a mixed forest stand of European beech and Norway spruce at the "Kranzberger Forst" near Freising after two years of experimental drought, which was applied taking advantage of a through-fall exclusion system ("Kranzberg Roof Experiment", acronym KROOF). In drought-stressed trees under through-fall exclusion (TE) and control (CO) trees, hydraulic vulnerability was studied in branches as well as in leaves sampled at the same height from sun-exposed tree crowns. In parallel, relevant xylem anatomical traits such as mean arithmetic and hydraulic diameter of conduits, conduit wall reinforcement and conduit density, and leaf pressure-volume relations were analyzed.

Through-fall exclusion resulted in prolonged drought with TE trees reaching pre-dawn water potentials down to -1.6 MPa. In both species, water potentials at 50% loss of xylem hydraulic conductivity were about 0.4 MPa more negative in TE than in CO branches. Likewise, foliage hydraulic vulnerability (expressed as water potential at 50% loss of leaf hydraulic conductance) and water potential at turgor loss point were 0.4 and 0.5 MPa

lower in TE compared to CO trees, respectively. Only minor differences were observed in xylem anatomical traits.

The second part of the study aimed at clarifying, in both European beech and Norway spruce, possible long term carry-over effects of a previous drought episode, and how dehydration-rehydration is affecting the relations between xylem embolism and stem non-structural carbohydrates (NSC). In particular, the capability of hydraulic recovery in the stem xylem upon re-irrigation and the relationship between hydraulic recovery and NSC dynamics were investigated. The experiment was conducted in potted saplings growing in a greenhouse at the Gewächshauslaborzentrum Dürnast (WZW, Technische Universität München). For both species, trees underwent two drought-re-irrigation cycles performed in two consecutive summers. After the first drought cycle, plants were kept well-irrigated over winter until the following summer. The target peak of drought was adjusted somewhat below the theoretical lethal thresholds of xylem embolism in conifers and angiosperms (50% and 88% percent loss of xylem hydraulic conductivity, PLC, respectively), i.e. in the range of 10-40% in Norway spruce and approximately 80% in European beech. Therefore target minimum leaf water potentials at re-irrigation were set to -3.0 to -3.5 MPa in spruce and -3.8 to -4.2 MPa in beech. In the second drought cycle, water potentials, PLC and NSC content (detected separately in stem wood and bark) were assessed three times, i.e. before and at the end of the drought period, as well as one week after re-irrigation.

In Norway spruce (part II A), PLC and NSC content measured in well-watered plants before the beginning of the second drought cycle showed no carry-over effects from the previous drought, indicating complete long-term recovery. The second drought treatment induced moderate PLC (about 20%) and did not affect total NSCs content, while starch was converted to soluble sugars in the bark. After one week of re-irrigation, PLC fully recovered with NSCs being depleted, only in the wood, by about 30%.

European beech (part II B) trees stressed in the first drought cycle had lower minimum water potentials and stem specific hydraulic conductivity than control trees, in the following growing season under well-watered conditions. Aboveground biomass and total leaf area decreased too, resulting in lower tree water consumption. PLC, instead, was similar to control trees, probably due to hydraulic recovery occurred in spring through the differentiation of new functional xylem conduits. In beech, the second drought treatment

induced an increase in PLC to values close to hydraulic failure (85% on average) with starch being converted to soluble sugars. Starch in the wood was almost completely depleted at the end of the second drought treatment. After one week of re-irrigation, no embolism repair was observed and soluble sugars were reconverted to starch. In the second drought cycle, the total NSC content in the wood of plants not stressed in the previous year decreased with time, whereas plants stressed in both years kept NSCs almost constant over time.

In conclusion, the study provides novel insights into the hydraulic acclimation capacity and resilience to fluctuations in water availability of European beech and Norway spruce. The results of the study on mature trees indicate significant and fast hydraulic acclimation under prolonged drought in both European beech and Norway spruce. Acclimation was well coordinated between branches and foliage, which might be essential for survival and productivity of mature trees under future drought periods. The data from the greenhouse experiment showed that in Norway spruce total NSCs in stems are not affected by relatively short (about 40 days long) droughts. Moreover, and most importantly, this study gives for the first time evidence that Norway spruce can repair drought-induced xylem embolism, in the short term (within one week) upon re-irrigation. In addition, when water is newly available, NSCs stored in xylem parenchyma can be mobilized over short term, possibly to sustain respiration and/or for processes involved in the recovery of xylem transport. This might imply dependency on sapwood NSCs for survival, especially if frequent drought spells occur. On the other hand, aboveground biomass and water consumption of European beech saplings are strongly reduced by previous severe drought spells that bring them at the edge of hydraulic failure. In these conditions, embolized vessels in beech stems are not actively refilled and therefore tree survival would likely depend on hydraulic recovery through formation of new functional vessels. Both hydraulic acclimation to drought and hydraulic recovery may be important for the survival of these important tree species in Central European forests under future climate change.

Zusammenfassung

Hydraulische Akklimatisierung gegen Trockenstress und Wiederherstellung der hydraulischen Leitfähigkeit wurden bei Rotbuche und Fichte untersucht. In ausgewachsenen Bäumen, die über einen Zeitraum von zwei Jahren künstlichem Trockenstress ausgesetzt waren, konnte eine Akklimatisierung in Zweigen und Blättern von beiden Baumarten nachgewiesen werden. In Trockenstress-Wiederbewässerungs-Zyklen wurde bei Topfpflanzen Emboliebildung mit gehalt an nicht-strukturellen Kohlenhydraten verknüpft: nach Wiederbewässerung wurde nur bei Fichte Embolliereparatur festgestellt begleitet von Kohlenhydratabbau.

Abbreviation list

$(t/b)_h^2$, conduit wall reinforcement

A, CO_2 assimilation rate (µmol m^{-2} s^{-1})

C_{1cycle}, control trees in the first drought cycle (greenhouse experiment)

CC, control trees in both drought cycles (greenhouse experiment)

CD, conduit density (mm^{-2})

CD, control in the first, drought in the second drought cycle (greenhouse experiment)

C_{FT}, capacitance at full turgor (mmol m^{-2} MPa^{-1})

CO, control treatment (through-fall exclusion experiment)

CO_{year3}, control three-year old cut segments (through-fall exclusion experiment)

D, mean arithmetic conduit diameter (µm)

D_{1cycle}, drought trees in the first drought cycle (greenhouse experiment)

DC, drought in the first, control in the second drought cycle (greenhouse experiment)

DD, drought trees in both drought cycles (greenhouse experiment)

D_h, mean hydraulic conduit diameter (µm)

E, leaf transpiration rate (mmol m^{-2} s^{-1})

g_s, stomatal conductance to water vapour (mmol m^{-2} s^{-1})

K_{max_leaf}/ K_{max_twig}, maximum leaf/end-twig hydraulic conductance (mmol MPa^{-1} s^{-1} m^{-2})

k_s, maximum specific hydraulic conductivity (kg MPa^{-1} s^{-1} m^{-1})

LMA, leaf mass per area (g m^{-2})

PLC, percent loss of xylem hydraulic conductance/conductivity (%)

SVWC, soil volumetric water content (%)

TE, through-fall exclusion treatment (through-fall exclusion experiment)

$V_{G,}$ vessel grouping index

ε, bulk modulus of elasticity (MPa)

π_0, osmotic potential at full turgor (MPa)

Ψ_{12_branch} /Ψ_{50_branch}/Ψ_{88_branch}, water potential at 12/50/88 % loss of branch xylem conductivity (MPa)

Ψ_{50_leaf}/Ψ_{50_twig}, water potential at 50% loss of leaf/end-twig conductance (MPa)

$\Psi_{md,}$ leaf midday water potential (MPa)

Ψ_{pd}, leaf pre-dawn water potential (MPa)

Ψ_{TLP}, water potential at turgor loss point (MPa)

Ψ_{xyl}, xylem water potential (MPa)

1. Introduction

1.1. Climate change and forests die-back

According to the last IPCC (Intergovernmental Panel on Climate Change) report, average land and ocean surface temperature increased of 0.85 °C over the 1880-2012 period (IPCC 2014). Relative to 1850-1900, best case scenarios predict an increase in global surface temperature of 1.5 °- 2.0 °C (IPCC 2014) by the end of the 21st century. Higher mean temperature will likely increase frequency of heat extremes on daily and seasonal timescales as well as their duration. In addition to that, changes in the world's hydrological cycle will include the decrease in mean precipitation in many mid-latitude and subtropical dry regions (IPCC 2014). Looking at the past few decades, shifts in precipitation and temperature patterns in Europe, as in other regions of the world (Dai 2013), have already led to extended and more frequent droughts during the growing season (Fuhrer et al. 2006) and to more recurrent dry years (Briffa et al. 2009).

Water limitation is one of the most critical challenges to plant survival and productivity. In the light of the ongoing climate change, increase in duration, intensity and frequency of dry periods, exacerbated by rising temperatures that lead to higher vapour pressure deficits (VPDs) and evaporation to the atmosphere, enhance drought stress experienced by plants (Williams et al. 2013). Such environmental constraints have been connected to episodes of tree mortality reported worldwide (Allen et al. 2010 for a review, Nardini et al. 2013, IPCC 2014) and are also the main determinants of forecasted changes in forest structure and composition (Williams et al. 2013). Forests are particularly sensitive to climate change because of their long life-spans. Wood plantations and perennial woody crop plants in orchards, which are expected to be productive for decades, are endangered as well, with impacts on yield and local economies (Lobell et al. 2006). Forest die-back is projected to occur in our century in several regions (IPCC 2014) and constitutes a large-scale risk for carbon storage, ecosystem structure and function, biodiversity, wood production, economic activities and human societies (Dale et al. 2000, Gitlin et al. 2006, McDowell et al. 2008, Millennium Ecosystem Assessment 2005).

1.2. Causes of tree die-off

In order to predict how climate change will affect different biomes, it is necessary to identify and understand the physiological drivers of tree decline and mortality. Three main mechanisms are considered to be responsible for drought-induced tree die-off: hydraulic failure, carbon starvation and phloem transport failure. Biotic agents play a significant role as well, given that higher temperatures increase insect infestation pressure (e.g. Logan et al. 2003, Gan 2004) and that drought stress may reduce tree vigor and weaken their defenses against pathogens (Schlyter et al. 2006, McDowell et al. 2008, Wiley et al. 2016). In the following paragraphs, each of the three main determinants of tree mortality will be separately explained, while more detailed information on interactions between hydraulic and carbon dynamics in relation to the objectives of this work will be given in the introduction sections 1.3.2 and 1.3.3.

1.2.1. Xylem embolism and hydraulic failure

Survival of plants depends on the maintenance of adequate long-distance water transport to sustain cell metabolism, photosynthesis and growth. Nevertheless, limited water supply can induce the formation of embolism, i.e. the disruption of the water column in the xylem pipeline as a consequence of increased xylem tensions to critical thresholds. This blockage is caused by entry of gaseous bubbles into the conduits ("air-seeding" hypothesis, Tyree and Zimmermann 2002) and induces a reduction in plant's water transport capacity.

Vulnerability to xylem embolism is often analyzed using "vulnerability curves" (see Figure 4.1 -2), which plot the loss in xylem hydraulic conductivity (usually expressed in percentage, PLC) as a function of the xylem water potential (Ψ_{xyl}; Tyree and Zimmermann 2002). PLC is low under well hydrated conditions (i.e. Ψ_{xyl} near zero) and increases, typically following a sigmoidal function, when Ψ_{xyl} becomes more negative. Usually, vulnerabilities are compared using the xylem pressure at which 50% PLC occurs, called Ψ_{50}. This value corresponds to the steepest part of the vulnerability curve, where a small drop in water potential induces the highest decrease in hydraulic conductivity. If embolism reduces xylem water transport to a critical threshold, partial desiccation or even death of tree individuals occurs. This compromised xylem integrity in a part of the crown or over the whole tree is referred to as "hydraulic failure" (McDowell et al. 2008). Recent studies have shown that the lethal PLC should correspond to 88% in angiosperms

(Barigah et al. 2013, Ulri et al. 2013) and to 50% in gymnosperms (Brodribb and Cochard 2009, Brodribb et al. 2010).

Despite that xylem vulnerability greatly varies across species (Maherali et al. 2004), a meta-analysis showed that a large number of species from the different biomes generally operates at Ψ_{xyl} close to Ψ_{50} (Choat et al. 2012). The smaller is the difference between Ψ_{xyl} and Ψ_{50} (called "safety margin", Johnson et al. 2012), the higher is the risk of potentially catastrophic embolism. Therefore, given that increasing aridity and temperature is a global trend and that safety margins do not depend on mean annual precipitation, all forest biomes would be equally threatened by hydraulic failure (Choat et al. 2012).

In view of climate change, the strong point of some woody species to counteract dangerous levels of embolism might reside in the capability of hydraulic acclimation (i.e. becoming more resistant to embolism) or to recover the lost xylem functionality through embolism repair mechanisms (Zwieniecki and Secchi 2015). Hydraulic acclimation and repair capability will be investigated in parts I and II of this work, respectively, in European beech and Norway spruce.

1.2.2. Carbon starvation

Water loss and consequent drops in water potentials are avoided by trees through stomatal control. On the other hand, stomatal closure has the disadvantage to limit CO_2 uptake for photosynthesis. Carbon starvation occurs when stored carbon is not sufficient to maintain cellular metabolism and turgor, leading to a sustained negative carbon balance (McDowell et al. 2008). Carbon starvation would also imply the inability of plants to produce secondary metabolites useful for protection against pathogens (Guérard et al. 2007, McDowell et al. 2008, 2011).

Among species, a continuum of stomatal responses to water availability exists and varies from a drought avoidance strategy (isohydry), in which water losses are strongly limited by an early stomatal closure, to a drought tolerance strategy (anisohydry), which allows for maintenance of relatively high transpiration rates due to the slower and less efficient stomatal reaction in response to drought (Tardieau and Simonneau 1998). Trees with a more isohydric strategy are suggested to be more prone to carbon starvation because carbon assimilation would be strongly limited by stomatal closure, especially during prolonged and mild drought periods (McDowell et al. 2008). During the first stages of

drought, growth rates decline stronger than photosynthesis, causing no changes or even a temporary increase in non-structural carbohydrate (NSC) concentrations (Müller et al. 2011). Nevertheless, in a second phase, after a prolonged period of low carbon assimilation, carbohydrate reserves would theoretically decline (McDowell et al. 2011).

Independently on plant water use strategies, rising temperatures would also contribute to the consumption of carbon reserves because respiration rates are strongly dependent on temperature (Adams et al. 2009).

1.2.3. Phloem transport failure

A third physiological mechanism responsible for tree mortality is the failure of sugar transport in the phloem and the incapability for cells to use available carbohydrates owing to dehydration during drought (e.g. Sala et al. 2010, Hartmann et al. 2013a, McDowell et al. 2013, Sevanto 2014). Phloem transport failure could occur under drought as consequence of phloem turgor collapse or increased phloem sap viscosity (Sevanto 2014). As the demand for carbohydrates to maintain plant metabolism may require mobilization of reserves, this mechanism could promote carbon starvation because it would determine the inability to utilize carbohydrates and/or reallocate them to starving tissues (Sala et al. 2010). Phloem failure could also favor hydraulic failure, if for example carbohydrates need to be mobilized and transported in order to refill the embolized xylem conduits (Sevanto 2014, see parts IIA and B of this work for more detailed explanation).

1.3. Hydraulics of European beech and Norway spruce in view of climate change

The angiosperm European beech (*Fagus sylvatica*) and the coniferous Norway spruce (*Picea abies*) dominate managed forests in Central Europe, covering 30% of the forested area (Pretzsch et al. 2014). Here, European beech is naturally distributed from the colline to mountainous zone and constitutes the most abundant native tree species. The high plasticity of structural and functional traits justifies the wide ecological amplitude of beech, which is also a relatively drought-sensitive species (Ellenberg et al. 2002). While its northern European margin is extended to the Scandinavian Peninsula, in Central Europe Norway spruce finds its natural habitat in the Alps and in the European midlands

between 800 m a.s.l. and the tree line (Ellenberg and Leuschner 2010). In the past 200 years, it had been a common practice to cultivate spruce in pure stands far beyond its natural range, in the lowlands, due to its high yield in case of abundant water availability. Nevertheless, in Central Europe several constraints like drought and biotic susceptibility have recently directed silviculture to reconvert declining spruce forests with beech (Spiecker et al. 2004) or to cultivate beech and spruce in mixture (Pretsch et al. 2010).

In Central Europe, water is clearly becoming a key determinant for competitive success of tree species. The occurrence of extreme drought episodes - the summer drought spell that particularly affected southern and central Europe in 2003 gave an example of expected future drought extremes consequences on tree productivity (Ciais et al. 2005, Jump et al. 2006) – has brought the understanding of physiological strategies adopted by tree species under drought to a higher attention of the scientific community.

In relation to the objectives of the present study, different physiological aspects related to tree responses to drought will be introduced in the following paragraphs. In particular, while part I is related to the effects of long-term soil drought on the sole hydraulic system of mature trees (hydraulic acclimation to drought), parts II A and II B will focus on interactions between stem hydraulics and carbon dynamics under drought and recovery, which will be considered separately for Norway spruce (part II A) and European beech (part II B).

1.3.1. Part I - Hydraulic acclimation in adult European beech and Norway spruce (Tomasella et al. 2017a)

Plant-functional traits can be used as predictors of plant population abundance dynamics and species distribution under climate change (Soudzilovskaia et al. 2013). During changing environmental conditions, the survival of long-lived woody plants does not only depend on the species' general resistance but also on their acclimation potential, i.e., the capability to adjust structural and/or functional traits to environmental changes within their life-span (Beikircher and Mayr 2009, Taiz and Zeiger 2010). A high phenotypic plasticity, which is the ability of a genotype to express different phenotypes in response to environmental factors (Sultan 2000), may thus allow individuals to better acclimatize to changing climate conditions. Acclimation differs from adaptation, which instead implies the occurrence of genetic changes, over many generations and through natural selection

(Debat and David 2001). Accordingly, species-specific predisposition to tolerate drought (Maherali et al. 2004) reflects adaptations to withstand mean stress levels, while a plastic response in cavitation resistance may play a central role for trees undergoing repeated drought events. It would allow trees to sustain more negative water potentials without incurring hydraulic failure during consecutive droughts.

Despite its importance, however, the degree of phenotypic plasticity in hydraulic traits under drought is still poorly understood (Anderegg 2015). For example, cavitation resistance has been claimed to be a plastic feature in some species (Jacobsen et al. 2007, Beikircher and Mayr 2009), but not in others (Martinez-Vilalta et al. 2009, Lamy et al. 2014), and evidence on hydraulic acclimation in leaves is largely absent (Martorell et al. 2015).

The available studies on tree hydraulic acclimation are based either on spatial, or temporal analyses. The first category mainly includes population comparisons along precipitation gradients (e.g. Cornwell et al. 2007, Schuldt et al. 2016), in which site effects have to be considered (Goldstein et al. 2013, Tokumoto et al. 2014). The second category comprises greenhouse/garden experiments performed mainly on juvenile trees (e.g. Aranda et al. 2015, Martorell et al. 2015) or dendrochronological analyses on mature trees (e.g. Montwé et al. 2014, Rita et al. 2015). A third type of temporal acclimation analysis is based on precipitation exclusion experiments, which, inducing drought stress on a small scale, allow for direct measurements of species' hydraulic adjustment potentials. Nevertheless, especially for hydraulic studies on trees, this approach has been rarely used (Martin-StPaul et al. 2013, Montwé et al. 2014).

The hydraulic vulnerability segmentation hypothesis (Tyree and Ewers 1991) predicts that distal segments of a tree have lower resistance to cavitation than the proximal segments to which they are connected. This would be beneficial for trees undergoing drought because distal components cavitate first, causing the reduction of tensions in the central and more 'expensive' segments and limiting further water losses by disconnecting leaves from the hydraulic system. The hydraulic segmentation of a branch can be characterised by its leaf-to-stem safety margin (for other definitions of safety margins see e.g. Johnson et al. 2012a), expressed as the difference between the water potential inducing 50% loss of leaf conductance (Ψ_{50_leaf}) and the water potential inducing 50% loss of branch xylem conductance (Ψ_{50_branch}). So far, only a few studies directly

compared stem and leaf vulnerabilities (Johnson et al. 2011, 2016, Beikircher et al. 2013, Scholz et al. 2014, Nolf et al. 2015) and no analysis on drought acclimation and respective changes of leaf-to-stem hydraulic safety margins is available. Furthermore, the coordination with other hydraulic leaf traits is not well understood. In leaves, osmotic adjustment is the main driver for maintaining turgor at more negative water potentials (Bartlett et al. 2012) and has been suggested to contribute to the acclimation of leaf hydraulic vulnerability under drought (Martorell et al. 2015).

In this part, the acclimation potentials of European beech and Norway spruce were investigated. These species are interesting from a hydraulic point of view, as European beech is suggested to follow an overall more anisohydric and Norway spruce a more isohydric strategy (Lyr et al. 1992). Hydraulic studies on adult trees of these important species are scarce and focused on within-tree and population comparisons (Herbette et al. 2010, Schuldt et al. 2016). In Norway spruce only a study on wood anatomical plasticity is available (Montwé et al. 2014) and in European beech hydraulic acclimation to changing light conditions was observed in branches (Lemoine et al. 2002, Herbette et al. 2010) and to drought in potted saplings (Aranda et al. 2015).

1.3.2. Part II - Stem hydraulics and non-structural carbohydrate dynamics in potted Norway spruce and European beech saplings under drought and subsequent re-irrigation

Facing drought, woody plants may adopt several structural/functional responses that act either on the short or long-term in order to avoid or limit hydraulic dysfunction. A typical short term regulation is the reduction of transpiration through stomatal closure. Long-term adjustments include the increase in embolism resistance owing to wood anatomical changes (Jacobsen et al. 2007, Montwé et al. 2014), the reduction of transpiring leaf area with respect to conductive (i.e. through lower leaf:sapwood area ratio, Martínez-Vilalta et al. 2009, Martin-StPaul et al. 2013) and/or absorbing (i.e. through higher root:leaf area ratio) elements and the increase in rooting depth (Kozlovsky and Pallardy 2002, Sperry et al. 2002, Nardini et al. 2016). Nevertheless, if physiological impairment owing to a drought episode persists even upon stress release, trees might become more vulnerable to following stressors like pathogens (Desprez-Loustau et al. 2006), frost or another summer drought (Bréda et al. 2006). Moreover, initiation and development of new shoots in spring

can be compromised by limited water transport owing to xylem embolism (Améglio et al. 2002, Galvez et al. 2013) and by insufficient nutrient and carbohydrate availability and mobility (Kozlovsky 1992).

Under the ongoing climate change, trees may face the challenge of undergoing multiple drought events along their lifespan. Seedlings exposed to drought stress can become more tolerant to a following drought than seedlings not previously stressed (Clemens and Jones 1978). Nevertheless, some experiments applying multiple drought cycles have shown that trees undergoing successive stresses need longer recovery times than when subjected to a single drought episode (Liu and Dickmann 1993, Stewart et al. 1995). It has been therefore suggested that the resistance to a stress event might be related to the availability of carbon reserves at the beginning of each stress cycle and to the time interval between two consecutive events, reflecting the time needed to recharge the carbon pool (Niinemets 2010).

Water shortage in trees causes impairment of long distance water transport (Tyree and Zimmermann 2002), but can also affect carbon relations and metabolism. In fact, stomatal regulation of leaf transpiration during drought can significantly decrease carbon assimilation rates and, in extreme cases (e.g. mild but prolonged droughts), lead to negative net carbon balance (McDowell et al. 2008), when trees must necessarily rely on non-structural carbohydrate (NSC) reserves to maintain metabolic processes (Klein and Hoch 2015). On the other hand, dehydration can reduce mobilization of carbon (Hartmann et al. 2013 a), modify carbon allocation (Hartmann et al. 2013 b), affect phloem functioning (Hölttä et al. 2009, Sevanto 2014) and compromise enzymatic activities involved in sugars metabolism (e.g. starch hydrolysis, Srichuwong and Jane 2007). Due to the complexity of interactions between variables affecting NSC pools during drought (in particular duration and intensity of drought episodes, Mitchell et al. 2013), and to species-specific water-use strategies (Petrucco et al. 2017), a strong evidence of whether, how and in which compartments NSC reserves are affected in tree species is needed (Sala et al. 2010, Mencuccini 2014).

Recent advances indicate that the causes of tree decline might be related to both hydraulic failure and carbon starvation mechanisms (Sala et al. 2010, McDowell et al. 2011 2013, Sevanto et al. 2014). In a carbon manipulation experiment, trees with higher NSCs availability kept higher (less negative) water potentials and survived longer to drought

(O'Brien et al. 2014). This highlights the importance of NSCs for maintaining cell turgor, phloem transport and sufficient hydraulic function during stresses (Sevanto 2014, Sevanto et al. 2014).

There is proof that stored NSCs and their metabolism are also involved in maintaining and restoring xylem transport capacity, allowing for water refilling of gas-filled conduits (e.g. Bucci et al. 2003, Salleo et al. 2009, Secchi and Zwieniecki 2011). In the current model proposed for embolism repair, developed during the past few decades (for a review see Secchi et al. 2017), soluble sugars are transferred from parenchyma cells (i.e. vessel associated cells, VACs) into embolized xylem ducts, in order to establish an osmotic gradient that reclaims water from VACs and/or phloem (Nardini et al. 2011) to the conduits and allows for repair. This mechanism requires the presence of living cells in the proximity of the embolized conduits, so that both spatial arrangement and amount of woody parenchyma would therefore be important traits affecting the process (Brodersen and McElrone 2013). For this reason woody angiosperms, having an average parenchyma fraction in the secondary xylem of about 26% against an average of 8% calculated in conifers (Morris et al. 2016), are more likely to show active post-drought hydraulic recovery than conifers (Johnson et al., 2012, Choat et al. 2015, Secchi et al. 2017). This anatomical dissimilarity between the two groups has been also connected to the fact that angiosperms, compared to conifers, generally operate at smaller (or even negative) safety margins (i.e. difference between minimum xylem pressure experienced and the pressure inducing 50% loss of xylem hydraulic conductance, PLC, Johnson et al. 2012). This might suggest that the higher risk of embolism spread in angiosperms would be compensated by a higher capability of embolism repair. On the other hand, pit membranes of conifers have a torus-margo structure: when embolism occurs, the torus is aspirated to the pit chamber aperture, operating as a sealing valve and isolating the embolized tracheids from adjacent functional ones (Pittermann et al. 2005). As isolation of gas-filled conduits is required during refilling under negative pressures (Zwieniecki and Holbrook 2009), in conifers the repair of embolized conduits would be favoured by this sealing mechanism (Mayr et al. 2014).

Water relation parameters and embolism dynamics during drought-irrigation cycles have been only studied in a few angiosperm species (Yazaki et al. 2010, 2015, Yoshimura et al. 2016, Savi et al. 2016). In some of these species, the degree of xylem embolism repair correlated to the amount of stem soluble sugars available at the end of the drought period

(Savi et al. 2016) and the conversion between NSC specimens (starch to soluble sugars and *vice versa*) in the sapwood was related to embolism formation-repair cycles (Yoshimura et al. 2016). Moreover, xylem refilling after winter embolism was associated with a decrease in stem starch content (Beikircher et al. 2016). Except for the few studies cited above, there's a lack of knowledge on stem hydraulics-NSC relations during dehydration-rehydration, especially in tree species threatened by climate change.

Part II A – Norway spruce

In conifers, studies on repair of drought-induced embolism are generally lacking. Refilling has been demonstrated to occur in some conifers after frost-induced embolism via needle water uptake upon thawing of snow (Mayr et al. 2014) or after drought-induced embolism via needle cuticle (Laur and Hacke 2014) or bark (Katz et al. 1989, Earles et al. 2016) water absorption. Evidence supporting the involvement of active refilling in conifers is scant (Borghetti et al. 1991, 1998, McCulloh et al. 2011, Klein et al. 2016), while some studies have shown no repair (Choat et al. 2015, Umebayashi et al. 2016) or have reported cambial re-growth as the main strategy for partial recovery of water transport (Brodribb et al. 2010).

Norway spruce is a conifer currently threatened by climate change in Central Europe (Hlásny et al. 2011) and is known to be relatively isohydric (Lyr et al. 1992). On the other hand, this strategy would theoretically put this species at risk of carbon store depletion, especially under prolonged and mild droughts (McDowell et al. 2008, Mitchell et al. 2013). In previous studies conducted on this species, drought has been reported to affect carbon allocation and translocation, with differences between aboveground and belowground organs (Hartmann et al. 2013a; Hartmann et al. 2013 b). In conifers, as mentioned above, the study of stem hydraulic and NSC dynamics under drought and subsequent re-irrigation is missing.

Part II B - European beech

European beech dominates natural forests in Europe and constitutes a relevant economic resource (Leuschner et al. 2006). Nevertheless, its drought-sensitivity (Ellenberg 1996) has been particularly stressed in the past decades, as growth decline of this species has been observed all over Europe (Jump et al. 2006, van der Werf et al. 2007), even over

several years after the occurrence of the drought episode (Power 1994, Stribley and Ashmore 2002). As an example, after the extraordinary drought spell occurred in 2003 beech was one of the European forest species with the largest losses in gross primary productivity (Ciais et al. 2005).

The anisohydric response strategy of European beech, consisting in a relatively low stomatal sensitivity to changes in water status, induces fast drops in xylem water potentials under drought and therefore potentially higher risks of xylem hydraulic dysfunction (McDowell et al. 2008). Under a severe drought treatment applied in saplings, death of beech and other angiosperm species has been related to hydraulic failure, which occurred at about 88% PLC (Barigah et al. 2013, Ulri et al. 2013). If this threshold determines the border line between surviving and succumbing individuals, European beech trees previously stressed to their hydraulic limits would be an important target of study under a subsequent drought event.

For this species there are no studies directly assessing stem hydraulics in combination with carbohydrate dynamics, and its repair capability under tension has not been tested yet. In fact, refilling of drought-induced embolism in European beech twigs was only reported at the onset of abundant precipitation in autumn and was attributed to root pressure and/or aboveground water uptake (Magnani and Borghetti 1995).

2. Objectives of the study

2.1. Part I - Hydraulic acclimation in adult European beech and Norway spruce

In this part of the study, the acclimation potentials of European beech and Norway spruce under prolonged and relatively moderate soil drought were investigated. A through-fall exclusion experiment allowed for studying mature trees within a mixed forest and thus to simulate drought in an otherwise intact forest system (Pretzsch et al. 2014). After two years of through-fall exclusion, (1) the acclimation in the vulnerability to xylem embolism at the branch level, (2) changes in xylem anatomical traits related to embolism resistance, (3) the acclimation in the vulnerability of leaves (European beech) and end-twigs (Norway spruce), and (4) adjustments of the leaf turgor loss point were examined. A stronger hydraulic acclimation was expected in beech, as safety margins in angiosperms are usually small (enabling only limited protection under prolonged drought) and wood formation, due to the presence of several different cell types, is probably plastic. In contrast, in spruce, less plastic responses were hypothesized. This would be in accordance with a recent meta-analysis (Anderegg 2015), in which angiosperms showed higher intraspecific variability in hydraulic traits than conifers.

2.2. Part II - Stem hydraulics and non-structural carbohydrate dynamics in potted Norway spruce ad European beech saplings under drought and subsequent re-irrigation

Potted juvenile Norway spruce and European beech trees were subjected to two drought-re-irrigation cycles performed in two consecutive growing seasons (summer 2014 and 2015). Both drought cycles aimed at reaching the same defined thresholds of leaf minimum water potentials, which were different in dependence on the species (see explanation below). In the second drought cycle (summer 2015), coupling water relations and hydraulic measurements with stem NSC content, were analyzed: (1) possible long-term (or carry-over) effects of the first drought cycle; (2) stem NSC dynamics under drought, as possibly influenced by the species' water use strategies; (3) the capability to recover xylem hydraulics in the short period (one week) after re-irrigation and (4) possible relations between hydraulic recovery and stem NSC content variations.

The experiment was carried out at the same time in the two species and the general experimental design and most of methods applied were also the same. Nevertheless, given that conifers and angiosperms differ in several hydraulic properties as well as in their theoretical recovery thresholds (see below), a direct comparison of the two species for this experiment cannot be made. Therefore, the two species will be considered in separate chapters, except for the "Materials and methods" section. In the following subchapters, species-specific targets and hypotheses will be clarified.

2.2.1. Part II A - Norway spruce

Norway spruce saplings were dehydrated in both drought cycles to target water potentials corresponding to embolism levels below theoretical lethal thresholds for conifers (i.e. below 50% percent loss of xylem hydraulic conductance, PLC, Brodribb and Cochard 2009, Brodribb et al. 2010). In Norway spruce the following hypotheses were tested: (1) in the long term (the following growing season), the previous drought event affects NSC pool size; (2) at the end of drought stem NSCs are depleted, due to the relatively isohydric strategy of the species; upon re-irrigation (3) hydraulic function is rapidly recovered and (4) stem NSCs content decreases because, in line with the current model for refilling (Secchi et al. 2017), sugars previously accumulated in the xylem apoplast would be washed away when the xylem conduits are refilled and water transport is restored.

2.2.2. Part II B - European beech

In European beech both drought treatments aimed at inducing levels of embolism close to the edge of hydraulic failure, which for angiosperms theoretically corresponds to 88% PLC (Barigah et al. 2013, Ulri et al. 2013). It was hypothesised that: (1) previously stressed plants are more affected by the second drought treatment, as a consequence of impairment of water transport and/or NSC reserves; (2)) at the end of drought total stem NSCs are not depleted, due to the relatively anisohydric strategy of the species and, in line with the findings of Yoshimura et al. (2016), conversion of starch to soluble sugars are triggered by PLC; upon re-irrigation (3) hydraulic function is at least partially recovered and (4) related to NSCs content. In particular, if recovery of hydraulics occurs, similarly to the hypothesis formulated above for spruce, stem NSCs are partially depleted.

3. Material and methods

3.1. Part I - Hydraulic acclimation in adult European beech and Norway spruce (Tomasella et al. 2017 a)

3.1.1. Experimental site and plant material

The study site is located in the Kranzberg Forest, Southern Bavaria, Germany (N 48°25'12", W 11°39'42'', elevation 450 m a.s.l.). Mean annual air temperature is 7.8 °C and mean precipitation 750-800 mm $year^{-1}$, whereas during the growing seasons (May-September) the respective values are 13.8 °C and 460-500 mm $year^{-1}$ (averaged from 1971 to 2000, Hera et al. 2011). The site is characterized by a mixed stand of European beech (*Fagus sylvatica* L.) and Norway spruce (*Picea abies* (L.) Karst) with a mean age of 83 ± 4 years and 63 ± 2 years, respectively (2014). The trees belong to study plots included in the "Kranzberg ROOF experiment" (KROOF, Goisser et al. 2016, Pretzsch et al. 2016). Each plot (sizes ranging between 110 and 200 m^2) included 4-6 European beech and a similar number of Norway spruce specimens. The plots were trenched in spring 2010 by vertical ditches down to 1 m soil depth (reaching a dense clay layer of tertiary sediments), subsequently lined with plastic tarp (waterproof and impermeable to root growth), and refilled with soil. Since May 2014, rainfall has been excluded at 6 out of 12 plots by means of automated roofs at about 3 m aboveground, which from April-May to November were closing in case of precipitation (Pretzsch et al. 2016). During winter, the roofs were permanently open.

The plant material was sampled in 8 plots (4 unroofed, control, CO; 4 roofed, with through-fall exclusion, TE), in which tree crowns were accessible through a canopy crane. Branches and single leaves (European beech) or end-twigs (Norway spruce) were taken from sun-exposed crown parts at about 30 m height, corresponding to the upper canopy of European beech trees. The sampling was strictly performed at this height to avoid shading (Lemoine et al. 2002) or height (Ambrose et al. 2009) effects on the studied hydraulic parameters. End-twigs were used for analyses in case of Norway spruce because the small needles of this species neither allow pressure-volume analyses nor rehydration kinetics measurements (see paragraphs 3.1.6 and 3.1.7). Still, this enabled to characterise hydraulics of distal crown parts and should sufficiently represent needle

hydraulics. It is important to note that the entire end-twigs analysed were grown from 2014 to 2016, when the through-fall exclusion experiment was performed.

The experimental drought applied in 2015 and 2016 strongly limited growth of Norway spruce TE trees, i.e. in 2016 the current and the previous year shoots were extremely short in comparison to CO twigs (max. 2 cm length, Figure 3-1d). For this reason, measurements (pressure-volume and leaf vulnerability analysis; see methods) on Norway spruce were performed on three-year-old end-twigs (i.e. built since spring 2014). CO and TE end-twigs used for measurements were 17.4 ± 0.7 and 12.6 ± 1.2 cm long, respectively. In order to identify potential effects of the current and previous year shoot (differently developed in CO and TE end-twigs), additional measurements were performed on three-year-old segments, deprived of the current-year and the previous-year segments (abbreviation CO_{year3}). A scheme with all measurements performed is given in Figure 3-1.

3.1.2. Soil volumetric water content

Soil volumetric water content (SVWC, %) was measured weekly via time domain reflectometry (TDR 100, Campbell Scientific, Inc., Logan, USA) in all experimental plots (6 CO and 6 TE). TDR probes were installed in the middle of each plot at four different depths (0-7 cm, 10-30 cm, 30-50 cm and 50-70 cm). In the results are reported the SVWC values measured at the shallower (0-7 cm) and deeper (50-70 cm) layers.

3.1.3. Pre-dawn and minimum seasonal water potentials

Pre-dawn water potentials (Ψ_{pd}) were measured in several campaigns over all growing seasons (2014-2016). One short end-twig was excised from each of eight trees per treatment and species at about 30 m height, between 03:00 and 04:30 h solar time (before sunrise). Immediately after harvest, samples were sealed in plastic bags and water potential was measured, using a pressure chamber (Model 3000 Pressure Extractor, Soil moisture Equipment Corp., Santa Barbara, USA).

Midday water potentials (Ψ_{md}) were measured during several campaigns in summer 2016 (third year of drought) as described above, between 12:00 and 14:30 h (sunny days). Minimum water potentials (per species and treatment) were defined as the lowest Ψ_{md}

reached during the growing season (corresponding to the July or August campaigns). These values, compared to branch xylem and leaf/end-twig vulnerabilities (see below), allowed to estimate the stomatal regulation in relation to leaf and branch hydraulic dysfunction.

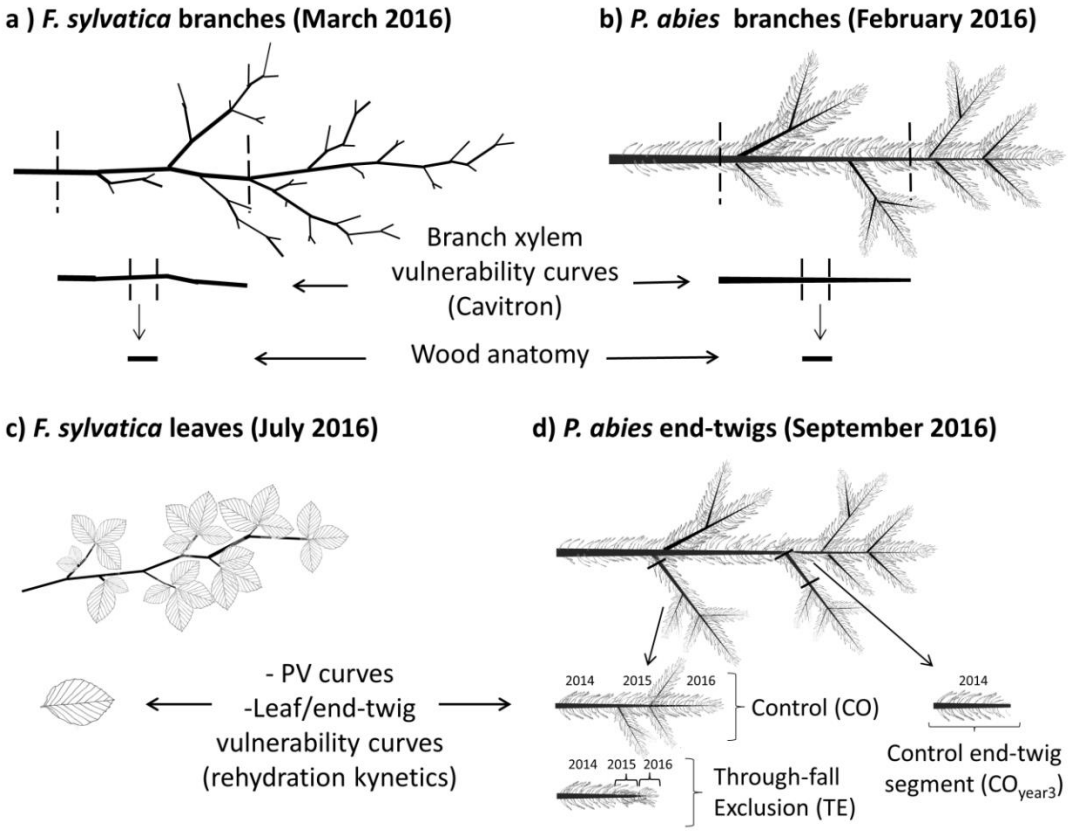

Figure 3 - 1 Hydraulic acclimation study in adult trees: scheme of plant material. Branch **(a, b)** xylem vulnerability analyses were performed with the Cavitron technique in February-March 2016. The central segment of the sample was used afterwards for anatomical analysis. PV curves and leaf/twig vulnerability curves were performed in European beech leaves (*F. sylvatica*, c) or Norway spruce end-twigs (*P. abies*, d), in summer 2016. Leaf/end-twig vulnerabilities were analysed by progressively dehydrating branches and then detaching single leaves/end-twigs in the lab for rehydration kinetics procedure. For measurements, control (CO) and drought stressed (TE) trees were used. In case of Norway spruce CO end-twigs, also samples lacking the previous and current year shoot were prepared (CO_{year3}, called "control end-twig segments" in the text). CO and TE end-twigs of Norway spruce were grown from 2014 to 2016, when the rainfall exclusion experiment was performed.

3.1.4. Branch xylem vulnerability curves

Vulnerability to xylem cavitation was assessed with the Cavitron technique (Cochard et al. 2005) in 7-8 trees per treatment (CO and TE), taking one branch per tree. Samples were collected between February and March 2016 (two years after starting the through-

fall exclusion), i.e. when the roofs of TE plots had been kept open for the whole winter (from December 2015) and prior spring flush, to avoid influences of phenological differences between trees on vulnerability analysis. After harvest, the cut ends of European beech and Norway spruce branches were shortened under water. Beech samples (placed in buckets with water) and spruce samples (wrapped tightly in plastic bags containing wet paper towels) were transported within one day to Innsbruck (Institute of Botany) for vulnerability measurements. Side twigs were removed and the main branch was re-cut several times under water according to Beikircher and Mayr (2016), till reaching a length of 27.5 cm. The mean diameter of samples (without bark) ranged between 3.5-5.5 mm in European beech and between 5.0 -7.0 mm in Norway spruce, while the central portion of the branch segments was 2-3 years old in beech and 3 years old in spruce. This implies that most of TE branches used for Cavitron and xylem anatomical analysis (see below) included xylem built the year before the start of through-fall exclusion. European beech segments were debarked (5 cm) at both ends; in Norway spruce, bark was removed from the entire sample, to avoid clogging of tracheids by resin. Immediately before Cavitron (Cochard 2002) measurements, beech segments were flushed at 0.08 MPa for 20 min at both cut ends (until reaching maximum conductivity), while connected to the Xylem Embolism Meter (XYL'EM, Bronkhorst, France), in order to remove native embolism. Native embolism in European beech branches was 44 ± 12 % (no difference between treatments), due to winter embolism, while no native embolism was detected in Norway spruce. Cavitron measurements and conductivity calculations followed Beikircher et al. (2010). After final trimming at both ends, samples were fixed in a 280 mm custom-built rotor inside a centrifuge (Sorvall RC-5, Thermo Fisher Scientific, Waltham, USA). Segment ends were kept inside transparent plastic reservoirs filled with distilled, filtered (0.22 µm) and degassed water containing 0.005% (v/v) 'Micropur' (Katadyn Products Inc., Wallisellen, Switzerland) to prevent microbial growth. Hydraulic conductivity (k) through the sample was calculated at successive higher xylem pressures, induced by increasing rotational speed. Percentage loss of conductivity (PLC) was calculated as:

$$PLC = 100\ (1 - k_f/k_i) \quad (1)$$

where k_i is the initial (maximum) hydraulic conductivity (obtained at a xylem pressure below 0.5 MPa) and k_f is the hydraulic conductivity at the xylem water potential at a given rotational speed (Ψ_{xyl}).

Curves were fitted with the software package R (R development core team 2014, version 3.1.2) using an exponential sigmoidal function, according to Pammenter and Vander Willingen (1998):

$$PLC = 100 / 1 + \exp[a_{branch}(\Psi_{xyl} - \Psi_{50\_branch})] \quad (2)$$

where a_{branch} is the coefficient related to the slope of the curve and Ψ_{50_branch} is the branch xylem water potential inducing 50% loss of conductivity. The xylem pressures inducing 12 (Ψ_{12_branch}) and 88 (Ψ_{88_branch}) PLC were also calculated:

$$\Psi_{12\_branch} = \log(100/12-1)/a + \Psi_{50} \quad (3)$$

$$\Psi_{88\_branch} = \log(100/88-1)/a + \Psi_{50}$$

3.1.5. Wood anatomical analysis

In order to relate xylem anatomical traits to the potential hydraulic plasticity under drought, conduit mean arithmetic diameter (D, µm), conduit mean hydraulic diameter (D_h, µm), conduit wall reinforcement $(t/b)_h^2$, conduit density (CD) and vessel grouping index (V_G, only for European beech) were calculated from xylem cross section analysis.

From the central portion of five randomly selected samples per treatment previously used for vulnerability curves, cross sections of 15-20 µm thickness were obtained with a microtome (Sledge Microtome G.S.L. 1, Schenkung Dapples, Zuerich, Switzerland) and stained with Etzold FCA mixture. Anatomical traits were analyzed from pictures captured with a digital camera (ProgRes CT3, Jenoptik, Jena, Germany) connected to a light microscope (Olympus BX41TF, Olympus Austria, Vienna, Austria), at a magnification of 20x for European beech and 40x for Norway spruce. For each section, analyses were conducted on a radial sector of sapwood including all relevant annual rings (3 years, formed from 2013 to 2015). Images were analyzed using the software ImageJ (v. 1.48; U. S. National Institutes of Health, Bethesda, Maryland, USA, http://imagej.nih.gov/ij/).

D_h was calculated according to the equation (Sperry and Hacke 2004):

$$D_h = \frac{\sum D^5}{\sum D^4} \quad (4)$$

where *D* is the conduit diameter, calculated from the conduit area and assuming a circular shape in beech and a squared shape in spruce.

Conduit wall reinforcement $(t/b)_h^2$ was calculated according to Hacke et al. (2001a), whereby t is the thickness of the double cell wall and b the hydraulic diameter of the conduit.

CD, expressed as number of conduits per 1 mm^2 (Scholz et al. 2013), was calculated from the complete radial sectors considered for D_h calculations, dividing the total number of conduits by the sapwood area analyzed. V_G is the ratio between total number of vessels and total number of vessel groupings (Carlquist 2001).

3.1.6. Pressure-volume analysis

Water potential isotherms (Tyree and Hammel 1972), also called pressure-volume (PV) curves, were measured in summer 2016 (i.e. during the third year of through-fall exclusion) in five samples (European beech leaves and Norway spruce end-twigs) per species and treatment. Curves were measured in July for beech and in September for spruce to ensure full maturation of tissues and completed xylogenesis in spruce twigs.

Small branches were cut in late afternoon and rehydrated overnight, until water potential was > -0.2 MPa. Leaves of European beech or end-twigs of Norway spruce were detached with a razor blade, wrapped in cling film, and initial water potential (Ψ_{leaf}/Ψ_{twig}) was measured with a pressure chamber (mod. 1505D, PMS Instrument co., Albany, USA). Ψ_{leaf}/Ψ_{twig} and fresh mass were determined periodically during slow dehydration (cling film was removed) on the bench. Measurements stopped when the relation between water loss and Ψ_{leaf}^{-1} (or Ψ_{twig}^{-1}) became linear ($R^2 > 0.95$). The spreadsheet tool of Sack and Pasquet-Kok (2011) was used to determine the following PV traits: water potential at turgor loss point (Ψ_{TLP}, MPa; a key trait to assess plant species' ecological drought tolerance, Lenz et al. 2006, Bartlett et al. 2012), osmotic potential at full turgor (π_0, MPa) and bulk modulus of elasticity (ε, MPa, i.e. the slope of turgor potential vs. relative water content, above and including turgor loss point).

Calculation of leaf/end-twig hydraulic conductance (K_{leaf} or K_{twig}, see below), required the determination of absolute leaf/end-twig capacitance, which is the ratio of changes in water content and respective Ψ_{leaf}/Ψ_{twig}, normalised by projected leaf area. Absolute leaf/end-twig capacitances were calculated at full turgor (i.e. above and including turgor loss point, C_{FT}, mmol m^{-2} MPa^{-1}) and below turgor loss point (C_{TLP}, mmol m^{-2} MPa^{-1}; see Brodribb and Holbrook 2003). Separate PV and capacitance analyses were made for entire control end-twigs (CO) and control segments grown in 2014 (CO_{year3}, see explanation above). As both methods are based on water potential measurements, cutting open a second end of twigs, as done for CO_{year3} end-twig segments, may cause the water column to relax and have an effect on the measured water potential. This effect was preliminarily checked to be very small and not significant.

3.1.7. Leaf/end-twig vulnerability

The response of hydraulic conductance (K_{leaf} in beech, K_{twig} in spruce) to decreasing Ψ_{leaf}/Ψ_{twig} was measured in European beech leaves and Norway spruce end-twigs. K_{leaf}/K_{twig} were determined using the rehydration kinetics technique described by Brodribb and Holbrook (2003). Branches (of about 60 cm length) of 7-8 trees per treatment were harvested in the early morning, transported to the laboratory and wrapped in a plastic bag containing a wet paper towel, for at least 30 minutes, in order to equilibrate water potentials. Measurements were performed under laboratory conditions (air temperature of 20-23 °C and artificial light). Initial water potential (Ψ_0, MPa) was determined in two leaves (beech) or end-twigs (spruce): if the difference between the two Ψ_0 was > 0.1 MPa, measurements were discarded. A third leaf/end-twig was cut while the cut end immersed in filtered (0.2 µm), degassed, 10 mM KCl and 1 mM $CaCl_2$ solution and let rehydrate for a rehydration time (t) of 5 to 10 s for beech and 30 to 70 s for spruce. In spruce, prior excision, the region of the twig to be cut for rehydration was stripped of its bark to avoid resin occlusion at the cut surface. The rehydrated leaves/end-twigs were then wrapped in plastic cling for 2 minutes to allow for equilibration of water potential. Final water potential (Ψ_f, MPa) was measured and K_{leaf} (or K_{twig} in spruce, mmol MPa^{-1} s^{-1} m^{-2}) was calculated as follows:

$$K_{leaf} = C_{FT} [\ln(\Psi_0 \Psi_f^{-1})] t^{-1} \quad (5)$$

When Ψ_0 was below Ψ_{TLP}, C_{FT} was substituted by C_{TLP}. As for PV curves, separate vulnerability curves were made in control end-twig segments grown in 2014 (CO_{year3}).

Maximum leaf/end-twig conductance K_{max_leaf} (or K_{max_twig}) was calculated as mean K_{leaf} (or K_{twig}) of well hydrated shoots (Ψ_0 > - 0.8 MPa) and percentage loss of conductance calculated as PLC for stems (Equation 1), substituting k_i by $K_{max\_leaf}/K_{max\_twig}$ and k_f by K_{leaf}/K_{twig}. Leaf/end-twig vulnerability curves were plotted as sigmoidal functions following Equation 2, where Ψ_{50_branch} was substituted by $\Psi_{50\_leaf}/\Psi_{50\_twig}$ (water potential inducing 50% loss of leaf/end-twig conductance) and a_{branch} by a_{leaf}/a_{twig}.

3.1.8. Leaf-to-stem safety margins

The leaf-to-stem safety margin was calculated as the difference between leaf/end-twig hydraulic safety (expressed as Ψ_{50_leaf} in European beech and as Ψ_{50_twig} in Norway spruce) and branch xylem hydraulic safety (expressed as Ψ_{50_branch}) for each treatment (i.e. Ψ_{50_leaf} -$\Psi_{50\_branch}/\Psi_{50\_twig}$ - Ψ_{50_branch}).

3.1.9. Statistical analyses

Values are given as means ± SE. For curve fitting, vulnerability data were pooled per treatment and segment (branches or leaves/end-twigs), while vulnerability thresholds were calculated per sample. All data were tested for normality (Shapiro-Wilk test) and homoscedasticity (Levene test). Branch vulnerability curve parameters (a_{branch}, Ψ_{12_branch}, Ψ_{50_branch} and Ψ_{88_branch}) were compared within and between species (four groups) with Welch *F*-test, followed by post hoc Games-Howell test. Student's *t*-test (when equal variances) or Welch *t*-test (when unequal variances) were used to test differences between CO and TE treatments in Ψ_{pd}, Ψ_{md}, anatomical parameters of both species and in PV traits, K_{max_leaf}, Ψ_{50_leaf} and a_{leaf} of European beech. In Norway spruce, PV traits, Ψ_{50_twig}, K_{max_twig} and a_{twig} were compared between CO, CO_{year3} and TE, using one-way ANOVA followed by Tukey-HSD post hoc test. All tests were performed at a probability level of $P < 0.05$ using SPSS (IBM SPSS Statistics for Windows, Version 23.0. Armonk, NY: IBM Corp.).

3.2. Part II - Stem hydraulics and non-structural carbohydrate dynamics in potted Norway spruce and European beech saplings under drought and subsequent re-irrigation

3.2.1. Plant material and experimental design

The experiment was conducted at the Greenhouse Center Duernast (48°24'16.1''N; 11°41'34.5''E, Duernast, Germany). In April 2014, four-year-old Norway spruce and two-year-old European beech trees of South Bavarian origin (Hoermann Pflanzen GmbH, Schrobenhausen, Germany), were transplanted in 20 L cylindrical plastic pots. The substrate used for planting was a mixture of 70% forest loamy soil (upper 20 cm of a luvisol, collected from a local stand of spruce at Kranzberg Forest, Freising) and 30% sand. Five g of slow-release fertiliser (Osmocote®, ICL Fertilizers Deutschland GmbH, Germany) was added to the soil and pesticides against aphids and fungi were sprayed on leaves at the beginning of the vegetation period. In spring 2015, 1.5 g of fertilizer (Hakaphos® Blau 15-10-15+2, COMPO Gmbh & Co., Germany) was added as solution to the soil. The soil was maintained at field capacity by an automated drip irrigation system. Pots were placed in a greenhouse equipped with a retractable roof. During the vegetation period, the roof was left open during the day with exception of rainfall events, in order to assure natural direct sunlight to the plants and avoid overheating. Pots were periodically and randomly moved within the greenhouse space.

Air temperature (°C), relative humidity (RH, %) and Photosynthetic Photon Flux Density (PPFD, µmol m^{-2} s^{-1}) were measured at tree height in the middle of the greenhouse and recorded every 10 min by a data logger (model DL2e, Delta-T Devices, Cambridge, UK).

The main results of the studies on spruce and beech derive from measurements carried out through a drought-recovery treatment applied in summer 2015 (see below) on plants that were drought stressed the year before (summer 2014). This was done in order to test the long-term effects of the previous drought on hydraulics, water relations and stem NSC pool size. In both drought cycles, plants were subjected to water shortage until leaf midday water potentials (Ψ_{md}) between -3.0 and -3.5 MPa for Norway spruce and between -3.8 and -4.2 MPa for European beech were reached. Afterwards plants were re-irrigated at soil field capacity. The target water potentials under drought corresponded to ~10-40% and ~80% loss of hydraulic conductance (PLC) in spruce and beech,

respectively, according to vulnerability curves available in the literature for the two species (Cochard 1992, Mayr et al. 2002, Barigah et al. 2013).

The first drought cycle started on 23 July 2014. 30 plants per species were kept watered at soil field capacity (C_{1cycle}, control trees) and 30 underwent drought (D_{1cycle}, drought trees), induced by withholding irrigation. After re-irrigation, all plants were kept well-watered until the second drought treatment, which started the following summer (2015). During the first drought cycle (summer 2014), air temperature and relative air humidity averaged 18.8 °C and 80 %, respectively. In winter 2014-2015, the minimum temperature reached in the greenhouse was -4.3 °C.

In the following summer, plants from C_{1cycle} and D_{1cycle} groups were randomly assigned to two groups that were, as for 2014, a control (kept well-watered by drip irrigation) and a drought treatment. Therefore, four groups were formed: CC (both years control), CD (first year control, second year drought), DC (first year drought, second year control) and DD (both years drought). During the second drought cycle period, maximum daily PPFD ranged between 340 and 1690 µmol m^{-2} s^{-1}, relative humidity (RH) oscillated between 20 and 90% and mean daily air temperature was between 23 and 30 °C. Maximum daily temperatures ranged between 23 and 43°C. In order to test possible long-term legacies of the 2014 drought, a first measurement campaign ("pre-drought") was carried out at the end of June 2015 (i.e. the week before the beginning of the second drought treatment), by measuring soil volumetric water content (SVWC), gas exchange, water potentials, stem PLC and NSC content. Twigs and needles were fully expanded at the beginning of measurements. Drought started on 30 June and irrigation of CD and DD trees was regulated in order to reach the target minimum water potentials almost at the same time in all trees, to avoid that different duration of the drought would affect NSC concentration. To this purpose, in the first four weeks of the treatment, drought trees were irrigated every second day with half of their individual daily water consumption, which was measured before starting the experiment by weighing each drought pot over a 24 h time interval. Afterwards irrigation was completely withheld in order to reach the target leaf water potentials. Trees not harvested for PLC and NSC content at the end of drought ("end-drought" campaign) were re-irrigated to soil field capacity and then were kept well-watered by drip irrigation as control trees. After six/seven days of re-irrigation, trees were harvested for a third ("re-irrigation") campaign. In Figure 3-2 the scheme of the

experiment is represented. Plants to be harvested in each campaign were randomly selected already before the start of the experiment.

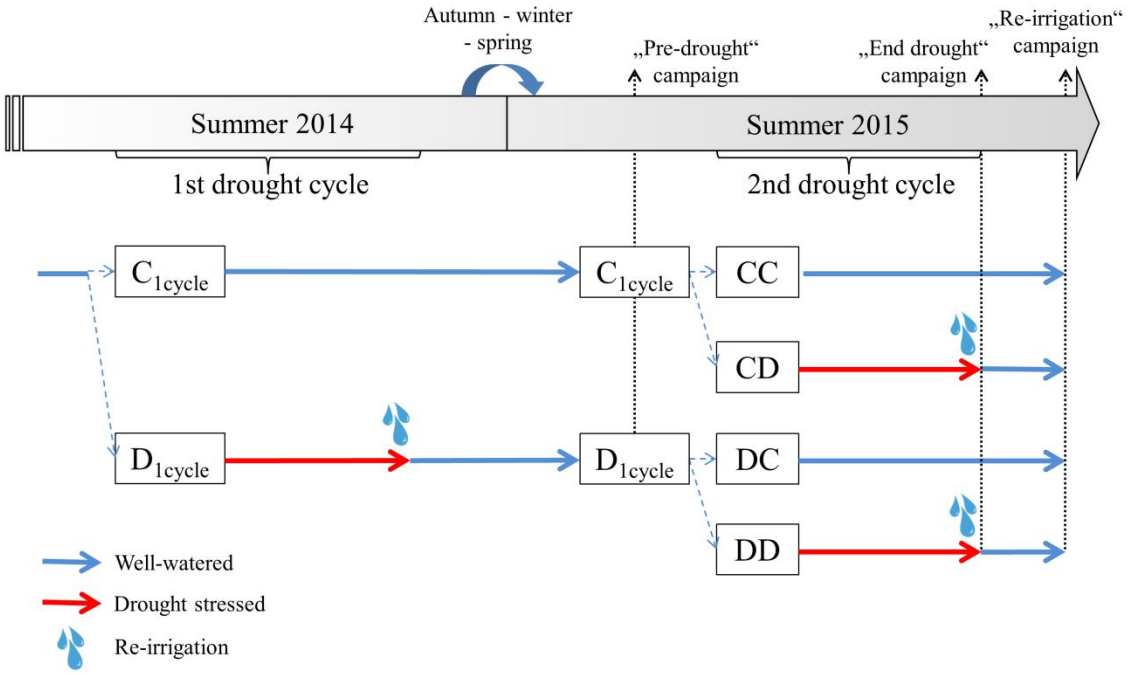

Figure 3 - 2 Greenhouse experiment: scheme of the experimental setup. In the first cycle (summer 2014), spruce and beech potted trees were split into two treatments: a control (C_{1cycle}), kept well-watered, and drought stressed one (D_{1cycle}). In both drought cycles, plants were dehydrated to a target Ψ_{md}, at which each single plant was re-irrigated. During the first drought cycle, irrigation was completely withheld in D_{1cycle} plants. After re-irrigation, all plants were kept well-watered until the following summer (2015), when the second drought cycle took place. In summer 2015 a first measurement campaign ("pre-drought") was performed in C_{1cycle} and D_{1cycle} plants, all well-watered. Afterwards, both C_{1cycle} and D_{1cycle} groups were divided into two groups, a well-irrigated and a drought-stressed one. Therefore, four groups were formed (CC, CD, DC and DD). In this second drought, CD and DD plants were dehydrated progressively, regulating the amount of irrigation in order to reach the target Ψ_{md} almost at the same time (within a few days). At the peak of drought and after one week of re-irrigation, a second ("end drought") and a third ("re-irrigation") measuring campaigns were performed, respectively. In the three measuring campaigns, water potentials, percent loss of stem hydraulic conductance (PLC) and stem non-structural carbohydrates (NSC) were measured. (Modified figure from Tomasella et al. 2017b).

3.2.2. Soil volumetric water content

Soil volumetric water content (SVWC, %) was measured weekly in all the pots, over the whole second drought cycle period, via time domain reflectometry (TDR 100, Campbell Scientific, Inc., Logan, Utah, USA). Probes 20 cm in length were inserted vertically into the pots for instantaneous measurements. A mean value over the total depth was given as

output. Measurements started on 30 June 2015 (start of drought, all trees well-watered) and ended on 14 August 2015 (when all pots were re-irrigated after the drought treatment).

3.2.3. Water potentials and gas exchange

Pre-dawn (Ψ_{pd}) and midday leaf water potentials (Ψ_{md}) were measured between 3:00 and 4:30 h and between 11:30 and 13:30 h (solar time), respectively, in current-year fully developed twigs with a Scholander-type pressure chamber (mod. 1505D, PMS Instrument co., Albany, USA). European beech twigs were bearing one-two leaves. In the first drought cycle (2014), only Ψ_{md} were measured, on subsamples (n=5) and on a weekly basis (see Supplementary Figures S1a and S4). In both drought cycles, Ψ_{md} were measured more frequently when values were approaching the target for re-irrigation. In the three main campaigns of the second drought cycle (2015), xylem water potentials (Ψ_{xyl}) were measured in parallel with Ψ_{md}, on twigs which were wrapped in plastic cling and aluminium foil the evening before, in order to stop transpiration and allow for equilibration of water potentials (Barigah et al. 2013).

In 2015, in order to monitor the effects of the drought treatment on leaf gas exchange, CO_2 assimilation rate (A, µmol m^{-2} s^{-1}), stomatal conductance (g_s, mmol m^{-2} s^{-1}) and leaf transpiration (E, mmol m^{-2} s^{-1}) were measured on 25 June (before starting the drought treatment), on 16 July and on 3 August (last week of drought). Measurements were carried out during sunny days (PPFD between 1100 and 1500 µmol m^{-2} s^{-1}), between 11.30 and 13.30 h (solar time), with a portable gas analyser (Licor 6400, LI-COR Inc., USA). CO_2 concentration was set to 400 ppm. Due to the limited size of spruce needles, a conifer chamber made of transparent plastic (6400-05 LI-COR Inc., USA; measurements under ambient light) was used on a current-year twig. In beech, a cuvette providing red-blue light (set to 1500 PPFD) was clamped to a single mature sun-exposed leaf. In each campaign, measurements were carried out in three to eight trees per treatment, on one twig/leaf per tree. In spruce, gas exchange parameters were normalized by the total needle area of the twig segment included in the chamber. Due to the three-dimensional structure of spruce needles, total projected area was multiplied by a factor 3.2 (Perterer and Koerner 1990).

3.2.4. Stem radius variation (only for Norway spruce - part II A)

Stem radius variation was detected in Norway spruce trees using diameter dendrometers (model DD-S, Ecomatik, Dachau/Munich, Germany), installed at the basal portion of the stem of two-three trees per treatment. From installation (March 2015) to tree harvest (August 2015), dendrometer signals were recorded every 10 min by the data logger used for environmental data (see above). The diameter variation, defined as the relative change in diameter with respect to the beginning of drought treatment (30 June), was calculated.

3.2.5. Water potential isotherms

In order to assess possible adjustments of turgor loss point due to the two drought cycles, water potential isotherms (or pressure-volume curves, Tyree and Hammel 1972) were measured before the beginning of the second drought cycle (end of June 2015) in C_{1cycle} and D_{1cycle} trees (n = 5) and after the second drought treatment (upon restored irrigation) in twigs of control and drought treatments (n = 5). Fully developed current-year twigs were detached in the early morning and allowed to rehydrate for 30 to 60 min (until $\Psi > -0.2$ MPa) while wrapped in plastic cling. The method and calculations (including leaf mass per area, LMA) are described in the method paragraph 3.1.6 (Part I).

3.2.6. Percentage loss of stem hydraulic conductance (PLC)

Percentage loss of stem hydraulic conductance (PLC, %) was assessed in the second drought cycle (2015) in the "pre-drought" (29-30 June), "end drought" (8-12 August) and "re-irrigation" (16-20 August) campaigns. Between 11:00 and 16:00 h (solar time), trees were cut under water in the proximity of the root collar and then trimmed several times under water, making multiple short cuts (Venturas et al. 2015; Nardini et al. 2017a), until the selected portion (two-year old) of the main stem reached a length of about 3-4 cm and 5-7 cm, in spruce and beech, respectively. According to the so called "Wheeler effect", cutting samples under tension, even if under water, produces artefactually higher PLC values (Wheeler et al. 2013). Nevertheless, those results have been confuted by follow-up studies (Trifilò et al. 2014, Venturas et al. 2015, Nardini et al. 2017a, Nolf et al. 2017) applying standard handling and sampling protocols. In the present experiment, trees were cut and trimmed several times under water, thus leading to relaxation of xylem tension.

In Norway spruce, segments were debarked completely to avoid tracheid occlusion by resin. In European beech, about 1 cm of bark was removed only at the cut end to be inserted to the Xylem Embolism Meter (XYL'EM - Plus, Bronkhorst, France) outlet. After final thin and sharp cuts at both ends, samples were connected to the XYL'EM. Hydraulic conductance measurements were performed at 25 °C under low water pressure (7 kPa) using degassed, filtered (0.2 µm) water with 10 mM KCl and 1 mM $CaCl_2$ added (Nardini et al. 2007; Barigah et al. 2013). Consecutive flushes of 10 min each were applied with the same solution at 0.1 MPa for spruce and 0.2 MPa for beech, until no further increase in conductance (maximum hydraulic conductance, K_{max_stem}) was detected. PLC was calculated similarly to Equation 1 (see above) as:

$$PLC = 100\ (1- K_{n\_stem}/K_{max\_stem}) \quad (6)$$

where K_{n_stem} is the initial native hydraulic conductance (i.e. measured before flushes).

Maximum specific hydraulic conductivity was calculated as:

$$k_s = K_{max\_stem}\ L\ A_{xyl}^{-1} \quad (7)$$

where L is the length and A_{xyl} the mean xylem area of the stem sample measured.

3.2.7. Stem non-structural carbohydrate (NSC) analysis

A 3-4 cm long stem segment adjacent to the portion used for hydraulic conductance measurements (see above) was taken from each tree harvested during the three main campaigns of the second drought cycle. Bark (including cambium) was separated from wood with a razor blade and both portions were treated as separate samples, microwaving them three consecutive times at 700 W for 30 s to stop enzymatic activity. After oven-drying at 70 °C until constant mass, each sample was ball milled to fine powder, and 20 mg of dry mass was used for soluble sugars extraction in distilled water, following Schloter et al. (2005). A first extraction was carried out in 1 ml water, vortexing and incubating the suspension for 10 min in 80 °C water bath. After centrifuging and collecting the supernatant, the procedure was repeated twice using 0.5 ml distilled water. The remaining dry pellet was re-suspended in 1.0 ml distilled water and starch was hydrolysed to glucose using heat-stable α-Amylase from *Bacillus licheniformis* (1250 U/ml, 30 min incubation at 80 °C) and amyloglucosidase from *Aspergillus niger* (3 U/ml,

overnight incubation at 37 °C). After centrifugation, final extracts were filtered (0.45 µm nylon filters) and stored at -20 °C until analysis. NSC analysis was performed with high-pressure liquid chromatography (Schambeck SFD, Bad Honnef, Germany) equipped with a Carbosep CHO-820 Ca^{2+} column (Transgenomic, Glasgow, UK), maintained at 90°C. Millipore water was used as mobile phase at a flow rate of 0.5 ml min^{-1} (Angay et al. 2014). Sugar specimens (glucose, fructose, sucrose, pinitol, galactose, stachyose and raffinose) were identified by retention time and concentration was quantified by comparing peak heights in chromatograms with calibration curves obtained from standard solutions. Starch content was quantified as glucose equivalents. Total NSC content was considered as the sum of all measured specimens: starch, glucose, fructose and sucrose constitute the major physiologically important carbon storage compounds, while the others are mainly synthetized in response to stresses like drought (Deslauriers et al. 2014).

3.2.8. Leaf desiccation assessment (only for European beech - part II B)

At the end of the second drought cycle, during the "end-drought" campaign (i.e. when drought stressed trees reached the target Ψ_{md}) leaf desiccation was assessed in European beech in all groups (no leaf desiccation was observed in Norway spruce). Percentage of desiccated leaves was calculated for each tree counting the total number of leaves and the number of damaged leaves.

3.2.9. Aboveground biomass

In the "end-drought" and "re-irrigation" campaigns (August 2015) the aboveground biomass of each tree harvested for PLC measurements was measured after being oven dried at 70 °C for 48 h. For data analysis, the two campaigns were considered as a single one.

3.2.10. Statistical analysis

Analyses were carried out at a probability level of $P < 0.05$, using R (v. 3.1.2, R development Core Team, 2014). All data were tested for normality (Shapiro-Wilk test) and homoscedasticity (Bartlett test) and, whenever necessary, log-, square root- or exponential- transformed.

Welch's t-test was used to test differences between C_{1cycle} and D_{1cycle} trees in all parameters measured before starting drought ("pre-drought" campaign), except for PLC of Norway spruce that was tested with Mann-Whitney U-test (non-normality).

Differences between treatments for A, g_s, E, Ψ_{pd}, Ψ_{xyl} and Ψ_{md} were tested per campaign with ANOVA followed by post-hoc Tukey-HSD. In Norway spruce, differences in A and PLC (non-normality) were tested in each campaign with the non-parametric Kruskal-Wallis test followed by Conover's-post-hoc (R package pmCMR).

In the "end-drought" and "re-irrigation" campaigns, the influence of the first and second drought cycle on stem NSC content was tested using a two-way ANOVA. NSC contents were compared with a two-way ANOVA (treatment and campaign as factors) followed by Tukey HSD post-hoc test. In Norway spruce, as the first drought cycle did not significantly affect NSC content (Supplementary Table S3), data of the "end-drought" and "re-irrigation" campaigns were pooled per water regime (well-watered treatments, CC & DC, and drought treatments, CD & DD). In European beech, all four groups were kept separated, but the DC group was not included in the statistical analysis because consisting on only two replicates per campaign (mean values are reported on graphs without error bars).

A two-way factorial ANOVA (first year and second year treatments as factors) followed by Tukey HSD test was used to test differences in aboveground biomass between treatments.

Correlations PLC-starch and PLC-soluble sugars were tested separately in the "end-drought" and "re-irrigation" campaigns, calculating Spearman's rank correlation coefficients (non-normality) in Norway spruce and Pearson's correlation coefficients in European beech.

4. Results

4.1. Part I - Hydraulic acclimation in adult European beech and Norway spruce (Tomasella et al. 2017 a)

4.1.1. Soil water content and pre-dawn water potentials

From the beginning of the through-fall exclusion (May 2014) on, soil volumetric water content (SVWC) was generally lower in precipitation-excluded (TE) than in control (CO) plots, in all the measured soil horizons (Figure 4.1-1; data not shown for 10-30 cm and 30-50 cm depths). The shallower horizons (0-7 cm, 10-30 cm), with respect to the deeper ones, showed the lowest SVWC and the highest differences between treatments. When the roofs were permanently open (over winter, see gray zones in Figure 4.1-1), water in the soil of TE plots was only partially recharged, due to scarce precipitation over winter 2014/15 as well as winter 2015/16. In summer 2015, CO plots reached similar low SVWC as TE plots because of a natural drought episode.

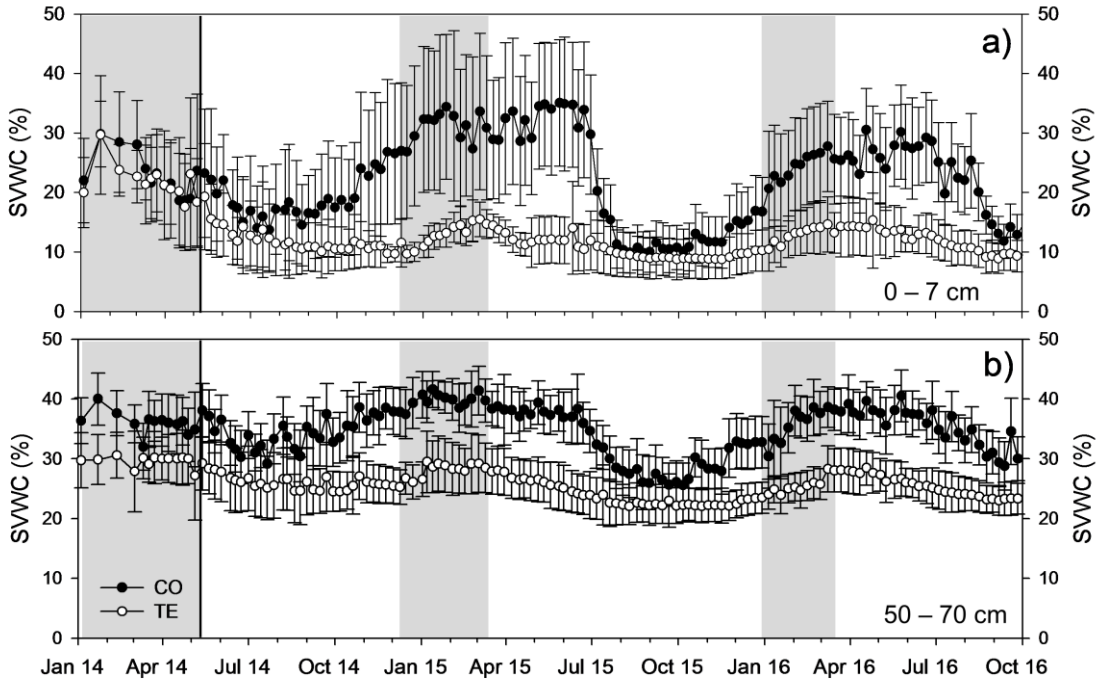

Figure 4.1 - 1 Soil volumetric water content (SVWC) at 0-7 cm (a) and 50-70 cm (b) depth. SVWC was assessed weekly (January 2014 to September 2016) in control (CO) and through-fall exclusion (TE) plots. The beginning of the through-fall exclusion (May 2014) is marked by a vertical black line. Gray background shows the time periods with permanently opened roofs (winter). Values are means ± SE (*n*=6).

Table 4.1 - 1 Pre-dawn leaf water potentials (Ψ_{pd}, MPa). Ψ_{pd} measured in five field campaigns within the three consecutive growing seasons subjected to through-fall exclusion (2014-2016), in control (CO) and through-fall exclusion (TE) treatments. Values are means ± SE (n = 6-8). * 0.01<P<0.05; ** P<0.01 between treatments of a species.

	European beech		Norway spruce	
Date	CO	TE	CO	TE
18.07.2014	-0.42 ± 0.03	-0.75 ± 0.08**	-0.89 ± 0.06	-1.39 ± 0.05**
21.07.2015	-0.76 ± 0.05	-1.32 ± 0.05**	-0.79 ± 0.04	-1.60 ± 0.05**
14.08.2015	-1.31 ± 0.13	-1.66 ± 0.10*	-1.31 ± 0.09	-1.63 ± 0.11*
18.07.2016	-0.32 ± 0.01	-0.56 ± 0.03**	-0.52 ± 0.01	-1.03 ± 0.07**
25.08.2016	-0.38 ± 0.03	-0.78 ± 0.05**	-0.59 ± 0.03	-0.85 ± 0.11

In both species and in all campaigns, pre-dawn water potentials (Ψ_{pd}) were lower in TE trees relative to CO (Table 4.1-1), supporting the effectiveness of the through-fall exclusion treatment and confirming SVWC data. Ψ_{pd} differences between treatments were about 0.2 MPa higher in Norway spruce than in European beech, with exception of August campaigns where scarce or absent precipitation events caused a drop of Ψ_{pd} in both species at the CO plots (Table 4.1-1). Most pronounced differences were observed in Norway spruce in July 2015 with 0.8 MPa lower Ψ_{pd} in TE *versus* CO trees.

4.1.2. Branch xylem vulnerability to cavitation

Both species showed a more cavitation resistant xylem in TE than in CO trees and thus a shift in branch vulnerability upon experimental drought (Figure 4.1-2; Table 4.1-2). In European beech, Ψ_{50_branch} was 0.4 MPa lower in TE (-3.82 ± 0.05 MPa) than in CO trees (-3.42 ± 0.07 MPa) and Ψ_{12_branch} and Ψ_{88_branch} similarly shifted by about 0.5 MPa and 0.3 MPa, respectively (Table 4.1-2). In Norway spruce, a similar trend was observed (although only significant regarding Ψ_{50_branch}), with an average of -3.74 ± 0.06 MPa in CO and of -4.09 ± 0.07 MPa in TE branches.

Overall, branches of Norway spruce exhibited slightly more negative vulnerability thresholds than European beech (CO trees; Table 4.1-2). The slope of the sigmoidal curves, indicated by the parameter a_{branch}, did not differ within and between species (Table 4.1-2).

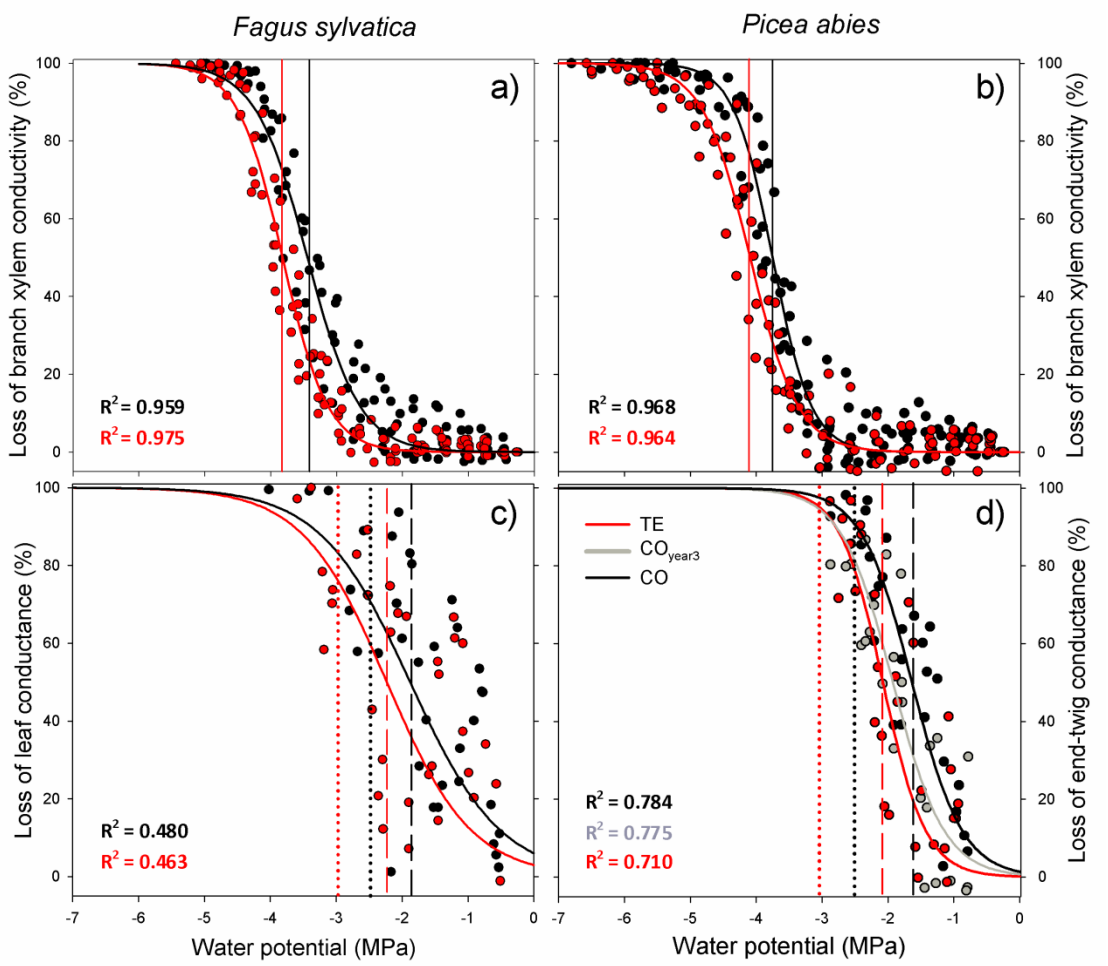

Figure 4.1 - 2 Branch and leaf/end-twig vulnerability curves. Branch vulnerability of European beech **(a)** and Norway spruce **(b)**; vulnerability of European beech leaves **(c)** and Norway spruce end-twigs **(d)** in control (CO) and through-fall exclusion (TE) treatments. The vulnerability curve of Norway spruce control end-twig segments grown in 2014 (CO_{year3}) is shown in panel d. Solid vertical lines indicate water potentials inducing 50% loss of branch xylem conductivity (Ψ_{50_branch}; n = 7-8), dotted vertical lines indicate water potentials at turgor loss point (Ψ_{TLP}), dashed vertical lines indicate water potentials at 50% loss of leaf/twig conductance (Ψ_{50_leaf}/ Ψ_{50_twig}; n = 7-8).

4.1.3. Wood anatomical traits

The observed conduit mean arithmetic diameter (D), conduit mean hydraulic diameter (D_h) and conduit wall reinforcement $(t/b)_h^2$ in branch cross sections did not differ significantly between treatments in both species. However, beech TE trees tended to have smaller vessels and higher conduit reinforcement, with D averaging about 15.1 µm and 12.3 µm ($P < 0.10$), D_h averaging about 28.2 µm and 27.4 µm and $(t/b)_h^2$ averaging about 1.4 and 1.8 in CO and TE, respectively (Table 4.1-3). In beech, also conduit density was (significantly) higher in TE (1218 ± 74 mm^{-2}) with respect to CO branches (872 ± 113 mm^{-2}), while no difference was observed in spruce (Table 4.1-3). The vessel grouping index (V_G) analyzed in beech revealed no differences between treatments.

Table 4.1- 2 Branch and leaf/end-twig hydraulic vulnerability. Slope of branch xylem vulnerability curve (a_{branch}), water potential at 12 (Ψ_{12_branch}), 50 (Ψ_{50_branch}) and 88% (Ψ_{88_branch}) loss of branch xylem conductivity; slope of leaf/twig vulnerability curve (a_{leaf}/a_{twig}), water potential at 50% loss of leaf/end-twig conductance (Ψ_{50_leaf}/ Ψ_{50_twig}), maximum leaf/end-twig hydraulic conductance (K_{max_leaf}/ K_{max_twig}) and hydraulic safety margin (Ψ_{50_leaf} - Ψ_{50_branch}/ Ψ_{50_twig} - Ψ_{50_branch}). CO = control, TE = through-fall exclusion, CO_{year3} = control end-twig segments grown in 2014. Different letters indicate significant differences (P < 0.05) across species and treatments for branch parameters, within species treatments for leaf/twig parameters. Values are means ± SE (n = 7-8).

	European beech		Norway spruce		
	CO	TE	CO		TE
a_{branch}	2.73 ± 0.26[a]	3.09 ± 0.18[a]	3.72 ± 0.43[a]		3.11 ± 0.35[a]
Ψ_{12_branch} (MPa)	-2.64 ± 0.14[a]	-3.16 ± 0.07[b]	-3.15 ± 0.09[b]		-3.39 ± 0.07[b]
Ψ_{50_branch} (MPa)	-3.42 ± 0.07[a]	-3.82 ± 0.05[b]	-3.74 ± 0.06[b]		-4.09 ± 0.07[c]
Ψ_{88_branch} (MPa)	-4.19 ± 0.04[a]	-4.48 ± 0.06[b]	-4.33 ± 0.10[ab]		-4.80 ± 0.16[b]
	CO	TE	CO	CO_{year3}	TE
a_{leaf}/a_{twig}	1.46 ± 0.38[a]	1.56 ± 0.42[a]	2.62 ± 0.43[a]	2.56 ± 0.45[a]	3.08 ± 0.66[a]
Ψ_{50_leaf}/ Ψ_{50_twig} (MPa)	-1.88 ± 0.16[a]	-2.23 ± 0.17[a]	-1.63 ± 0.07[a]	-1.92 ± 0.07[b]	-2.07 ± 0.08[b]
K_{max_leaf}/ K_{max_twig} (mmol $MPa^{-1}s^{-1}m^{-2}$)	34.2 ± 2.2[a]	30.4 ± 3.2[a]	33.1 ± 2.3[a]	42.1 ± 2.6[b]	35.4 ± 2.6[a]
Ψ_{50_leaf} -Ψ_{50_branch}/ Ψ_{50_twig} - Ψ_{50_branch} (MPa)	1.54	1.59	2.11	1.82	2.02

Table 4.1 - 3 Wood anatomical traits. Conduit mean arithmetic diameter (D), conduit mean hydraulic diameter (D_h), conduit wall reinforcement [$(t/b)_h^2$], conduit density (CD) and vessel grouping index (V_G) calculated from cross sections of control (CO) and through-fall exclusion (TE) branches (n = 5). Single asterisks indicate 0.05 < P < 0.1; double asterisks indicate P < 0.05 between treatments of a species. Values are means ± SE.

	European beech		Norway spruce	
	CO	TE	CO	TE
D (µm)	15.1 ± 1.3*	12.3 ± 0.5*	9.8 ± 0.5	9.6 ± 0.3
D_h (µm)	28.2 ± 1.3	27.4 ± 1.3	13.9 ± 0.7	13.8 ± 0.4
$(t/b)_h^2$ x10^{-2}	1.44 ± 0.16	1.76 ± 0.27	7.26 ± 1.06	7.24 ± 1.00
CD (mm^{-2})	872 ± 113**	1218 ± 74**	3995 ± 192	3928 ± 153
V_G	2.51 ± 0.39	2.90 ± 0.27	-	-

4.1.4. Pressure-volume traits

Both European beech and Norway spruce TE trees exhibited about 0.5 MPa lower leaf/end-twig water potentials at turgor loss point (Ψ_{TLP}) than CO trees. This adjustment in Ψ_{TLP} was based, in both species, on an about 0.4 MPa more negative osmotic potential at full turgor (π_0) in TE versus CO trees (Figure 4.1-3). In addition, a lower bulk modulus of elasticity (ε) was found in TE end twigs of Norway spruce indicating higher cell wall elasticity. In both species, absolute capacitances at full turgor (C_{FT}) and below turgor loss point (C_{TLP}, data not shown) did not significantly differ between treatments, even though tended to be higher in TE than in CO leaves/twigs (Figure 4.1-3). In spruce, control end-twig segments grown in 2014 (CO_{year3}) showed intermediate Ψ_{TLP} and $\pi_{0,}$ higher C_{FT} and C_{TLP}, and lower ε with respect to CO and TE twigs (Figure 4.1-3).

4.1.5. Total leaf/end-twig vulnerability, safety margins and minimum seasonal water potentials

European beech TE leaves lost 50% of hydraulic conductance at about 0.35 MPa more negative water potential (Ψ_{50_leaf}) than CO leaves. The average maximum whole-leaf hydraulic conductance (K_{max_leaf}) observed was 34.2 mmol MPa^{-1} s^{-1} m^{-2} in CO and 30.4 mmol MPa^{-1} s^{-1} m^{-2} in TE leaves (no significant difference; Table 4.1-2).

In Norway spruce, mean Ψ_{50_twig} was 0.44 MPa lower in TE than in CO samples (Table 4.1-2). CO_{year3} samples showed intermediate Ψ_{50_twig} with respect to CO and TE end-twigs but the highest K_{max_twig} (42.1 ± 2.6 mmol MPa^{-1} s^{-1} m^{-2}). No difference in K_{max_twig} was found between CO and TE samples. In TE trees, leaf-to-stem safety margins of both species were overall similar to CO trees (Table 4.1-2).

Minimum Ψ_{md} measured in summer 2016 in European beech twigs was significantly lower in TE (-2.33 ± 0.10 MPa) than in CO trees (-1.97 ± 0.07 MPa; $P < 0.05$). In Norway spruce, no differences in minimum Ψ_{md} were found between CO (-1.95 ± 0.05 MPa) and TE (-2.09 ± 0.04 MPa) treatments.

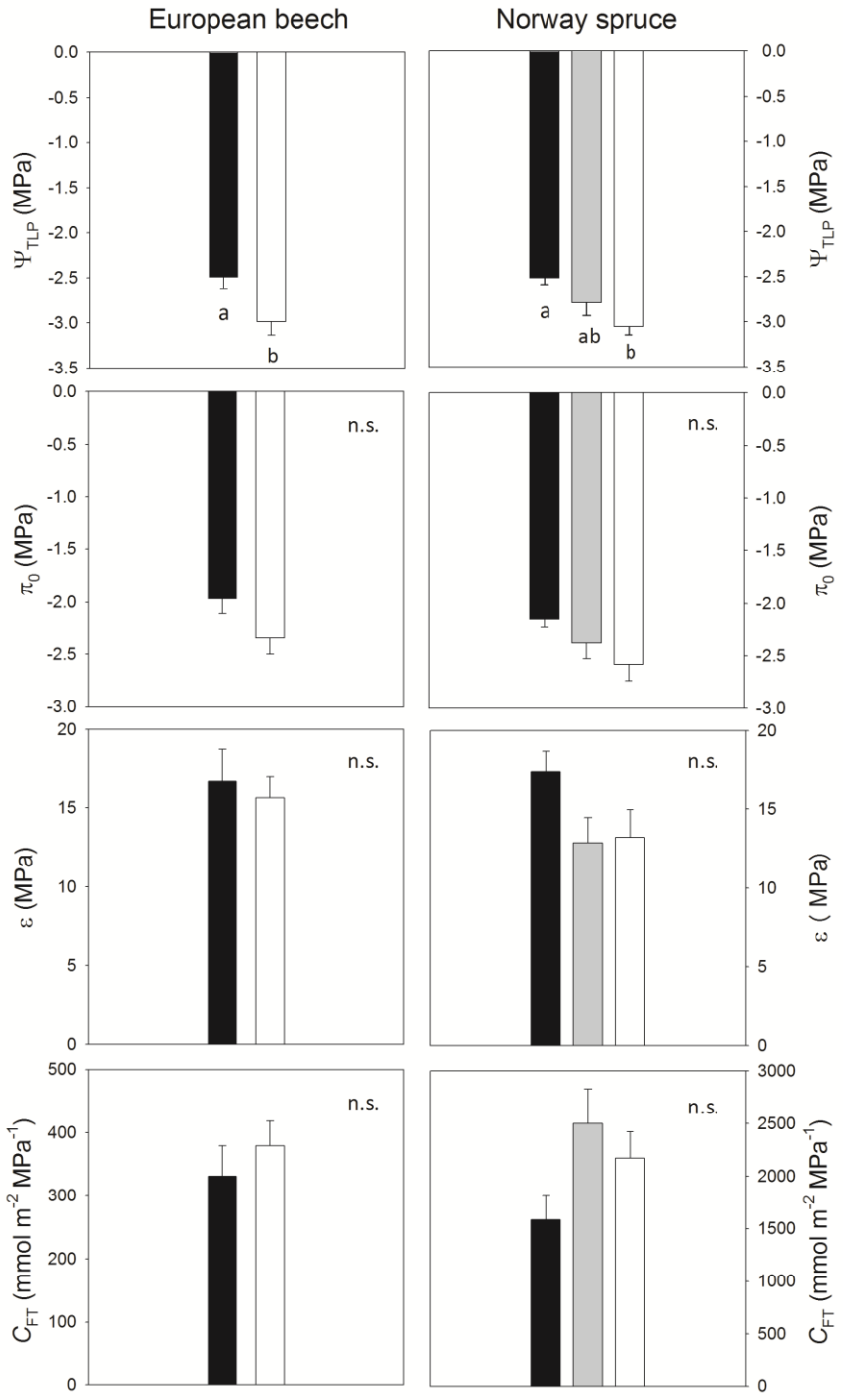

Figure 4.1 - 3 Leaf/end-twig pressure-volume parameters. In leaves (European beech) and end twigs (Norway spruce) of control (CO, black bars), through-fall exclusion (TE, white bars) and control segment (CO_{year3}, beech , gray bars) samples, were analysed: water potential at turgor loss point (Ψ_{TLP}), osmotic potential at full turgor (π_0), bulk modulus of elasticity (ε) and absolute capacitance at full turgor (C_{FT}). Different letters indicate significant differences ($P < 0.05$) across treatments. Bars are means ± SE ($n = 6$ in beech, $n = 5$ in spruce).

4.2. Part II A - Stem hydraulics and non-structural carbohydrate dynamics in potted Norway spruce saplings (Tomasella et al. 2017b)

4.2.1. Environmental and water relations data

In the first drought cycle (summer 2014), plants reached the target midday water potentials (Ψ_{md}, average -3.24 ± 0.04 MPa) in 57 to 95 days (Figure S1a). In the following summer, under well-watered conditions (i.e. in the "pre-drought" campaign, end June 2015), no significant effects were found in leaf water relations, except for xylem water potentials (Ψ_{xyl}), which were less negative in previously stressed plants (i.e. in D_{1cycle}, $P = 0.01$, Table S1).

During the second drought cycle, the soil water content (SVWC) in the two drought treatments (CD and DD) gradually decreased, reaching 8% in the last week of the experiment (Figure 4.2-1). Gas exchange parameters (A, g_s and E) measured in drought stressed plants were close to zero after only two weeks of drought, while control plants maintained over the whole period almost constant values. No difference in gas exchange was found between the two control (CC and DC) as well as between the two drought (CD and DD) treatments (Figure 4.2-2).

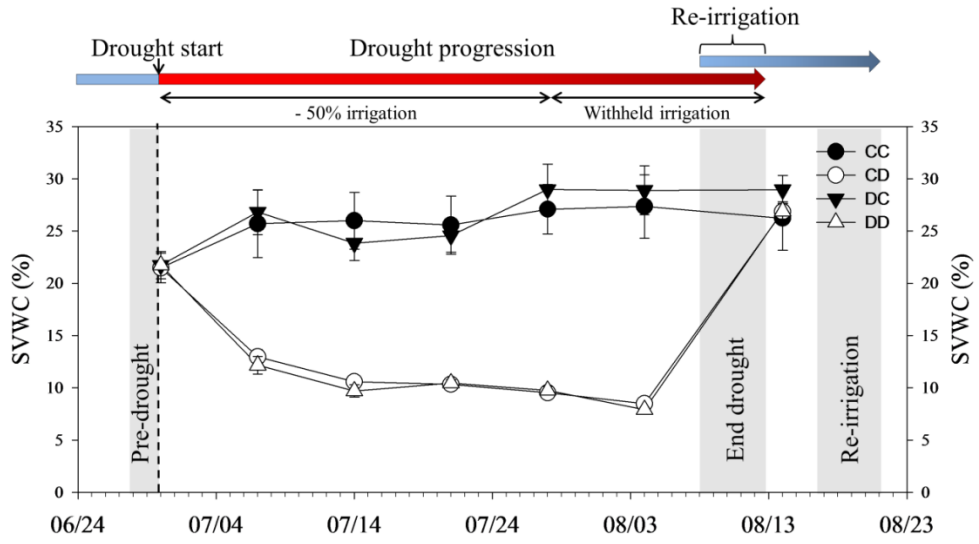

Figure 4.2 - 1 Soil volumetric water content (SVWC) measured over time in Norway spruce pots during the second drought cycle (summer 2015). CC = control in 2014 and 2015; CD = control in 2014, drought in 2015; DC = drought in 2014, control in 2015; DD = drought in 2014 and 2015. Values are means ± SE (n = 3-14 per treatment and campaign). The dashed vertical line shows the beginning of the drought cycle and the shaded areas highlight the time periods where, in order of time, the "pre-drought", "end drought" and "re-irrigation" campaigns were performed. Above the graph, the irrigation regime for drought stressed plants is explained.

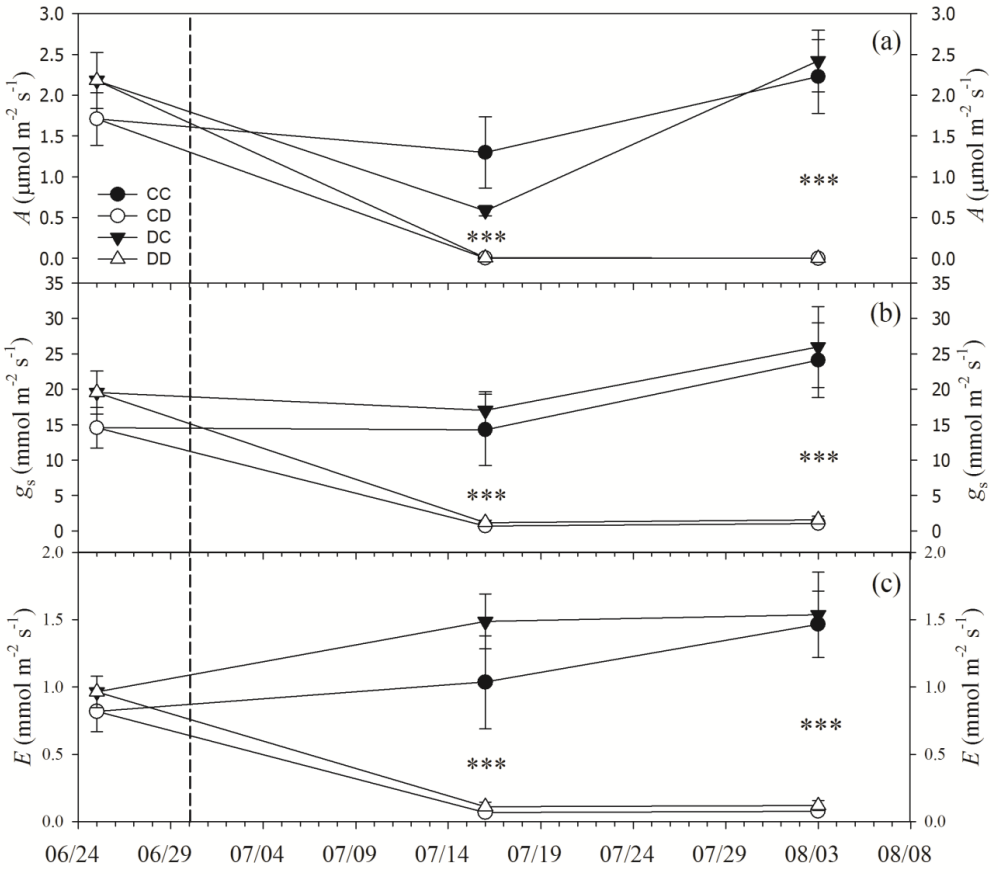

Figure 4.2 - 2 Leaf gas exchange measured over time, before (25 June, "Pre-drought" campaign) and throughout the second drought cycle (summer 2015) in Norway spruce. (a) CO_2 assimilation rate (A), **(b)** stomatal conductance (g_s) and **(c)** leaf transpiration (E). The beginning of the drought treatment is represented by the vertical dashed line. CC = control in 2014 and 2015; CD = control in 2014, drought in 2015; DC = drought in 2014, control in 2015; DD = drought in 2014 and 2015. Values are means ± SE and asterisks indicate significant differences ($P < 0.001$) between drought (CD and DD) and control (CC and DC, well-watered throughout the whole drought cycle) treatments.

The two drought treatments reached the target Ψ_{md} (average of about -3.2 MPa; range from -3.0 MPa to -3.5 MPa) after 39 to 44 days of drought, and pre-dawn water potentials (Ψ_{pd}) and Ψ_{xyl} were close to Ψ_{md} in both groups (Figure 4.2-3a, b). At the end of the drought cycle, both control treatments maintained Ψ_{md} at about -1.3 MPa and Ψ_{xyl} was less negative in DC than in CC plants ($P = 0.03$, Figure 4.2-3b). Upon re-irrigation, water potential isotherm parameters and LMA (Table S2, supplementary material) did not differ between irrigated and stressed plants. On 16 August, after re-irrigation, Ψ_{pd} were about 0.5 MPa lower in DD plants than in the two control groups (about -0.2 MPa) and CD plants showed intermediate values (Figure 4.2-3a). Six to seven days after re-irrigation, Ψ_{xyl} and Ψ_{md} were similar to control values (about -0.6 MPa and -1.0 MPa, respectively; Figure 4.2-3b, c).

4.2.2. Native xylem embolism

In the second drought cycle (summer 2015), percentage loss of stem xylem hydraulic conductance (PLC) measured in well-watered plants, was close to zero (Figure 4.2-3d). Drought induced a significant increase in PLC, and at the end of the drought period ("end drought" campaign) mean values of about 25% and 15% were measured in CD and DD trees, respectively, with no significant difference between the two treatments (P = 0.81). After irrigation, drought stressed plants showed complete recovery of PLC to pre-stress values (i.e. close to zero, Figure 4.2-3d).

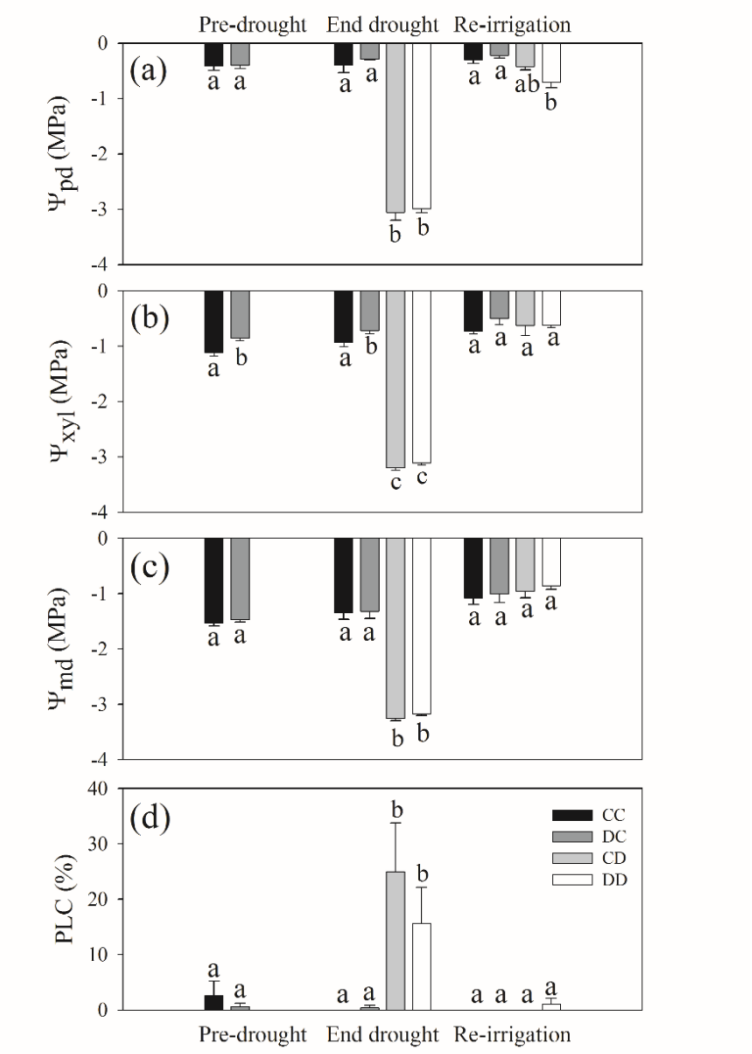

Figure 4.2 - 3 Water potentials and xylem embolism dynamics of Norway spruce in the second drought cycle (2015). (a) Predawn (Ψ_{pd}), **(b)** xylem (Ψ_{xyl}) and **(c)** midday water potentials (Ψ_{md}) and (d) percentage loss of stem xylem hydraulic conductance (PLC) measured in "pre-drought", "end drought" and "re-irrigation" campaigns. CC = control in 2014 and 2015; CD = control in 2014, drought in 2015; DC=drought in 2014, control in 2015; DD = drought in 2014 and 2015. Bars are means ± SE. Different letters indicate differences among treatments within each campaign. The "pre-drought" campaign shows values measured in well-watered plants before that C_{1cycle} and D_{1cycle} plants would have been split into two groups (for explanation see Figure 3-2).

4.2.3. Stem diameter variation

During the second drought cycle (summer 2015), control trees showed a continuous increase in stem diameter (Figure 4.2-4a, c). In both drought treatments (CD and DD), water shortage induced the complete stop (or a slight reduction) of radial growth. While in the first 30 days of drought diurnal cycles of shrinking-swelling were still maintained (Figure 4.2-4b, d), in the final phase of drought (about 10 days before re-irrigation), when irrigation was completely stopped, daily fluctuations were almost negligible and a pronounced shrinkage was observed. Upon re-irrigation, stems of drought trees started to gradually swell and diameters reached the pre-stress values after one day.

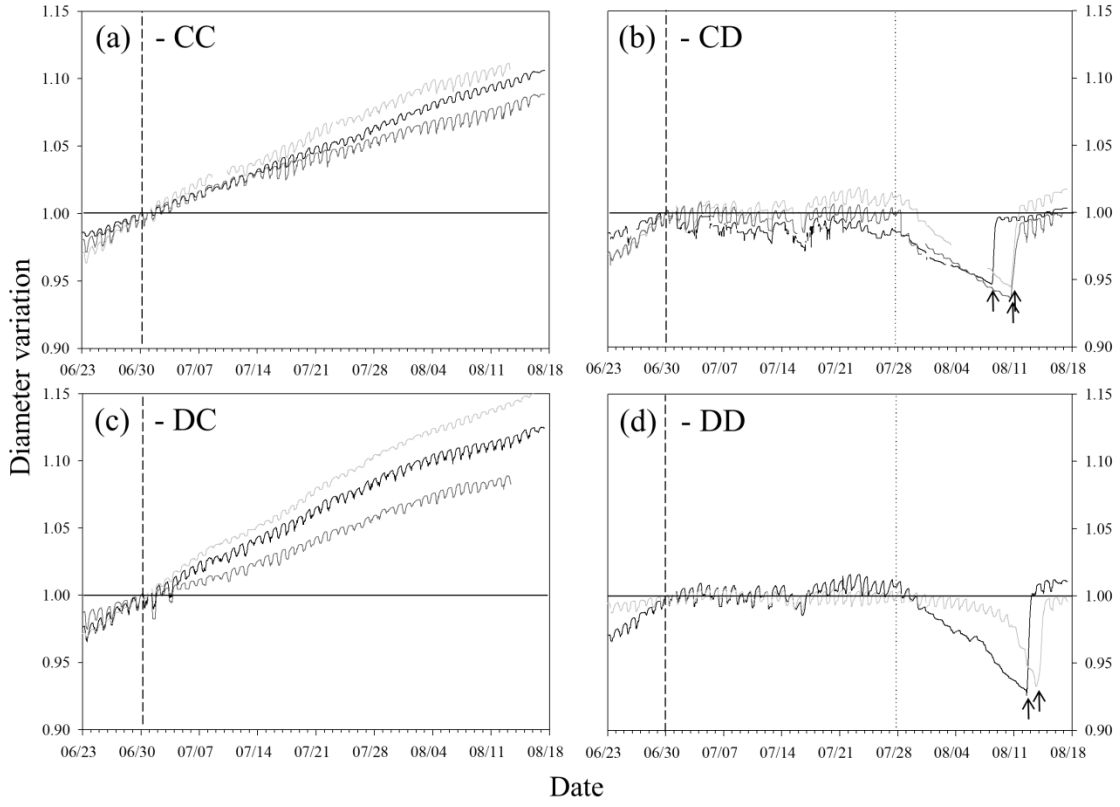

Figure 4.2 - 4 Stem diameter variation over the second drought cycle (summer 2015) in Norway spruce. Stem diameter variations measured in **(a)** CC (control in 2014 and 2015), **(b)** CD (control in 2014, drought in 2015), **(c)** DC (drought in 2014, control in 201) and **(d)** DD (drought in 2014 and 2015) treatments**.** Values are expressed as stem diameter variation from the diameter measured at the beginning of the drought treatment at the basal stem of two-three trees per treatment. Line colours indicate different tree individuals. Vertical dashed and dotted lines show, respectively, the beginning of the drought treatment and the time when irrigation was completely withheld in drought trees. Arrows indicate the time when each tree individual was re-irrigated after drought.

4.2.4. Stem non-structural carbohydrate content

The first drought cycle in summer 2014 did not influence neither the NSC content measured under well-watered conditions in the "pre-drought" campaign of 2015 (Table S1), nor most of NSC specimens concentration measured in the "end-drought" and "re-irrigation" campaigns of 2015 (Table S3, supplementary material). Only sucrose concentration measured in the bark at the end of drought was higher (P = 0.03) in plants stressed the year before. Most differences in NSC content measured at the end of drought and upon re-irrigation could be ascribed to the current year drought (i.e. second drought cycle, Table S3). Hence, for sake of clarity, NSC data of the two control treatments (CC and DC) as well as those of the two drought treatments (CD and DD) were pooled together (Figures 4.2-5 and S2).

NSC content was much (about ten-folds) higher in the stem bark than in the wood. In the wood, drought significantly affected only pinitol content (P < 0.001), which doubled to ca. 8 mg g^{-1}, and stachyose content (P = 0.03, Figure S2). In the bark, at the end of drought, starch was almost completely depleted (average of 0.6 mg g^{-1}) in drought stressed trees, and fructose content was about 50% higher than in control trees (Figure 4.2-5). In both wood and bark, the drought treatment did not affect the amount of total soluble sugars as well as the total NSC content.

After one week of re-irrigation ("re-irrigation" campaign), the content of NSC specimens measured in the wood of drought stressed trees decreased: sucrose, glucose and total NSC content were depleted by about 30% (Figure 4.2-5). In the bark, no difference between treatments was detected at recovery, for all main NSC specimens (Figure 4.2-5).
PLC measured at the end of drought in D trees negatively correlated with the respective starch concentration in the wood (ρ = -0.528, P = 0.024), but did not correlate with soluble sugars content (ρ = 0.222, P = 0.375; see also Figure S3 supplementary material).

4.2.5. Aboveground biomass

Only the first year drought cycle substantially (P = 0.060) affected trees aboveground biomass, which at the end of the experiment (August 2015) was 137 ± 14 g in C_{1cycle} and 103 ± 9 g in D_{1cycle} trees.

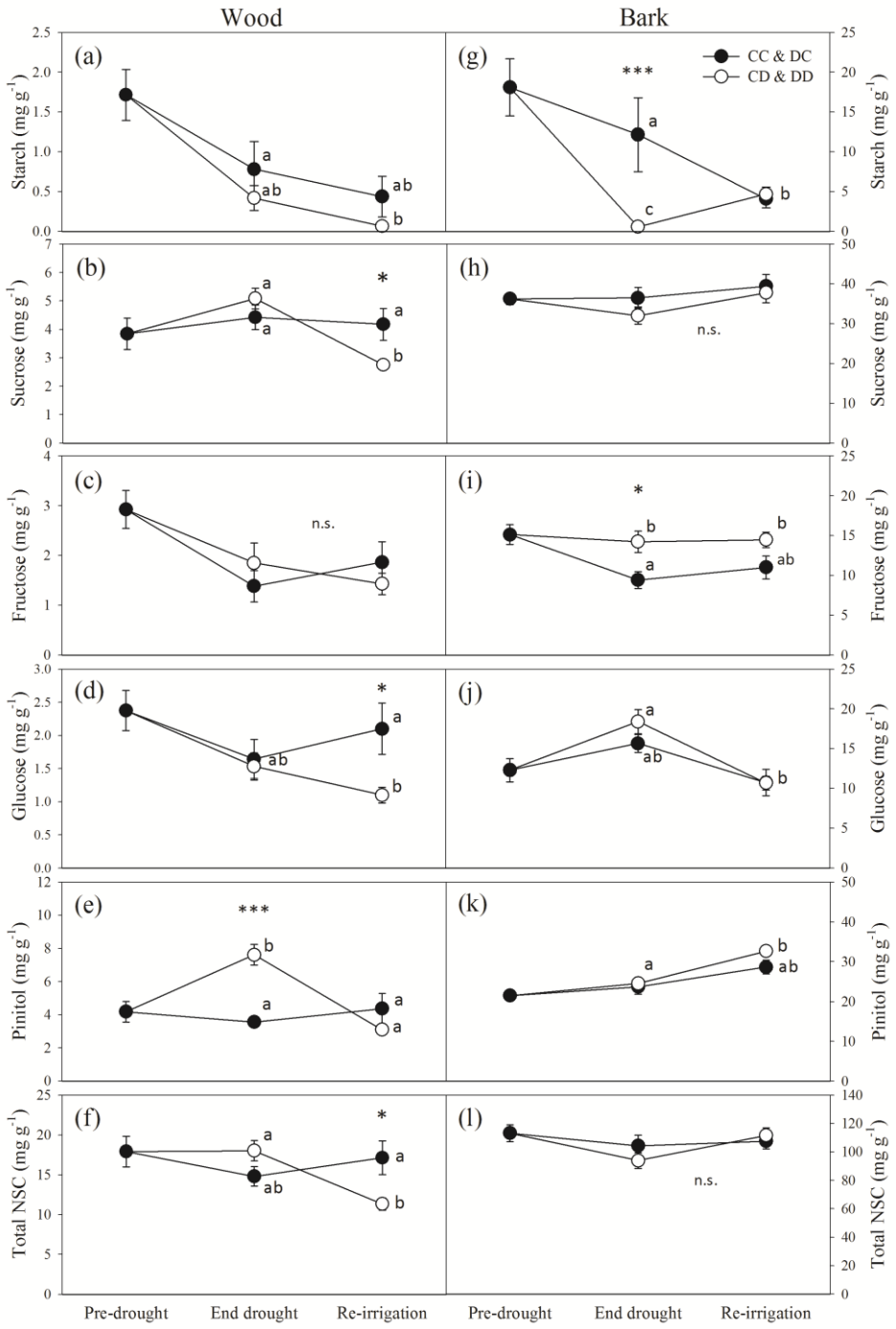

Figure 4.2 - 5 Non-structural carbohydrate (NSC) dynamics in Norway spruce stems during the second drought cycle (2015). NSC concentration (in mg g^{-1} of dry mass) in stem wood **(a-f)** and bark **(g-l)**, measured in "pre-drought", "end drought" and "re-irrigation" campaigns. In the "pre-drought" campaign, data were pooled in one single group (n = 8). In the "end drought" and "recovery" campaigns, well-watered (CC and DC) as well as drought (CD and DD) treatments were pooled, resulting in one control (CC & DC) and one drought (CD & DD) group. Please note the different scales between wood and bark NSC content. "Total NSC" is the sum of all NSC specimens (starch, sucrose, fructose, glucose, pinitol, stachyose, raffinose and galactose) analysed. Symbols are means ± SE (n = 6-12). Different letters indicate significant differences between treatments and campaigns (two-way ANOVA and Tukey-HSD, only data of "end drought" and "re-irrigation" are compared). *n.s.* = no significant difference. Asterisks denote the significance of differences among treatments within a given campaign (*0.01 <P < 0.05, **0.001 < P < 0.01, ***P < 0.001). Modified figure from Tomasella et al. 2017b.

4.3. Part II B - Stem hydraulics and non-structural carbohydrate dynamics in potted European beech saplings

In the first drought cycle (summer 2014), drought lasted 36 to 66 days, when stressed plants reached the target leaf midday water potentials ($\Psi_{md,}$ -4.04 ± 0.14 MPa on average). In some drought stressed plants, complete leaf desiccation occurred before the target Ψ_{md} could be measured. Therefore these plants were re-irrigated like the others, but discarded from the following steps of the experiment (i.e. not included in the second drought cycle). Except one, all plants re-irrigated after reaching the target Ψ_{md} in summer 2014 survived, while those which were re-irrigated at complete leaf desiccation died either before or after flush in the following spring (see Supplementary Figure S5).

4.3.1. Parameters measured in the "pre-drought" campaign

In the "pre-drought" campaign (end June 2015), well irrigated trees that were drought stressed the year before (D_{1cycle}) had more negative Ψ_{md} (P = 0.048), fewer leaves, higher leaf mass per area (LMA) and about 30% lower daily water consumption (measured as evapo-transipiration, ET) than control trees (C_{1cycle}, Table 4.3-1). Maximum specific hydraulic conductivity (k_s) and water potential at turgor loss point (Ψ_{tlp}) were also substantially lower in D_{1cycle} than in C_{1cycle} plants (P = 0.091 and P = 0.071, respectively). On the other hand, percentage loss of xylem hydraulic conductance (PLC), pre-dawn water potential (Ψ_{pd}) and leaf gas exchange parameters did not differ between the two groups (Table 4.3-1). NSC content was also similar between the two treatments, except for glucose content measured in the bark that was higher in D_{1cycle} plants (P = 0.006, Supplementary Figure S6).

4.3.2. Water relations and stem hydraulics (second drought cycle)

Two weeks after the start of the second drought cycle, Ψ_{md} dropped to about -2.5 MPa and -2.2 MPa in CD and DD trees, respectively, and similar values were measured two weeks later. Ψ_{md} measured in control plants were kept rather constant, at about -1.5 MPa, during the whole drought period (Figure 4.3-1b). Ψ_{pd} measured on 8 August (end of the drought cycle, 0 to 5 days before re-irrigation) were about -2.6 and -2.0 in CD and DD trees, respectively (Figure 4.3-1a). At the end of the drought treatment ("end drought" campaign), stressed plants (CD and DD) reached Ψ_{md} between -3.73 and -4.16 MPa.

Table 4.3 - 1 Parameters measured in well-irrigated European beech saplings in the "pre-drought" campaign of the second drought cycle (summer 2015). C_{1cycle} are control and D_{1cycle} are drought treatments of the first drought cycle (summer 2014). PLC = percentage loss of xylem hydraulic conductance; k_s = maximum specific hydraulic conductivity; Ψ_{pd} = leaf predawn water potential; Ψ_{xyl} = xylem water potential; Ψ_{md} = midday leaf water potential; A = CO_2 assimilation rate, g_s =stomatal conductance to water vapor, E = leaf transpiration rate, Ψ_{tlp}= water potential at turgor loss point; π_0 = osmotic potential at full turgor; ε = bulk modulus of elasticity; LMA = leaf mass per area; ET = daily evapotranspiration.Values are means ± SE and asterisks indicate significant differences between treatments ($^{(*)}0.05<P<0.10$; * $0.01<P<0.05$; *** $P<0.001$).

Parameter	C_{1cycle}	D_{1cycle}
PLC (%)	17.7 ± 6.2	41.4 ± 21.5
k_s (kg MPa^{-1} s^{-1} m^{-1})	2.28 ± 0.26	1.64 ± 0.05$^{(*)}$
Ψ_{pd} (MPa)	-0.14 ± 0.03	-0.14 ± 0.02
Ψ_{xyl} (MPa)	-0.36 ± 0.06	-0.49 ± 0.05
Ψ_{md} (MPa)	-0.87 ± 0.12	-1.26 ± 0.14*
A (µmol m^{-2} s^{-1})	4.57 ± 1.02	5.70 ± 0.71
g_s (mmol m^{-2} s^{-1})	57.2 ± 11.1	70.2 ± 12.2
E (mmol m^{-2} s^{-1})	1.37 ± 0.22	1.75 ± 0.19
Ψ_{tlp} (MPa)	-1.34 ± 0.10	-1.58 ± 0.05$^{(*)}$
π_0 (MPa)	-1.12 ± 0.11	-1.25 ± 0.09
ε (MPa)	14.5 ± 2.0	10.7 ± 1.5
LMA (g m^{-2})	49.0 ± 3.4	58.4 ± 1.5*
Leaf number	332 ± 26	214 ± 33*
ET (g day^{-1})	326 ± 14	235 ± 12***

After two weeks of drought, CO_2 assimilation rates (A) and stomatal conductance to water vapour (g_s) significantly decreased in drought stressed plants (CD and DD groups), whereas control plants maintained almost constant values over time (Figure 4.3-2 a, b). In the last measurement campaign (4 August), which occurred 4 to 9 days before the peak of drought, DD plants still maintained A at about 1 µmol m^{-2} s-1, while CD plants completely stopped photosynthesis. With respect to the pre-drought campaign (25 June), leaf transpiration rates (E) increased by about the double in control plants, while were kept almost constant over time in drought stressed plants, due to the higher VPDs

registered in the second and third gas exchange campaign with respect to the first one (data not shown).

The drought applied in the second cycle induced a significant increase in stem xylem embolism: at the end of drought, PLC was 85 ± 9 % and 83 ± 7 % in CD and DD treatments, respectively (Figure 4.3-3). Ψ_{tlp} and π_0 were about 0.7 and 0.5 MPa lower, respectively, in drought stressed plants (Table 4.3-2). After re-irrigation, although being less negative than in the "end-drought" campaign, Ψ_{pd} and Ψ_{md} were still about 0.5 MPa and 1.2 MPa, respectively, lower in drought than in control groups (Figure 4.3-1). No significant change in PLC was observed after one week of re-irrigation (Figure 4.3-3).

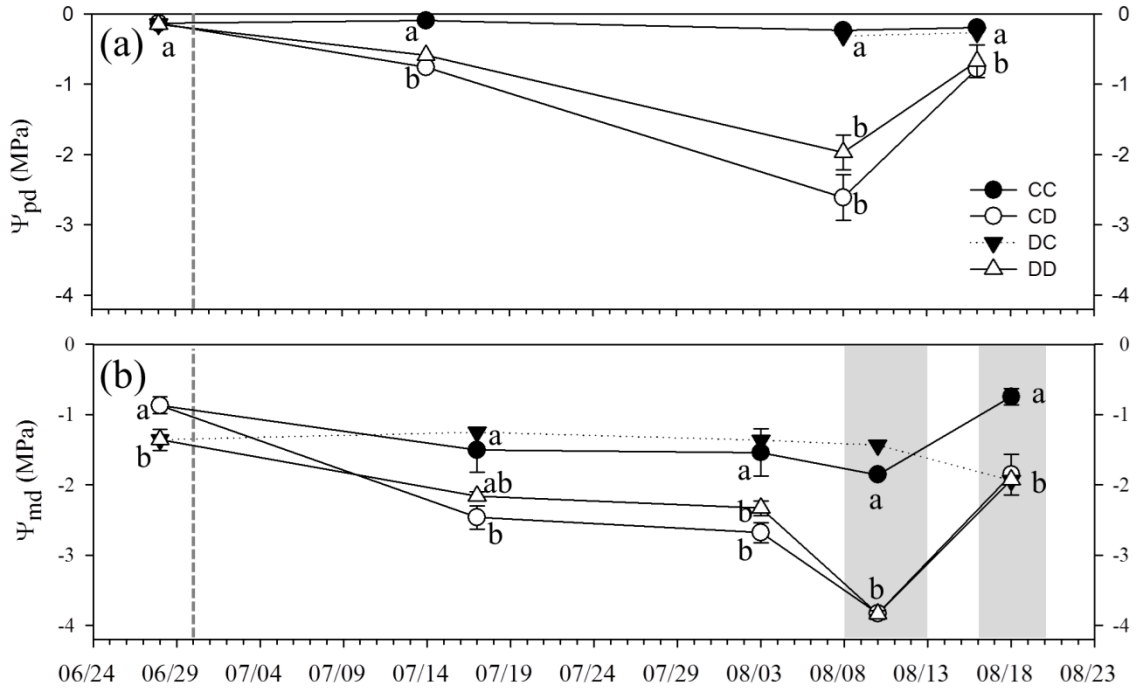

Figure 4.3 - 1 Water potentials measured along the second drought cycle (summer 2015) in European beech saplings. (a) Pre-dawn (Ψ_{pd}) and **(b)** midday (Ψ_{md}) water potentials measured along the second drought cycle (summer 2015). Values are means ± SE and for each sampling date, different letters indicate significant differences between treatments ($P < 0.05$, Tukey HSD test following significant ANOVA). For the DC group (black triangles, n = 2), statistical analysis was not performed and bars are omitted. Vertical dashed lines show the beginning of the drought treatment, while shaded areas highlight the time periods in which the "end drought" (8-13 August) and the "re-irrigation" (16-20 August) campaigns were performed.

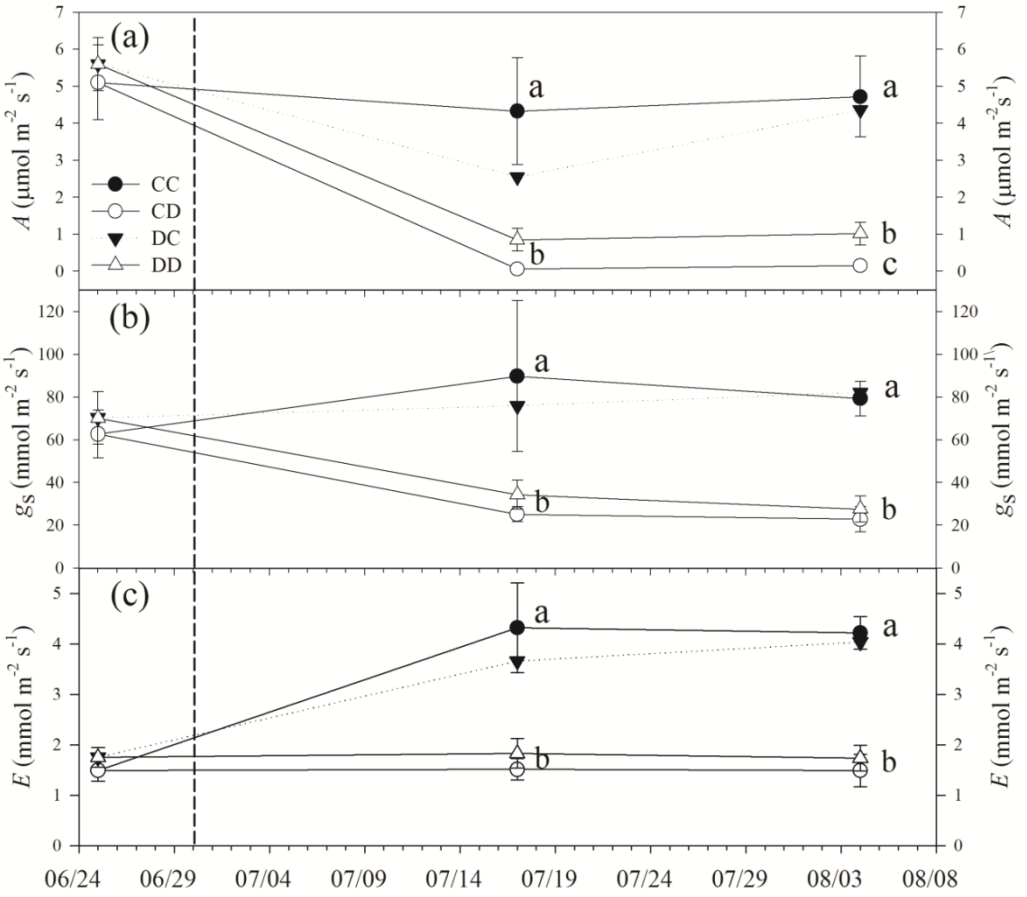

Figure 4.3 - 2 Leaf gas exchange measured over time, before (25 June, "Pre-drought" campaign) and throughout the second drought cycle (summer 2015) in European beech. (a) CO_2 assimilation rate (A), (b) stomatal conductance (g_s) and (c) leaf transpiration (E). The beginning of the drought treatment is represented by the vertical dashed line. Values are means ± SE and different letters indicate significant differences between treatments within each campaign ($P < 0.05$, Tukey HSD test following significant ANOVA). For the DC group (black triangles, n = 2), statistical analysis was not performed and bars are omitted.

Table 4.3 - 2 Water potential isotherm parameters measured in European beech at re-irrigation in the second drought cycle (summer 2015). Water potential at turgor loss point (Ψ_{tlp}), osmotic potential at full turgor (π_0), bulk modulus of elasticity (ε) and leaf mass per area (LMA) measured the week after re-irrigation, in the second drought cycle, in twigs of control (i.e. well-irrigated, CC and DC, n = 3) and drought (CD and DD, n = 5) plants. Values are means ± SE and asterisks indicate significant differences between treatments (* $0.01 < P < 0.05$; ** $0.001 < P < 0.01$; Welch's t-test).

	CC & DC	CD & DD
Ψ_{tlp} (MPa)	-1.68 ± 0.15	-2.36 ± 0.08*
π_0 (MPa)	-1.47 ± 0.13	-2.00 ± 0.09*
ε (MPa)	27.2 ± 11.6	22.7 ± 9.7
LMA (g m^{-2})	46.6 ± 1.4	70.1 ± 3.9**

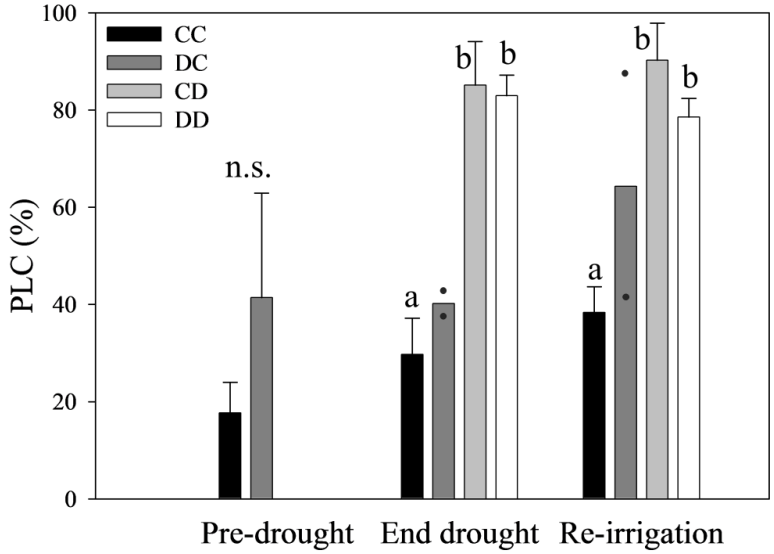

Figure 4.3 - 3 Percentage loss of xylem hydraulic conductivity (PLC) measured in in European beech the second drought cycle (summer 2015). Bars are means ± SE. The "pre-drought" campaign shows values measured in well-watered plants before that C_{1cycle} and D_{1cycle} would have been split into two groups (for explanation see Figure 3-2). In the "end-drought" and in the "re-irrigation" campaigns, different letters indicate significant differences ($P < 0.05$) between treatments and campaigns (n = 3-6, two-way ANOVA with treatment and campaign as factors, followed by Tukey HSD test). The DC group (n = 2, error bars omitted) was not included in the statistical analysis and single PLC values are given as dots.

4.3.3. Non-structural carbohydrate content

At the peak of the second drought cycle ("end drought" campaign), stressed plants (CD and DD) accumulated high amounts of soluble sugars in both wood and bark compartments (Figure 4.3-4b, e). At the same time, starch content decreased: in CD trees starch was almost completely depleted in both wood and bark, while in DD trees starch content in the wood remained relatively higher (about 17 mg g^{-1}) than in CD trees.

After re-irrigation, soluble sugar content of drought treatments significantly decreased in both wood and bark, but remained significantly above controls in the wood. On the other hand, upon re-irrigation, starch content generally increased in both drought treatments, reaching values similar to those of control plants (Figure 4.3-4a, d).

In the "end-drought" campaign, differences in NSC content were only determined by the drought treatment currently applied (i.e. CD and DD plants differed from CC and DC plants, see results of two-way ANOVA reported on top of each single graph in Figures 4.3-4 and Supplementary S6, and in Table S4). After re-irrigation, differences in soluble sugars content in wood and bark, as well as in total NSC in the bark, were still determined by the most recent drought treatment. Conversely, differences in starch and total NSC

content measured in the wood were related to the previous year drought treatment: trees which underwent drought the year before (DC and DD groups) had higher starch and total NSC content than those which didn't (i.e. CC and CD; Figure 4.3-4 a, c, d, f). The amount of the additional sugar specimens analysed (stachyose, raffinose, galactose) was very small and did not significantly change during the measuring campaigns (Figure S6, supplementary material). Pinitol content was not detected.

In both "end-drought" and "re-irrigation" campaigns, total soluble sugars measured in the wood positively correlated with PLC (Figure 4.3-5a). Starch content negatively correlated with PLC at the "end-drought" campaign, whereas no correlation was found after re-irrigation (Figure 4.3-5b).

4.3.4. Leaf desiccation

Drought plants started to show leaf desiccation a few days before reaching the target Ψ_{md} for re-irrigation: the percentage of damaged leaves at the end of drought was significantly higher in CD (61 ± 9 %) than in DD (20 ± 11 %) plants (P = 0.012). Control groups (CC and DC) did not show any foliar damage or desiccation. Leaves of CD trees showed also visible heat damage symptoms (e.g. sunburn spots), which, instead, were rarely present in DD plants.

4.3.1. Aboveground biomass

Differences in aboveground biomass measured at the end of the experiment (August 2015) were related to the drought stress applied in the previous year (i.e. first drought cycle P= 0.012) and not to the second one (P=0.423). Aboveground biomass of plants which were stressed the year before was lower (34.9 ± 2.4 g) than that of well irrigated plants (53.6 ± 5.9 g).

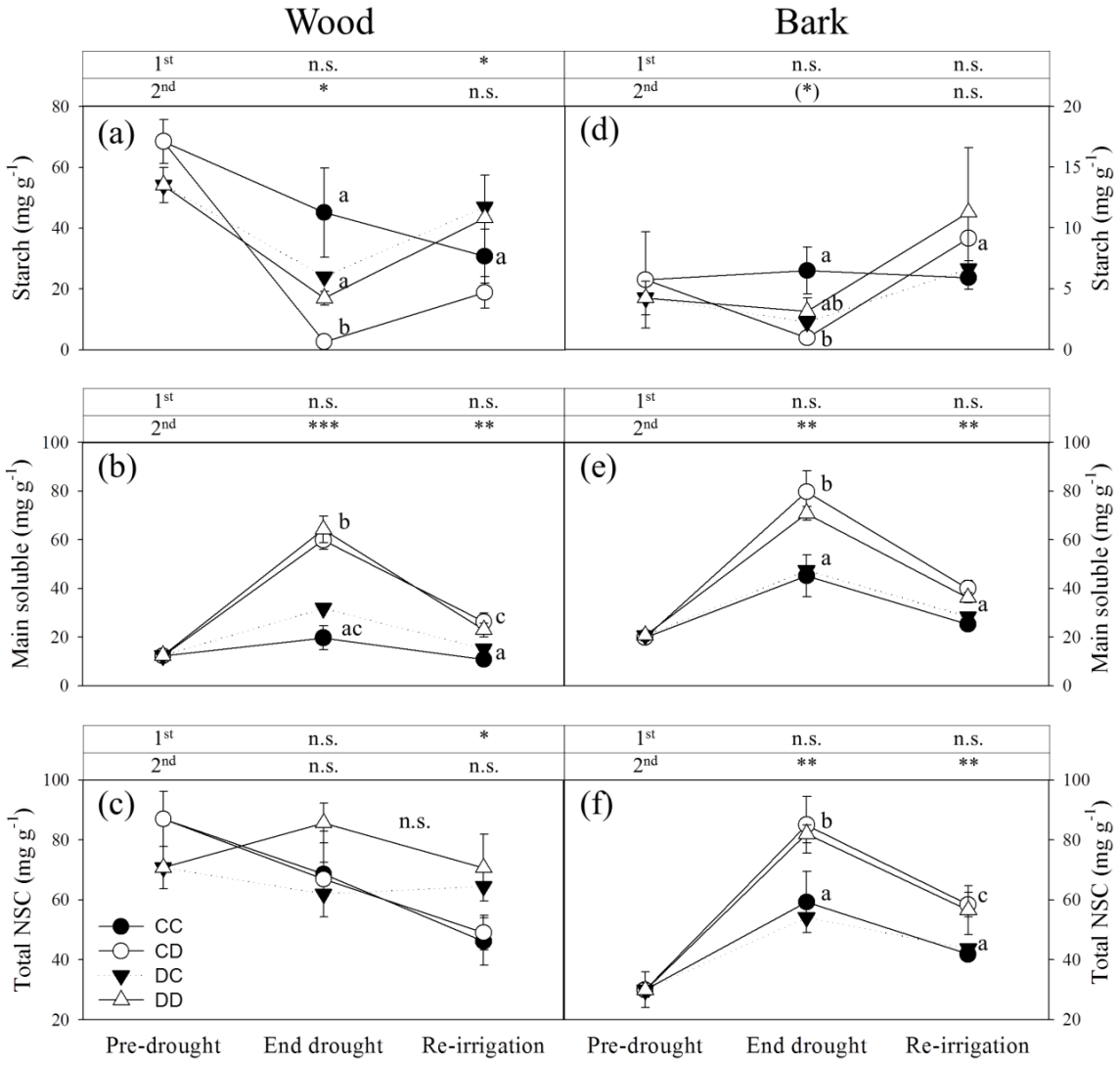

Figure 4.3 - 4 Non-structural carbohydrate (NSC) dynamics in European beech stems during the second drought cycle (2015). NSC concentration (in mg g^{-1} of dry mass) in stem wood **(a-c)** and bark **(d-f)**, measured in "pre-drought", "end drought" and "re-irrigation" campaigns. "Main soluble" is the sum of sucrose, glucose and fructose; "Total NSC" is the sum of all NSC specimens measured. In the "pre-drought" campaign, all plants were well irrigated and only two groups were present (control, C_{1cycle}, and drought, C_{1cycle}, treatments of the first drought cycle, n = 4). In the "End-drought" and "Re-irrigation" campaigns, different letters indicate significant differences between treatments and campaigns (n = 3-6, two-way ANOVA with treatment and campaign as factors, followed by Tukey HSD test). The DC group (n = 2, error bars omitted) was not included in the statistical analysis. For starch content, please note the different scales between wood and bark fractions. On top of each panel, the results of two-way ANOVA, examining the effect of the first (1st) and second drought cycle (2nd) on NSC content measured in the "end drought "and "re-irrigation" campaigns, are shown (*0.01 < P < 0.05, **0.001 < P < 0.01, ***P < 0.001, n.s. = not significant).

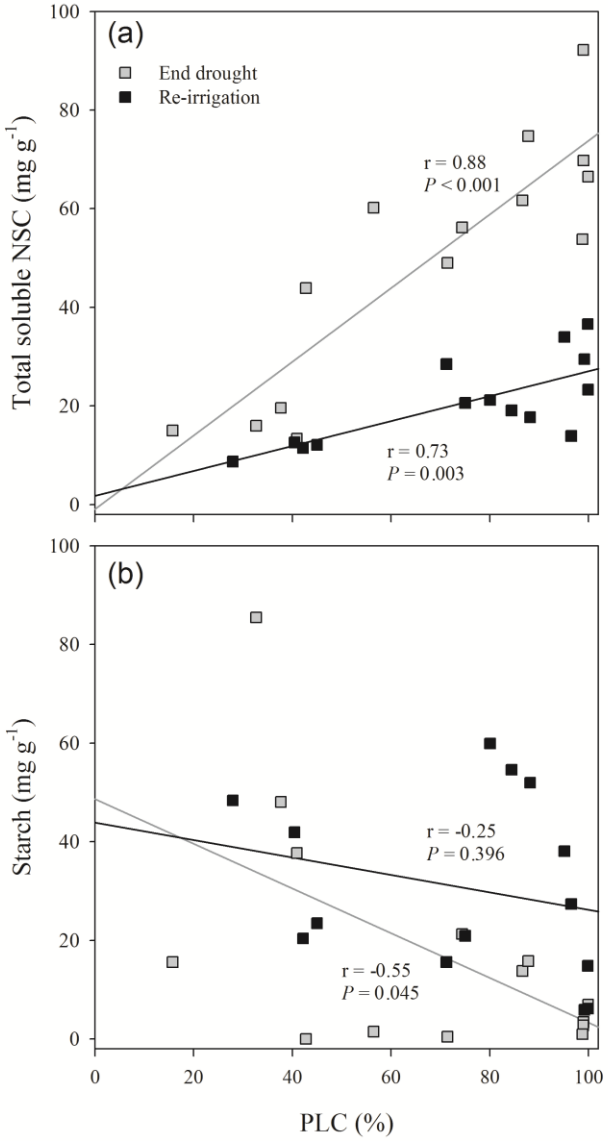

Figure 4.3 - 5 The relationship between starch and total soluble non-structural carbohydrates (NSC) in the stem wood and PLC at the end of the second drought cycle and upon re-irrigation (summer 2015) in European beech. The correlation between percentage loss of xylem hydraulic conductance (PLC) and total soluble NSC **(a)** or starch content **(b)** measured in the stem wood at the end of the drought period (end-drought, black squares) and one week after re-irrigation (re-irrigation, gray squares). Regression lines, Pearson's correlation coefficient (r) and *P*-value (*P*) are reported.

5. Discussion

The results of the experiment conducted on mature European beech and Norway spruce trees support the working hypotheses of short term hydraulic acclimation and of coordination between branch xylem and leaf hydraulics under prolonged soil drought. Nevertheless, whereas for the conifer species a smaller plasticity with respect to the angiosperm species was expected, the two co-occurring species showed similar shifts in the vulnerability curves.

Contrary to the initial hypotheses, in the juvenile trees subjected to two drought-re-irrigation cycles in the greenhouse, stem hydraulics and NSCs content of both European beech and Norway spruce were not impaired by the drought stress applied the previous year (although other drought effects were clearly observed in European beech). At the end of the second drought cycle, the hypothesis of NSC depletion in the isohydric Norway spruce was also confuted, whereas in European beech, according to the hypotheses, starch was converted to soluble sugars and NSCs correlated with PLC. After re-irrigation, the recovery of xylem function and contemporary depletion of stem NSCs were observed only in Norway spruce (in which the NSC consumption was limited to the stem wood), but not in European beech saplings, in which hydraulic recovery did not occur.

In the following, specific discussion sessions to parts I, IIA and IIB are developed, and are ensued by a general discussion.

5.1. Part I - Hydraulic acclimation in adult European beech and Norway spruce (Tomasella et al. 2017a)

5.1.1. Acclimation of xylem hydraulic vulnerability

The through-fall exclusion experiment demonstrated that, under prolonged but overall moderate drought (see pre-dawn water potential data, Ψ_{pd}; Table 4.1-1), both study species exhibited significant and short-term acclimation in vulnerability to xylem cavitation (Figure 4.1-2). With respect to pre-dawn water potentials (Table 4.1-1), Norway spruce showed slightly higher levels of drought stress than European beech upon drought treatment. This can be explained by the shallow rooting system of spruce (the majority of fine roots are restricted to the upper 30 cm; Haeberle, personal

communication) as upper soil layers developed the lowest water contents (Figure 4.1-1). During through-fall exclusion, in Norway spruce water uptake of TE trees almost stopped, while in beech it continued, albeit at lower rates (Kallenbach, personal communication). Therefore, given that soil water content detected by sensors (reaching a maximum depth of 70 cm) did not further decrease during prolonged drought (Figure 4.1-1), it is very likely that European beech roots had access to water from deeper soil layers. Overall the difference in drought stress between species was minor and it is thus remarkable (and in contradiction to the hypothesis formulated in the introduction) that not only the more anisohydric angiosperm European beech but also the isohydric conifer Norway spruce showed acclimation.

Previous studies showed plasticity in cavitation resistance of European beech (Herbette et al. 2010) and provided evidence of an environmental control of this hydraulic trait (Wortemann et al. 2011, Aranda et al. 2015). Accordingly, Schuldt et al. (2016) have recently shown an increase in cavitation resistance with decreasing water availability in European beech populations distributed along a geographical gradient of precipitation. The results obtained in this work sustain and strengthen the above cited findings. The applied through-fall exclusion system allowed the comparison of adult trees within the same forest stand and thus permitted to exclude possible population genetic or site (e.g. nutrient availability and soil water storage capacity differences, Goldstein et al. 2013, Tokumoto et al. 2014) effects. Norway spruce seedlings were found to become more vulnerable to xylem cavitation upon drought (Chmura et al. 2016), probably because of "cavitation fatigue" (Hacke et al. 2001b). A dendrochronological study conducted in a mature Norway spruce plantation equipped with a through-fall exclusion system, instead, showed under drought the formation of conduits with smaller mean hydraulic diameter and higher cell wall reinforcement [$(t/b)_h^2$], which might be more resistant to cavitation (Montwé et al. 2014). In the study here presented, a clear trend in anatomical parameters was overall lacking: just the increased wall reinforcement $(t/b)_h^2$ and conduit density (also see Giagli et al. 2016, Hajek et al. 2016, Schuldt et al. 2016) in TE branches of beech might be related to increased cavitation resistance. It is likely that changes in pit architecture are more relevant for adjustments in hydraulic safety of both conifers (Hacke and Jansen 2009, Jansen et al. 2012, Bouche et al. 2014) and angiosperms (Lens et al. 2011), while anatomical parameters analysed in the present study only partly or indirectly reflect functional hydraulic traits.

It should be noted that all branch samples of European beech were flushed to remove native embolism prior to vulnerability measurements. Due to potential cavitation fatigue (Hacke et al. 2001b), flushing might have caused a general overestimation of vulnerabilities but did not influence the observed differences between CO and TE branches as native embolism was similar (see material and methods). Moreover, requiring a sample length of 28 cm for the Cavitron technique, it was not possible to analyse branch segments entirely formed during the though-fall exclusion period. Accordingly, the central segment of these samples used for anatomical analysis, contained also xylem formed the year before the start of the drought treatment. Thus, it can be expected that xylem segments completely formed during the TE period would show even bigger shifts in Ψ_{50_branch} and in anatomical parameters than those observed. Despite this possible underestimation of drought effects, acclimation was proven to occur during only two growing seasons, in which drought was induced. Overall plasticity in cavitation resistance upon exposure to drought is probably species-specific. For instance, Martin-StPaul et al. (2013) did not find any acclimation in branch vulnerability in a 7-years precipitation exclusion experiment on *Quercus ilex*.

5.1.2. Acclimation in turgor loss point and leaf/end-twig vulnerability

European beech leaves showed significant acclimation in the water potential at the turgor loss point (Ψ_{TLP}; Figure 4.1-3), which enables TE trees to maintain turgescence of the foliage at lower water potentials. Corresponding trends in Ψ_{TLP} and osmotic potentials at full turgor (π_0) indicate adjustments in Ψ_{TLP} to be based on osmoregulation (e.g. Bartlett et al. 2012). The observed acclimation in Ψ_{TLP} thereby was similar to the acclimation in leaf hydraulic vulnerability ($\Psi_{50\_leaf}/\Psi_{50\_twig}$; vertical lines Figure 4.1-2c), according to correlations between Ψ_{TLP} and leaf vulnerability published in previous studies (Blackman et al. 2010, Nardini and Luglio 2014, Martorell et al. 2015).

In European beech maximum leaf hydraulic conductance (K_{max_leaf}) was within the range reported for angiosperms (Brodribb et al. 2005), while K_{max_twig} of Norway spruce was much higher than the needle conductance reported for conifers (values between 1.6 and 24.1 mmol MPa^{-1} s^{-1} m^{-2}; Brodribb et al. 2005, Charra-Vaskou and Mayr 2011, Johnson et al. 2009, 2016). Differences in K_{max_twig} measurements are likely related to the definition of reference areas as K_{max_twig} calculations use a normalization by the projected leaf area

(Brodribb and Holbrook 2003), not accounting for needle geometry. In Norway spruce needles, the total leaf area is 2.2 to 4.0 times the respective projected area (Sellin 2000).

The loss of hydraulic conductance in dehydrating leaves is the result of xylem cavitation (Nardini et al. 2001, Johnson et al. 2012b), partial leaf xylem collapse (e.g. Cochard et al. 2004) and reduction in the extra-xylary conductance (Heinen et al. 2009, Voicu et al. 2009, Scoffoni et al. 2014). All these mechanisms might be responsible for the observed adjustment in leaf vulnerability (Table 4.1-2, Figure 4.1-2), as in both species under study vulnerability thresholds of leaves/end-twigs were more negative in TE than in CO trees. However, in the case of Norway spruce, the observed difference may also be substantially based on the reduced growth of new flushes (Figure 3-1d) and less on acclimation. Accordingly, control end-twig segments grown in 2014 (CO_{year3}) and TE twigs (carrying very small shoots from the previous and current year), had similar Ψ_{50_twig}. In contrast, in intact CO sample twigs, the bigger proportion of younger twigs and needles (formed in the previous and current year) caused overall higher Ψ_{50_twig}. This also indicates age-related changes in the vulnerability of end-twigs, probably related to mesophyll developments and thus to extra-xylary pathways. Indeed, in the conifer *P. pinaster*, Charra-Vaskou et al. (2012) and Bouche et al. (2016) found the hydraulic safety of needle xylem to be similar to branch xylem and higher than in the entire needle, indicating extra-xylary components to be hydraulically limiting. Ontogenetic changes might also explain the shifts in Ψ_{TLP} and π_0 observed in Norway spruce TE end-twigs, which are similar to the shifts in twig vulnerability (Figure 4.1-2d) as noted above for beech.

5.1.3. Coordination of hydraulics

Leaf-to-branch safety margins were positive and relatively wide in both species, whereby the safety margin was smaller in the more anisohydric European beech than in Norway spruce (Table 4.1-2). According to the hydraulic segmentation hypothesis (Bucci et al. 2013, Pivovaroff et al. 2014), recently validated between branches and leaves of both angiosperm and conifer species (Johnson et al. 2016), the here presented findings indicate that in both species leaves/needles act as hydraulic fuses, which protect proximal sections of hydraulic pathways. Considering the quantitatively similar and unidirectional changes in vulnerability of branches and leaves/end-twigs as well as in turgor upon drought, hydraulic traits and respective acclimations seem to be well coordinated within trees.

In European beech minimum water potentials (Ψ_{md}) measured in the field in summer 2016 were in both treatments similar to Ψ_{50_leaf} calculated from vulnerability curves (Table 4.1-2). This indicates that stomata regulate in dependence of the hydraulic limits (and thus vulnerabilities) of the distal components of the hydraulic pathway. In contrast, TE end-twigs of Norway spruce had a lower risk of hydraulic dysfunction due to their higher leaf hydraulic resistance and the absence of changes in Ψ_{md}. Reductions in conductivity located in extra-xylary part of leaves/twigs might be reversible (Cochard et al. 2004, Scoffoni et al. 2014) so that the observed Ψ_{md} were still safe for the hydraulic integrity of leaves/twigs.

5.2. Part II A - Stem hydraulics and non-structural carbohydrate dynamics in potted Norway spruce saplings under drought and subsequent re-irrigation (Tomasella et al. 2017 b)

Long-lasting mild droughts are supposed to induce carbon depletion, especially in relatively isohydric species like Norway spruce (McDowell et al. 2008). The first drought cycle, which lasted two to three months, did not induce in the studied spruce saplings any relevant long term impairment of water transport and, most importantly, stem NSC pool size. The new functional xylem built in spring from the cambium, is known to contribute to restore xylem functionality in case that residual embolism is still present after winter (Améglio et al. 2002). Nevertheless, it is likely that, similarly to what was observed in the second drought cycle (see discussion below), a fast hydraulic restoration could have occurred already upon re-irrigation, after the first drought treatment in 2014. Even during the second drought cycle, no carry-over effect was observed, indicating for spruce complete resilience to the drought stress undergone the previous year.

Under drought stress, spruce showed a typical isohydric behaviour: the almost complete stomatal closure observed in the second drought cycle allowed for reduction of leaf water loss, albeit at the expense of carbon assimilation (Figure 4.2-2). It is very likely that high temperatures registered in summer 2015, induced fast dehydration (e.g. in comparison with the 2014 drought), which was additionally exacerbated in the last two weeks of drought when irrigation was completely withheld. The target water potential range reached at the end of the drought treatment induced xylem embolism in the main stem: the measured percentage loss of xylem conductance (PLC) was in the range expected

from xylem vulnerability curves reported for the species in the literature (Cochard 1992, Mayr et al. 2002).

5.2.1. Stem NSC dynamics under drought

Contrary to the hypothesis, the drought treatment applied in 2015 did not alter stem carbon balance, in both wood and bark compartments (Figures 4.2-5 and S2). There is evidence that short-term and severe droughts, like the one undergone by our spruce saplings in 2015, can lead to little or no changes in NSC pool sizes even in relatively isohydric species (Anderegg and Anderegg 2013). It must be noted that stem diameter growth stopped at the time when drought started (Figure 4.2-4b, d), thus likely reducing carbon sink consumption and helping to preserve carbon pools when CO_2 uptake was drastically reduced. It is also possible that NSC depletion occurred in other tree compartments (e.g. in roots, Hartmann et al. 2013a, b, Yang et al. 2016). Nevertheless, while total NSC content did not change, starch in the bark was almost completely depleted by drought and was accompanied by an increase in monosaccharides (glucose and in particular fructose). This could be an indication of osmotic adjustment of turgor loss point (Silva et al. 2010, Hartmann et al. 2013a). Moreover, there are suggestions that solutes accumulated in the phloem might also be effective for refilling if they are delivered to the VACs through parenchyma rays (Nardini et al. 2011, Secchi and Zwieniecki 2015, Secchi et al. 2017). The consumption of local starch reserves under drought could be also a consequence of impeded phloem translocation (Sala et al. 2010, Hartmann et al. 2013a) and/or reduced sugar availability at the source (i.e. in the leaves) due to photosynthesis inhibition (Figure 4.2-1a).

Some NSC compounds are known to be involved in plant cell protection (as antioxidant and/or osmoprotectant) under stresses like drought. The relevant accumulation of pinitol in the wood of stressed plants at the end of drought, accompanied by a subsequent decrease to pre-stress values upon re-irrigation (Figure 4.2-5e), can be explained by the role played by this sugar alcohol as hydroxyl radical scavenger and osmolite in some plant species, including conifers (Deslauriers et al. 2014).

5.2.2. Embolism repair and NSC depletion only in the stem wood

In this experiment, spruce plants experienced water potentials which were low enough to induce xylem embolism, but still far from those theoretically endangering conifers' survival (PLC below the threshold of 50%, Figure 4.2-3). In Norway spruce, multiple drying-rewetting cycles, where plants were dehydrated to minimum leaf water potentials slightly below our target values, caused complete and short-term recovery of sapflow rates and stem diameter (as here observed, Figure 4.2-4) in each re-irrigation episode (Hartmann et al. 2013a). In the present study was obtained evidence that this species is able to recover xylem hydraulics in the main stem over short term after re-irrigation (six-seven days, Figure 4.2-3c). The possibility that water uptake via needle cuticle or bark, previously reported in some conifer species (Katz et al. 1989, Laur and Hacke 2014, Earles et al. 2016), could have been responsible for refilling of spruce stems, can be excluded. In fact, relative humidity during the recovery time of the experiment never exceeded 81%, while aboveground uptake is supposed to occur during fog (RH of 100%) or rain events. Also the possibility that newly built xylem conduits (new growth upon re-irrigation) would have allowed for fast hydraulic recovery, can be excluded by dendrometer data (no regrowth, Figure 4.2-4) and cannot explain the observed complete hydraulic recovery. Studies involving in vivo imaging have reported the occurrence of refilling under low xylem pressures (e.g. Brodersen et al. 2010) and in *Vitis riparia* positive root pressure was not required as a driving force of the process (Knipfer et al. 2016). Positive root pressure, which requires maximum soil water availability (i.e. $\Psi_{pd} \sim 0$) and complete stop of transpiration, has been shown to contribute to refilling in some monocots (e.g. Yang et al. 2012) or in some woody angiosperms prior spring flush (Strati et al. 2003, Brodersen and McElrone 2013), while in conifers this phenomenon has not been detected so far. Pre-dawn water potentials at recovery show that embolism repair occurred at relatively high xylem tensions (Figure 4.2-3a) and therefore do not support the involvement of root pressure in embolism removal in our trees.

One of the main working hypotheses was that recovery of xylem hydraulics should be accompanied by changes in NSC content in stem wood and/or bark. Upon hydraulic recovery, NSCs of drought plants were depleted only in the wood, but remained unaltered in the bark (Figure 4.2-5). This suggests that the NSC pool in wood parenchyma was partially degraded upon drought relief, and was still not recharged one week later. Here

below are proposed some scenarios which might explain the present findings. After re-irrigation, NSCs could have been used in the cambium as source of carbon to sustain new cell formation (albeit re-growth was not detected by dendrometers, Figure 4.2-2). This hypothesis, however, would not provide an explanation for sugar depletion only in the wood and not in the bark. Alternatively, sugar reserves might be used to supply carbon demand for stem respiration after re-irrigation, especially if photosynthesis is still depressed. Although gas exchange rates were not measured after re-irrigation, a delay in recovery of photosynthesis after drought has been previously reported in conifer species (Brodribb and Cochard 2009, Brodribb et al. 2010). Moreover, an increase in stem respiration at re-irrigation has been associated with an increase in energy demand for xylem transport restoration (Yoshimura et al. 2016).

According to the current paradigm for embolism refilling, soluble sugars released by the wood parenchyma into embolized conduits would drive water entry after drought relief (Bucci et al. 2003, Salleo et al. 2009, Secchi and Zwieniecki 2011). If this happened in Norway spruce, soluble sugars could have first entered the embolized tracheids and then, once the conduits had been refilled and become newly functional, removed by the transpiration stream (Secchi and Zwieniecki 2016). This mechanism could also explain the drop in starch content in drought stressed trees, as its breakdown could have contributed to generate the osmotic gradient for refilling. From the data collected, it is not possible to unequivocally relate NSCs depletion to active refilling of embolized conduits. Nevertheless, considering the Van't Hoff's equation, it is possible to estimate the theoretical minimum NSC content (expressed in glucose concentration) needed to generate the osmotic pressure (π) for the refilling of the gas-filled tracheids, in a wood sample of given size and given Ψ_{xyl} at recovery (Nardini et al. 2017b). Given the PLC measured before re-irrigation (20%), the sapwood area occupied by tracheids (25%, calculated in our samples from cross sections), the wood density of samples (0.51 g cm^{-3}) and the Ψ_{xyl} measured at recovery of hydraulics (-0.6 MPa, Figure 4.2-3), and assuming that a π of -0.7 MPa (i.e. 0.1 MPa more negative than $\Psi_{xyl;}$ assumption value) was necessary to counterbalance xylem tensions and reclaim water, the corresponding minimum glucose content required to reverse embolism would be 5 mg g^{-1} of DW (see calculations in the supplementary material). Therefore, ca. 6 mg g^{-1} DW in total NSC content, that is the drop in NSC content observed in the wood of stressed plants from

drought to recovery conditions in our study, should have been theoretically sufficient to provide the osmotic pressure required for the process.

In conifers, due to their wood anatomy, the occurrence and kinetics of refilling could depend on the amount and arrangement of ray parenchyma within the wood and on the distance between rays and embolized conduits (Brodersen and McElrone 2013), because water must come from living cells. In the stems of spruce saplings used in this experiment was measured a xylem parenchyma fraction of about 6 %, which is in line with the average value reported for conifers (8%, Morris et al. 2016). In Norway spruce, parenchyma rays are well spread within the wood and, albeit present in low percentage, have been already proven to be capable of driving water into embolized tracheids upon needle water uptake, after winter embolism (Mayr et al. 2014). Therefore, it is likely that for this species wood parenchyma rays could also contribute to restore xylem functionality in summer when, after a drought spell, a rain event occurs and water in the soil becomes again available for the plant. In our experiment, the amount of embolized conduits was limited and probably low enough to allow for relatively rapid recovery of xylem function. It is then possible that when a larger fraction of xylem area is embolized, refilling in conifers does not occur (Brodribb et al. 2010, Umebayashi et al. 2016) or is only partial or requires longer time and/or higher NSC availability.

5.3. Part II B - Stem hydraulics and non-structural carbohydrate dynamics in potted European beech saplings under drought and subsequent re-irrigation

5.3.1. Long-term carry over effects of the first drought cycle

Previous droughts and/or freeze-thaw events can cause accumulation of xylem embolism at the end of winter (Améglio et al. 2002). Therefore, in spring, restoration of xylem water transport through removal of residual embolisms (Beikircher et al. 2016) or via formation of new functional conduits by cambial activity (Cochard et al. 2001) is fundamental to sustain growth processes and transpiration rates of newly formed leaves (Améglio et al. 2002). In the experiment here presented, stressed beech saplings were re-irrigated in both drought cycles at the same target midday leaf water potentials (Ψ_{md}). At the end of the first drought cycle, although percentage loss of xylem hydraulic

conductance (PLC) was not measured, it can be inferred that drought plants (D_{1cycle}) reached PLCs similar to those measured at the end of the second drought cycle (i.e. values of about 85%). PLC measured in well-watered plants before the start of the second drought cycle (i.e. in the "pre-drought" campaign, Figure 4.3-2) in one year old stems probably indicates that the production of new functional vessels during spring contributed to the recovery of stem hydraulic conductance. After winter embolism, increase in hydraulic conductivity of young terminal branches of mature European beech trees was observed in spring at the onset of cambial activity (Magnani and Borghetti 1995, Cochard et al. 2001).

Several effects of the first drought cycle were detected in the following growing season (summer 2015). Firstly, previously stressed plants (D_{1cycle}) had lower leaf midday water potentials than control (C_{1cycle}) plants, albeit they did not differ in pre-dawn leaf water potentials (Ψ_{pd}, both groups were well-watered) and maintained similar leaf transpiration rates (*E*, Table 4.3-1). This indicates that D_{1cycle} plants exhibited higher resistance (or, *vice versa*, lower conductance) to water flow. The increase in hydraulic resistance (or a decrease in conductance) was confirmed by the reduction in maximum specific hydraulic conductivity (k_s, Table 4.3-1). This might be the consequence of changes in wood anatomical characteristics, such as the production of narrower vessels: according to the Hagen-Poiseuille law, hydraulic conductivity is primarily related to the fourth power of the conduit diameter (Tyree and Zimmermann 2002).

More negative Ψ_{md} could have induced the substantial adjustment of leaf water potentials at turgor loss point (Ψ_{tlp}, Table 4.3-1). Moreover, leaves produced in spring 2015 in D_{1cycle} plants were fewer and had a higher leaf mass per area (LMA). Higher leaf mass investment per unit area is an indication of increased sclerophylly. In addition, there is indication that buds developing during a drought period can produce, in the following growing season when they expand, shorter twigs and fewer and smaller leaves (Coder 1999). This might have happened in the experiment in stressed European beech saplings because the first drought cycle started at the time when buds were formed (i.e. July-August, Eschrich et al. 1989). As leaf specific transpiration rates (*E*) did not significantly change, the reduction of total leaf area in D_{1cycle} plants coupled with a reduced k_s were likely the factors determining a reduction in the whole plant water consumption (measured as "evapotranspiration", ET). Overall, these adjustments determined lower aboveground biomass investment and underline the negative effects of extreme droughts

on productivity of European beech, as documented in the past after extreme drought spells (Ciais et al. 2005).

Contrary to the initial hypotheses, the first drought cycle didn't induce significant stem NSC depletion in the following growing season (Figure 4.3-3, "pre-drought" campaign). Nevertheless, NSC depletion might have occurred in other tree compartments (e.g. roots, Hartmann et al. 2013a) and/or carbohydrate reserves could have been preserved by reducing growth rates, as this would imply the use of lower amounts of carbohydrates for structural growth (Daudet et al. 2005, Deslauriers et al. 2014).

5.3.2. Stem hydraulics and NSCs dynamics under drought and subsequent re-irrigation

In the second cycle, drought strongly limited gas exchange rates already after two weeks of water limitation. The almost complete stop of CO_2 assimilation in stressed trees, albeit stomata were not completely closed (Figure 4.3-1c, d), might have been the result of high PPFD in combination with high temperatures and drought, which together are known to contribute to increase damages to the photosynthetic apparatus (Flexas et al. 1999, Ishida et al. 1999).

The levels of embolism measured at the end of the second drought cycle in stressed trees were close to or in some plants even overcame the thresholds for survival of angiosperms (88%, Ulri et al. 2013). The previously experienced drought did not determine any change in resistance to xylem embolism in the stems, at least when comparing the PLC measured in the "end-drought" campaign in CD (plants stressed only in the second cycle) and DD (plants stressed in both drought cycles) groups (Figure 4.3 - 2).

At the end of the second drought cycle, the increase in soluble sugars concentration observed in both wood and bark can indicate osmoregulation in order to maintain cell turgor at lower water potentials (Kozlovsky and Pallardy, 2002). Osmotic adjustment of turgor loss point was also found at the leaf level, still in the week after re-irrigation(Table 4.3-2). At the peak of drought, it is interesting to note that in the wood a decrease in starch content of about 30 mg g^{-1} was accompanied by an increase in soluble sugars of about 40 mg g^{-1}. On the other hand, in the bark, an increase in soluble sugars of ca. 25 mg g^{-1} was accompanied by only a 3 mg g^{-1} drop in starch content (average values calculated by pooling the two well irrigated groups, CC and DC, and the two drought stressed ones,

CD and DD). This surplus of soluble sugars, especially in the bark, could have been transported from other tree compartments (e.g. roots) and/or produced by bark tissue photosynthesis. In different species, included European beech (Berveiller et al. 2007, 2010), stem chloroplasts are known to be an important *in-situ* source of carbon: CO_2 re-fixation can help sustaining growth and plant metabolism especially when, during drought, photosynthesis is limited and/or phloem transport is compromised (Vandeghuchte et al. 2015).

At the peak of the second drought cycle, starch in the wood was completely depleted only in CD plants, while soluble sugar levels were maintained similar to those of DD plants (Figure 4.3-3). This might indicate that CD plants reached a threshold point: further demands of NSCs could not have been locally satisfied and soluble sugars were important as osmoprotectants to preserve cell integrity.

It is important to note that, in the wood, only total NSCs of plants which were not stressed the previous year (CC and CD), progressively decreased with time (of about 50%, corresponding to 40 mg g^{-1}, from end June to mid-August 2015, Figure 4.3-3a). Carbon can be utilized, in addition to several other purposes, for respiration and structural growth (Deslauriers et al. 2014). In the second drought cycle, plants were subjected to high temperatures, as an extreme warm spell occurred in the region in the period of the experiment (see environmental data in materials and methods). Given that increasing temperatures accelerate respiration rates, there is evidence that high temperatures could contribute to NSC depletion more than soil drought (Adams et al. 2009). Nevertheless, this does not explain why DD plants maintained high and constant total NSC levels in the wood over the whole second cycle. A possible explanation could be that the plants that were not previously stressed maintained higher growth rates than plants that suffered drought the previous year. As a consequence, at the end of the experiment, when all plants were re-irrigated, plants previously stressed (i.e. DC and DD groups) had higher starch and total NSC content (Figure 4.3-3a, c). Higher NSC contents can prolong tree survival under drought (O'Brien et al. 2014) and in general increase plant defences against several stressors. Unfortunately, due to the limited amount of plants and to the destructive methods utilized, only short term recovery after drought could be studied. A prolonged recovery time could have given indication if this higher amount of NSCs in the wood of DD plants could have been beneficial for long-term recovery from drought.

After one week of re-irrigation, drought stressed plants did not show any recovery of xylem function (Figure 4.3-2). The results of this study indicate that the availability of NSCs was not the limiting factor for xylem embolism repair under tension: utilizing the calculations proposed in Norway spruce (see above, Nardini et al. 2017b), only 8 mg g^{-1} of solutes (calculated as glucose) would have been theoretically necessary to completely refill the embolized xylem fraction. Moreover, after one week of re-irrigation, soluble sugars accumulated in the wood during drought were in great part re-converted to starch (Figure 4.3-3a). In previous work on other angiosperms, there was an indication that embolism triggers starch-to-soluble sugar conversion in the sapwood and that during rehydration the reconversion into starch is accompanied by a decrease in PLC (Yoshimura et al. 2016). In the present study, albeit the pattern in NSCs was the same observed by Yoshimura et al. (2016), refilling did not occur (Figure 4.3-4): this might indicate that in European beech NSC conversion during dehydration-rehydration in the sapwood is merely due to osmoregulation processes. The PLC levels reached at the end of drought were extremely high and at the limit of beech survival: it could be possible that, in these conditions, refilling does not occur. Nevertheless, a previous study on other angiosperm species that reached stem PLCs around 80% and with high stem NSC availability at the peak of drought, showed partial hydraulic recovery upon re-irrigation (Savi et al. 2016).

5.4. General discussion

5.4.1. Overview of hydraulic methods

The degree of xylem embolism, alternatively called percentage loss of hydraulic conductivity (PLC) of stems/branches is an important and common parameter used to investigate the effect of drought on xylem water transport in plants. PLC can be determined by measuring the sample's hydraulic conductivity using a balance or a flow meter, and allowing water to flow through a cut branch segment by connecting it to a water reservoir positioned above the sample (Sperry et al. 1988). The Xylem Embolism Meter used in this thesis for conductivity measurements of stems in European beech and Norway spruce saplings is based on this principle. In addition, vulnerability curves, which constitute part of the results reported in this work, can be measured using several methods. Progressively dehydrating long cut branches in the lab (bench drying technique)

or potted plants represents a valid possibility, but it is a time consuming method that requires several branches for the construction of one complete curve. A faster method (1-2 h for one curve), which has been used to measure branch xylem vulnerability in the adult trees belonging to the Kranzberg experiment, is the Cavitron technique. It uses the centrifugal force to generate progressively higher xylem tensions in the xylem, and the conductivity of the segment can be directly detected, as water is flowing through the sample during centrifugation (Cochard 2002). It is suggested that this technique would not be appropriate when applied in long-vesselled species such as oaks (*Quercus* spp.), because of the presence of cut open vessels in the samples used for measurements (Cochard et al. 2010). For this reason, it is important to check that the maximum vessel length of the branches does not exceed the length of the segment that fits in the rotor of the centrifuge. In the branch samples measured in the present work, maximum vessel length was shorter than the length of the sample to be centrifuged (27.5 cm): in Norway spruce, being a conifer, tracheids are very short (some mm) and in European beech maximum vessel length of branches was checked to be 20 cm.

A current unsolved debate in the plant hydraulics scientific community regards whether or not in certain species, especially in long-vesselled ones, xylem embolism occurs already under well hydrated conditions (e.g. at xylem water potentials above -1 MPa; Cochard et al. 2010; Hacke et al. 2015). This means that vulnerability curves for these species could also have a different shape than the "common" sigmoidal one (see the xylem vulnerability curves of the study species, Figure 4.1-2), implying that for these species embolism formation (and repair) occurs routinely, even on a daily basis. Another question recently raised regards possible artefacts caused by cutting branches under tension that would determine an overestimation of native PLC (Wheeler et al. 2013, Torres-Ruiz et al. 2015). The protocol for sample preparation is therefore very important to avoid this effect and tests have been performed to validate them (Trifilò et al. 2014, Venturas et al. 2015, Nardini et al. 2017a, Nolf et al. 2017). This method, based on cutting and trimming the samples several times under water has been used in the present work for PLC measurements in stems of the potted saplings (see paragraph 3.2.6). There is currently a growing interest in the use of *in vivo* imaging techniques such as magnetic resonance imaging or X-ray micro CT for PLC estimation. This is due to the fact that they constitute reliable alternatives to the more common hydraulic methods, which require the harvest of the sample for measurements. Moreover, although their scarce availability and

high costs of instrumentation represent a limitation for a routine use of them in all labs, *in vivo* imaging methods represent good standards to validate the hydraulic techniques cited before (Torres-Ruiz et al. 2015, Nardini et al. 2017a, Nolf et al. 2017). In this context, the Ph.D. work here presented, is part of a project called "Tree Ecophysiology and Engineering", acronym "Tree'n'ing", funded by the International Graduate School of Science and Engineering (IGSSE). In this project, a portable low-field Magnetic Resonance Imager was used to visualize the water content in stems of the saplings subjected to drought in the greenhouse experiment here presented. Given the limited resolution of the imager (0.5 mm), it was possible to clearly visualize embolized areas only in the stems of Norway spruce, because, being a gymnosperm, its xylem consists almost entirely of xylem conduits. This method allowed us to prove for spruce the reliability of the PLC measurements performed with the Xylem embolism meter by comparing them with the MRI pictures taken immediately before cutting the stem for hydraulic measurements (Meixner et al., in prep.).

5.4.2. Drought experiments in the field and in the greenhouse: a comparison

Plant ecophysiology studies are conducted either in natural field conditions or under more controlled conditions in greenhouses, growing chambers, experimental gardens. The second type is evidently more suitable for experimental setups in which plant species are undergoing different levels of a particular environmental factor, such as water availability. Moreover, specific mechanistic studies are evidently better managed in small plants growing e.g. in pots. A question that often and unavoidably rises from these studies is if the results obtained can be translated to plants growing in the field, especially in natural ecosystems, where complexity is higher and several other factors contribute to the plant reactions. For this reason, both field and greenhouse approaches were chosen for the present thesis.

In this work, hydraulic aspects of European beech and Norway spruce were investigated inducing drought in mature trees in a through-fall exclusion experiment as well as in potted saplings growing in a greenhouse. Long-term field studies in mature forest systems probably represent the most realistic type of experiment for the investigation of drought effects in trees, allowing for simulation of prolonged water limitation in almost intact natural conditions. In the study at the "Kranzberger Forst", the approach of through-fall

exclusion demonstrated to be valuable for the investigation of the effects of a long term drought. On the other hand, more severe short-term droughts can be more easily simulated in potted trees in the greenhouse, where the limited amount of substrate in the pots (and therefore the total amount of water available for the plant) allows for quicker plant dehydration. For this reason, small potted trees are the most common plant material utilized for drought experiments (e.g. Hartmann et al. 2013a, b, Aranda et al. 2015, Savi et al. 2016). Albeit obvious advantages exist, several factors like root confinement, increased soil temperature due to interception of solar radiation by the pots and high soil surface exposure to the air exacerbate the effects of drought (Poorter et al. 2012). Non-structural carbohydrate (NSC) manipulation experiments are also often limited to potted trees (e.g. Hartmann et al. 2013 b, O'Brien et al. 2014, Sevanto et al. 2014), because changes in NSC pools (and especially C depletion) can occur more easily in saplings than in mature trees. This is due to the fact that, with respect to mature trees, a larger part of the total NSC pool of seedlings relies on recently assimilated carbon (Niinemets 2010). Conversely, in mature trees, storage NSCs, located mainly in the stem sapwood and in living roots, constitute a big total carbon fraction that can be mobilized in order to support plant function, also during prolonged unfavorable conditions (Carbone et al. 2013).

Several differences in physiological traits related to drought susceptibility of a tree species may exist when considering it at different ontogenetic stages. An example can be extrapolated from the present work, where vulnerability to xylem embolism was measured in both juvenile and adult trees. In particular, vulnerability curves have been measured in branches of adult trees (Figure 4.1 – 2 a, b), whereas in potted saplings PLC has been measured during dehydration of soil in pots (Figure 5.4 – 1 c, d). While in Norway spruce vulnerability to xylem embolism was very similar between mature and juvenile trees, in European beech stems of saplings were clearly more vulnerable than branches of adult trees. This finding in beech can also be confirmed by comparing the xylem vulnerability curves of saplings in Barigah et al. (2013) and of branches of mature trees in Urli et al. (2013). In addition to this, it must be highlighted that the study of xylem vulnerability to embolism is clearly more complex in adult trees than in saplings. Within the whole tree hydraulic pathway, adult trees are composed by several portions, from fine roots to leaves, including the main stem and several branch orders. These portions contribute to the whole resistance to water transport of a tree and have been demonstrated to differ in their vulnerability to hydraulic dysfunction in several studies. In

mature trees, distal organs like leaves and branches are the most commonly used plant material for vulnerability analyses. It has been confirmed in several studies, included the present one, that leaves are more vulnerable than branches, supporting the hydraulic vulnerability segmentation hypothesis (Tyree and Ewers 1991, Bucci et al. 2013, Pivovaroff et al. 2014). Nevertheless, due to clear difficulties of measuring the hydraulics of tree trunks, little is known about the vulnerability of all the segments of the hydraulic pathway (roots, main trunk, branches and leaves). The main trunk of some coniferous and angiosperm species was found to be less resistant to embolism than terminal branches (Johnson et al. 2016). This would imply that in mature trees the overall vulnerability to xylem embolism could be higher than that estimated by the sole analysis of branches.

5.4.3. Responses of European beech and Norway spruce to drought

European beech and Norway spruce are supposed to exhibit different stomatal control of transpiration-induced xylem tension under drought, i.e. an anisohydric vs. a more isohydric strategy, respectively. These different strategies have been proven in the mature trees of the through-fall exclusion experiment described in part I, analyzing the stomatal conductance response to variations in pre-dawn water potentials and vapor pressure deficit (Goisser et al., in preparation). It is generally expected that, under drought, more isohydric species would avoid quick drops in water potentials and consequent xylem embolism for a longer period than more anisohydric species (McDowell et al. 2008). Nevertheless, according to a global meta-analysis, the majority of woody plant species across forest biomes, independently if isohydric or anisohydric, tend to experience in the field comparable embolism levels and under drought operate relatively close to the thresholds of hydraulic dysfunction (Choat et al. 2012). In addition to that and against intuitive expectations, in an ecosystem-scale experiment the more anisohydric *Juniperus monosperma* showed very little embolism in comparison to the co-occurring isohydric *Pinus edulis*, i.e. in *P. edulis* stomatal closure occurred at less negative xylem water potentials, but the species was more vulnerable to embolism than *J. monosperma* (Garcia-Forner et al. 2016). This study demonstrates that stomatal response to drought alone does not give an indication of the predisposition of a species to hydraulic failure and that it must be related to the species' embolism resistance. Hydraulic properties such as vulnerability to xylem embolism represent one relatively "static" aspect of the drought susceptibility of a species. Acclimation in hydraulic vulnerability helps to preserve

hydraulic integrity (and therefore to avoid or postpone hydraulic impairment during drought), and in the present study has been demonstrated to occur in both beech and spruce in a relatively short period of experimental drought. Compared to *P. edulis* and *J. monosperma,* which largely differed in their vulnerability to embolism (Garcia-Forner et al. 2016), the co-occurring mature European beech and Norway spruce trees at Kranzberg forest differed only by about 0.3 MPa in the water potential at 50% loss of branch xylem hydraulic conductivity (see Table 4.1 - 2). Therefore, Norway spruce is also more effective to preserve xylem integrity than the respective more anisohydric European beech. Similar conclusions for beech and spruce can be drawn from the data collected in the greenhouse experiment in saplings. Plotting leaf gas exchange parameters and native PLC in dependence of midday water potentials (Ψ_{md}), stomatal closure in Norway spruce saplings occurred already at Ψ_{md} of about -1.7 MPa and stem embolism occurred at Ψ_{md} below -3.0 MPa. On the other hand, European beech stems reached 50% PLC already at Ψ_{md} below -2.0 MPa (even in control plants), when stomatal conductance was still above 25 mmol m^{-2} s^{-1}.

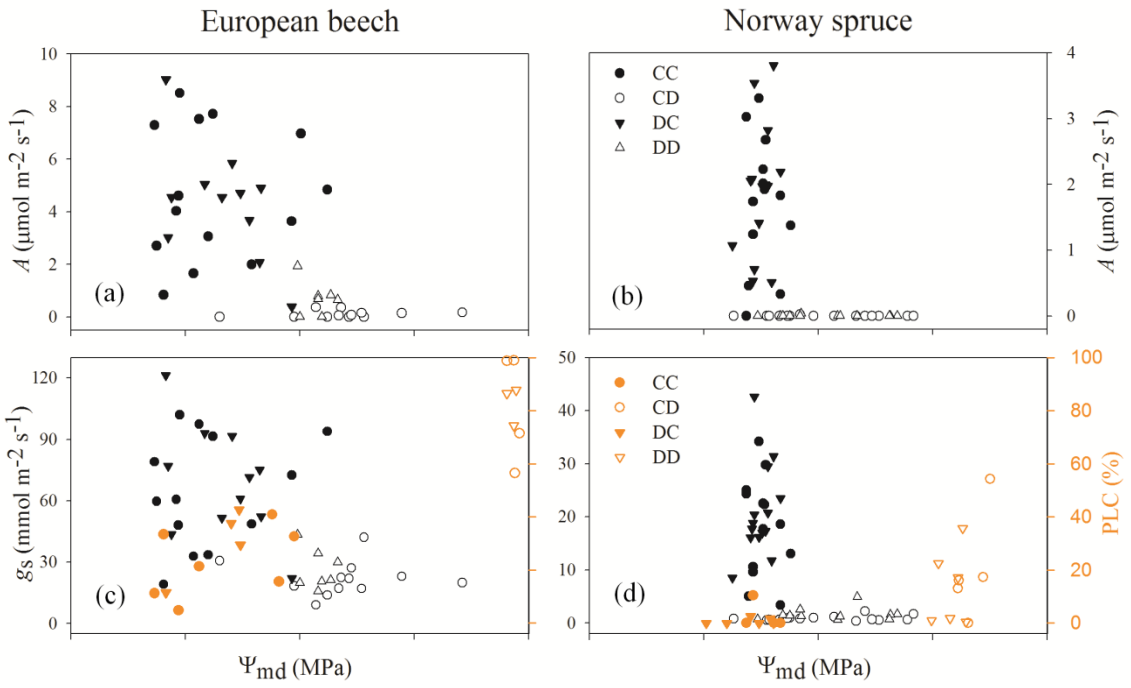

Figure 5.4 - 1 Leaf gas exchanges and PLC plotted against midday leaf water potentials (Ψ_{md}) in European beech and Norway spruce (greenhouse experiment). CO_2 assimilation rate (*A*, panels a, b), stomatal conductance (g_s) and PLC (panels c, d) plotted against Ψ_{md}. Data have been taken from the campaigns performed in second drought cycle (summer 2015); for PLC, data from the "re-irrigation" campaign are not included. For gas exchange parameters, please note the different scales between the species. In c and d, axes on the right indicate PLC (values and scale are in orange).

The xylem water potential at 50% loss of hydraulic conductance/conductivity is commonly used to compare xylem vulnerabilities between tree species or treatments (see part I). Nevertheless, when subjected to drought, angiosperms are generally able to survive at higher stem PLCs (88%, Urli et al. 2013) compared to conifers (50%, Brodribb and Cochard 2009, Brodribb et al. 2010). Despite the fact that these thresholds need to be tested for a bigger number of species, for angiosperms the xylem water potential at 88% PLC (Ψ_{88_branch}) has been recently suggested to be a more meaningful reference for the calculation of hydraulic safety margins than the xylem water potential at 50% PLC (Ψ_{50_branch}, Choat 2013). If different reference water potentials for the two groups had been used in the global meta-analysis of safety margins (Choat et al. 2012), the differences in hydraulic safety margins (calculated as the difference between the minimum water potential experienced in the field and the Ψ_{50_branch} or Ψ_{88_branch} in conifers and angiosperms, respectively) between angiosperms and gymnosperms would have been smaller (Choat 2013). In the same way, if this concept is applied to the data presented in this thesis, the difference between European beech and Norway spruce hydraulic safety margins would be small too.

Within the species-specific water use strategies, not only stomatal responses to dehydration and xylem vulnerability, but also rooting depth, which determines the exploitation of deeper water sources, plays an important role to predict the drought-induced decline of a tree species (Nardini et al. 2016). In pot experiments, the root system of seedlings is limited to the pot volume and therefore the real root architecture and rooting depth of a species is obviously not appropriately represented. This factor makes a direct comparison of beech and spruce water use strategies in the greenhouse experiment here presented more difficult. In a mature forest, during droughts and heat spells, European beech is likely to profit from its deeper rooting system with respect to Norway spruce. As already discussed in paragraph 5.1.1., the different rooting depth of the two species could explain why in the through-fall exclusion experiment predawn water potentials in drought (TE) plots were overall more negative in spruce than in beech. This could buffer to a certain degree the more “water spending” strategy of beech, in comparison to spruce, and allow for maintaining higher sap flow and growth rates under drought for longer time, as already observed at the Kranzberg site (Kallenbach, unpublished).

Preservation of xylem integrity represents only one aspect determining the overall resistance to drought in woody species. In addition to hydraulic failure, drought-induced tree mortality can be caused by carbon starvation, phloem transport failure and biotic attacks, as well as by the combination of two or more of them (McDowell et al. 2011).

Drought and carbon relations

In the increasing number of studies on carbon dynamics during drought, a large variability in behavior and responses seems to emerge between species (Mencuccini 2014). Mitchell et al. (2014) distinguished three different phases of tree carbon balance during drought progression: in the first phase, carbon uptake and growth, albeit decreasing, are still positive (no change in NSC content); in the second phase, growth ceases but photosynthesis continues (at lower rates) and therefore NSCs content increases; in the third phase, also carbon assimilation stops and NSCs are depleted. Within this scheme, carbon depletion could be also brought about by daily cycles of cavitation-refilling, as refilling of embolized conduits is an energy-requiring process. According to this scheme, short-term severe droughts are supposed to cause no change or even an increase in NSCs, because carbon investment for structural growth is reduced faster than CO_2 assimilation rates via stomatal closure, implying a transient accumulation of NSCs. Carbohydrate accumulation has been also observed in tree saplings at time of death after a drought treatment: this has been associated to the fact that NSCs could not have been utilized and mobilized due to extreme dehydration (Hartmann et al. 2013b). Even in the greenhouse experiment, the 40-45 days long drought treatment applied in the second cycle (summer 2015) did not induce changes in total NSC content in both wood and bark fractions of stems of Norway spruce (Figure 4.2 - 5), whereas in European beech total NSCs content increased in the bark, and progressively decreased or was kept constant in the wood fraction of CD and DD plants, respectively. In the mature trees of the Kranzberg experiment, even the multiple-year drought induced by through-fall exclusion did not affect NSC content in the study species (Goisser et al., unpublished). On the other hand, in the trunk of mature European beech trees, the radial decrease in NSC (and especially starch) content was stronger in declining than in healthy trees, suggesting mobilization of long term storage carbohydrates (Gérard and Bréda 2014). Nevertheless, although the amount of NSC reserves in mature trees can be high enough to sustain negative carbon balances for long periods (Hoch et al. 2003), their unavailability

to the sinks where they are needed could determine indirect carbon starvation (Sala et al. 2010). Therefore, it is perhaps more likely that in several mature tree species subjected to chronic drought, the strong decrease in phloem transport velocity or, in general, phloem failure, may constitute one major cause of tree mortality. This process would also in theory preclude the capability of active refilling after drought relief (recovery), if phloem is involved in the process (Nardini et al. 2011, Sevanto 2014). Further studies going in this direction are urgently needed.

Drought and biotic attacks

Bark beetles and associated fungi represent one of the greatest threats to conifers survival. In comparison to European beech, Norway spruce is more severely threatened by biotic agents and in particular is endangered by the spruce bark beetle *Ips typographus* (L.) and associated fingi. Its susceptibility to this insect increases especially when tree vitality is affected by drought or frost, and beetle attacks are further favored by exceptional warm summers (Schlyter et al. 2006). The soil drought applied in the through-fall exclusion experiment gave a clear example of the susceptibility of drought-weakened spruce trees to biotic agents: whereas CO trees were not infested, through-fall exclusion (TE) spruce trees belonging to two out of a total of six TE plots were severely attacked by bark beetles already in the second summer (2015) of the drought experiment. A successful defense of a tree against pathogens is thought to largely depend on production of secondary metabolites. A recent study on *Pinus contorta* revealed that higher susceptibility to a mountain pine beetle was related to the local (i.e. where the insect/pathogen attack occurred) reduction in NSC availability (Wiley et al. 2016).

5.4.4. Factors influencing the occurrence and detection of xylem hydraulic recovery

It is widely accepted that, at comparable levels of native embolism (i.e. PLC), angiosperms are potentially more prone to active refilling than gymnosperms, given that the former have higher wood parenchyma fraction and wood NSC content than the latter (Johnson et al. 2012, Brodersen and McElrone 2013, Morris et al. 2016, Secchi et al. 2017). This is probably the reason why the "hydraulic point of no return" in angiosperms is generally found at higher PLCs than in gymnosperms (Johnson et al. 2012). In the greenhouse experiment presented here, the target PLC for re-irrigation of drought stressed European beech and Norway spruce saplings was therefore chosen in dependence of the

different PLC thresholds for mortality in angiosperms and gymnosperms, respectively. Whereas spruce trees reached at the peak of drought an average PLC of about 20%, which is still far from the theoretical lethal value for conifers (50%, Brodribb and Cochard 2009, Brodribb et al. 2010), beech trees approached the hydraulic failure threshold for angiosperms (around 88%, Ulri et al. 2013). This makes a direct comparison of the hydraulic recovery capability of the two species rather difficult. In this work, a fast hydraulic recovery under tension has been observed in the conifer Norway spruce. Conversely, the angiosperm European beech did not recover xylem hydraulics after reaching PLCs close to the threshold for hydraulic failure, albeit still being able to survive, as exemplified after the first drought cycle.

Several aspects should be considered when determining the occurrence of hydraulic repair in a tree species. First of all, independently of being angiosperms or gymnosperms, the refilling capacity might be species-specific. Some species might simply not have evolved this strategy, as hypothesized here for European beech, which, when able to preserve a minimum water transport, might simply restore xylem functionality through re-growth in the following spring. In *Sequoia sempervirens*, inhabiting high rainfall/fog regions, saplings showed no refilling when water was only supplied in the soil (Choat et al. 2015), whereas xylem was partially refilled when branches were soaked in water, in order to simulate rain/fog events (Earles et al. 2016).

A second point to be taken into account when considering the xylem recovery capacity, is the fraction of embolized stem xylem (or PLC) reached at the peak of drought and to be refilled. Umebayashi et al. (2016) showed with MRI that in stems of *Pinus thunbergii* saplings, reaching PLC largely above 50%, no embolism repair occurred after re-irrigation. However, repair in conifers subjected to drought should be tested when PLC is still below 50% PLC. Likewise, PLC reached by European beech saplings in the present experiment was at the edge of theoretical hydraulic failure. Therefore, further studies on refilling of this species should in addition be performed in less severely stressed trees.

Another aspect to be considered is the technique used for detection of refilling under tension. *In vivo* imaging techniques (e.g. magnetic resonance imaging, X-ray micro CT) are considered the "gold standard" to validate destructive hydraulic methods (see above, Nardini et al. 2017a, Nolf et al. 2017). Nevertheless, when studying processes involving

cellular activities like active xylem refilling, it should be ensured that any damage of the living tissue has been induced during measurements. For example, the X-ray dose received by plants during X-ray micro CT scanning, recently used to test for the refilling capability of some species (e.g. Choat et al. 2015), might affect the physiology of phloem and parenchyma cells, the integrity of which is essential for the occurrence of refilling (Savi et al. 2017). Magnetic resonance imaging could represent perhaps a valuable *in vivo* alternative to investigate embolism repair (Zwieniecki et al. 2013), if cellular damage by overheating of the analyzed stem portion is avoided.

6. Conclusions and outlook

In this work, the effects of long-lasting (chronic) droughts were investigated in mature European beech and Norway spruce trees in a through-fall exclusion experiment. In addition, short-term repeated severe droughts, followed by re-irrigation, were analyzed in potted juvenile trees in a greenhouse drought-recovery experiment.

In the through-fall exclusion experiment performed in a mature forest system, the co-occurring European beech and Norway spruce showed under drought analogous hydraulic adjustments, well-coordinated between branch and leaf/end-twig levels. This is particularly interesting as the two study species obviously contrast in xylem anatomy, foliage type, crown architecture, and ecophysiology (including hydraulic strategies). In Norway spruce, growth limitation might also indicate a possible trade-off between increased hydraulic safety and decreased productivity. These results thus suggest that the two forest species studied might exhibit sufficient hydraulic plasticity to better cope with future drought periods. As hydraulic acclimation was observed upon prolonged drought, these results also highlight the importance of long-term field drought experiments. More intense or longer droughts, however, may exceed the species' capacity for hydraulic acclimation (Gutschick and BassiriRad 2003), and mild but extremely prolonged droughts may induce in the long term consumption of carbohydrate reserves to critical levels (McDowell et al. 2008). Moreover, trees weakened by hydraulic limitation and/or carbon-starvation are usually also more susceptible to biotic attacks (Schlyter et al. 2006). All these variables might affect tree species differently and modify competition between co-occurring species. In the case of the study species, it is likely that the shallower rooting system and other secondary effects of drought such as bark beetle attacks would put at higher risk Norway spruce than European beech.

The greenhouse study gave new insight on the capability of saplings of a conifer species, Norway spruce, to recover stem xylem hydraulic function after relief of soil drought. In conifers, there is little evidence for xylem hydraulic recovery after drought, and therefore this study introduces new perspectives for future studies. Moreover, hydraulic recovery was associated with NSC depletion, which was specifically localized in the stem sapwood fraction. Therefore, the possible causes of NSC depletion in the stem wood in the phase of recovery from drought were discussed: the here proposed hypotheses of utilization of NSC for the recovery of xylem hydraulics should be tested in further studies, especially

on other coniferous species and in field experiments. Given that aquaporins in VACs have been shown to promote refilling in conifer needles (Laur and Hacke 2014), research on aquaporin expression in the parenchyma of conifers' secondary xylem could be important. On the other hand, the results of the drought-irrigation study in the angiosperm European beech demonstrate that, under severe droughts, strongly embolized stems of this species cannot be repaired. However, in the case that living tissues are not compromised and a minimum water transport for survival is preserved at the end of the drought spell, surviving plants may partially restore xylem functionality in the following spring through cambial growth. It is possible that European beech might simply not have evolved the capability to actively refill embolized vessels. This hypothesis should be verified in future studies under less extreme drought conditions, i.e. inducing lower levels of stem xylem embolism. For both species, separation of stem wood and bark fractions for NSC analysis has been important for the study, as different patterns were identified under drought and/or re-irrigation between the two parts. This should be taken into consideration in future studies. The occurrence and kinetics of refilling after re-irrigation at different PLCs should be studied, especially with the support of appropriate non-invasive imaging techniques

Fast hydraulic acclimation capability and/or high resilience to fluctuations in water availability may be the key-factors determining the success of tree species in several forest ecosystems affected by climate change. Applying multiple cycles of drought-recovery in species showing refilling capability (e.g. in Norway spruce), could reveal whether progressive depletion of NSCs in the wood occurs and if it is connected to the refilling capability and kinetics of the species. In that case, the time needed to recover NSCs to control values after re-irrigation might be crucial. In the light of the predicted climate change scenarios, possible consequences of NSC consumption due to drought-recovery cycles on productivity, survival and general drought susceptibility should be taken into account. Further field hydraulic studies in natural or managed eco-systems are urgently needed to estimate the performance of tree species under future climate.

References

Adams HD et al. (2009) Temperature sensitivity of drought-induced tree mortality portends increased regional die-off under global-change-type drought. *Proceedings of the National Academy of Sciences of the USA* 106, 7063–7066.

Allen CD et al. (2010) A global overview of drought and heat-induced tree mortality reveals emerging climate change risks for forests. *For Ecol Man* 259, 660-684.

Ambrose AR, Sillett SC, Dawson TE (2009) Effects of tree height on branch hydraulics, leaf structure and gas exchange in California redwoods. *Plant Cell Environ* 32, 743-757.

Ameglio T, Bodet C, Lacointe A, Cochard H (2002). Winter embolism, mechanisms of xylem hydraulic conductivity recovery and springtime growth patterns in walnut and peach trees. *Tree physiol* 22, 1211-1220.

Anderegg WRL (2015) Spatial and temporal variation in plant hydraulic traits and their relevance for climate change impacts on vegetation. *New Phytol* 205, 1008-1014.

Anderegg WRL, Anderegg LDL (2013) Hydraulic and carbohydrate changes in experimental drought-induced mortality of saplings in two conifer species. *Tree Physiol* 33, 252-260.

Angay O et al. (2014) Sweets for the foe – effects of nonstructural carbohydrates on the susceptibility of *Quercus robur* against *Phytophthora quercina*. *New Phytol* 203, 1282-1290.

Aranda I. *et al.* (2015) Variation in photosynthetic performance and hydraulic architecture across European beech (*Fagus sylvatica* L.) populations supports the case for local adaptation to water stress. *Tree Physiol* 35, 34-46.

Barigah T.S. *et al.* (2013) Water stress-induced xylem hydraulic failure is a causal factor of tree mortality in beech and poplar. *Annals of Bot* 112, 1431-1437.

Bartlett M.K., Scoffoni C., Sack L. (2012) The determinant of leaf turgor loss point and prediction of drought tolerance of species and biomes: a global meta-analysis. *Ecol Lett* 15, 393-405.

Beikircher B, Ameglio T, Cochard H, Mayr S (2010) Limitation of the cavitron technique by conifer pit aspiration. *J Exp Bot* 61, 3385-3393.

Beikircher B, De Cesare C, Mayr S (2013) Hydraulics of high-yield orchard trees: a case study of three *Malus domestica* cultivars. *Tree Physiol* 33, 1296-1307

Beikircher B, Mayr S (2009) Intraspecific differences in drought tolerance and acclimation in hydraulics of *Ligustrum vulgare* and *Viburnum lantana*. *Tree Physiol* 29, 765-775.

Beikircher B, Mayr S (2016) Avoidance of harvesting and sampling artefacts in hydraulic analyses: a protocol tested on *Malus domestica*. *Tree Physiol* 36, 797-803.

Beikircher B, Mittmann C, Mayr S (2016). Prolonged soil frost affects hydraulics and phenology of apple trees. *Front Plant Sci* 7, 867; https:doi.org/10.3389/fpls.2016.00867.

Berveiller D, Fresneau C, Damesin C (2010) Effect of soil nitrogen supply on carbon assimilation by tree stems. *Ann For Sci* 67, 609; https:doi.org/10.1051/forest/2010022.

Berveiller D, Kierzkowski D, Damesin C (2007) Interspecific variability of stem photosynthesis among tree species. *Tree Physiol* 27, 53-61.

Blackman CJ, Brodribb TJ, Jordan GJ (2010) Leaf hydraulic vulnerability is related to conduit dimensions and drought resistance across a diverse range of woody angiosperms. *New Phytol* 188, 1113-1123.

Borghetti M, Cinnirella S, Magnani F, Saracino A (1998) Impact of long-term drought on xylem embolism and growth in *Pinus halepensis* Mill. *Trees* 12, 187-195.

Borghetti M, Edwards WRN, Grace J, Jarvis PG, Raschi A (1991) The refilling of embolized xylem in *Pinus sylvestris* L. *Plant Cell Environ* 14, 357-369.

Bouche PS et al. (2016) Are needles of *Pinus pinaster* more vulnerable to xylem embolism than branches? New insights from X-ray computed tomography. *Plant Cell Environ* 39, 860–870.

Bouche PS, Larter M, Domec JC, Burlett R, Gasson P, Jansen S, Delzon S (2014) A broad survey of hydraulic and mechanical safety in the xylem of conifers. *J Exp Bot* 65, 4419-4431.

Bréda N, Huc R, Granier A, Dreyer E (2006) Temperate forest trees and stands under severe drought: a review of ecophysiological responses, adaptation processes and long-term consequences. *Ann For Sci* 63, 625-644.

Briffa KR, van der Schrier G, Jones PD (2009) Wet and dry summers in Europe since 1750: evidence of increasing drought. *Int J Climatology* 29, 1894–1905.

Brodersen CR, McElrone AJ (2013) Maintenance of xylem network transport capacity: a review of embolism repair in vascular plants. *Front Plant Sci* 4, 108; https:doi.org/10.3389/fpls.2013.00108.

Brodersen CR, McElrone AJ, Choat B, Matthews MA, Shackel KA (2010) The dynamics of embolism repair in xylem: in vivo visualizations using high-resolution computed tomography. *Plant Physiol* 154, 1088-1095.

Brodribb TJ, Cochard H (2009) Hydraulic failure defines the recovery and point of death in water-stressed conifers. *Plant Physiol* 149, 575-584.

Brodribb TJ, Holbrook NM (2003) Stomatal closure during leaf dehydration, correlation with other leaf physiological traits. *Plant Physiol* 132, 2166-2173.

Brodribb TJ, Holbrook NM, Zwieniecki MA, Palma B (2005) Leaf hydraulic capacity in ferns, conifers and angiosperms: impacts on photosynthetic maxima. *New Phytol* 165, 839-846.

Brodribb TJ, Bowman DJMS, Nichols S, Delzon S, Burlett R (2010) Xylem function and growth rate interact to determine recovery rates after exposure to extreme water deficit. *New Phytol* 188, 533-542.

Bucci SJ, Scholz FG, Goldstein G, Meinzer FC, Sternberg LDASL (2003) Dynamic changes in hydraulic conductivity in petioles of two savanna tree species: factors and mechanisms contributing to the refilling of embolized vessels. *Plant Cell Environ* 26, 1633-1645.

Bucci SJ et al. (2013) The stem xylem of Patagonian shrubs operates far from the point of catastrophic dysfunction and is additionally protected from drought-induced embolism by leaves and roots. *Plant Cell Environ* 36, 2163-2174.

Carbone MS et al. (2013) Age, allocation and availability of nonstructural carbon in mature red maple trees. *New Phytol* 200, 1145-1155.

Carlquist S (2001) Comparative wood anatomy – Systematic, ecological, and evolutionary aspects of Dycotiledon wood, 2nd Ed. Springer Verlag, Berlin.

Charra-Vaskou K et al. (2012) Hydraulic efficiency and safety of vascular and non-vascular components in *Pinus pinaster* leaves. *Tree Physiol* 32, 1161-1170.

Charra-Vaskou K, Mayr S (2011) The hydraulic conductivity of the xylem in conifer needles (*Picea abies* and *Pinus Mugo*). *J Exp Bot* 62, 4383-4390.

Charrier G et al. (2016) Evidence for hydraulic vulnerability segmentation and lack of xylem refilling under tension. *Plant Physiol* 172, 1657-1668.

Chmura DJ, Guzicka M, McCulloh KA, Zytkowiak R (2016) Limited variation found among Norway spruce half-sib families in physiological response to drought and resistance to embolism. *Tree Physiol* 36: 252-266.

Choat B (2013) Predicting thresholds of drought-induced tree mortality in woody plant species. *Tree Physiol* 33, 669-671.

Choat B et al. (2012) Global convengence in the vulnerability of forests to drought. *Nature* 491, 752-756.

Choat B, Brodersen CS, McElrone AJ (2015) Synchrotron X-ray microtomography of xylem embolism in *Sequoia sempervirens* saplings during cycles of drought and recovery. *New Phytol* 205, 1095-1105.

Ciais P et al. (2005) Europe-wide reduction in primary productivity caused by the heat and drought in 2003. *Nature* 437, 529-533.

Clemens J, Jones PG (1978) Modification of drought resistance by water stress conditioning in *Acacia* and *Eucaliptus*. *J Exp Bot* 29, 895-904.

Cochard H (1992) Vulnerability of several conifers to air embolism. *Tree Physiol* 11, 73-83.

Cochard H (2002) A technique for measuring xylem hydraulic conductance under high negative pressures. *Plant Cell Environ* 25, 815–819.

Cochard H, Froux F, Mayr S, Coutand C (2004) Xylem wall collapse in water-stressed pine needles. *Plant Physiol* 134, 401-408.

Cochard H et al. (2010) Does sample length influence the shape of xylem embolism vulnerability curves? A test with the Cavitron spinning technique. *Plant Cell Environ* 33, 1543-1552.

Cochard H, Lemoine D, Ameglio T, Granier A (2001) Mechanisms of xylem recovery from winter embolism in *Fagus sylvatica*. *Tree Physiol* 21, 27-33.

Cochard H et al. (2005) Evaluation of a new centrifuge technique for rapid generation of xylem vulnerability curves. *Physiol Plant* 124, 410-418.

Coder KD (1999) Drought damage in trees. http://www.dnr.state.mn.us/fd/oct03/droughtstress.html.

Cornwell WK, Bhaskar R, Sack L, Cordell S, Lunch CK (2007) Adjustment of structure and function of Hawaiian *Metrosideros polymorpha* at high vs. low precipitation. *Funct Ecol* 21, 1063-1071.

Dai A (2013) Increasing drought under global warming in observations and models. Nature Climate Change 3, 52-58.

Dale VH, Joyce LA, McNulty S, Neilson RP (2000) The interplay between climate change, forest and disturbances. *The Science of the Total Environment* 262, 201-204.

Daudet FA et al. (2005) Experimental analysis of the role of water and carbon in tree stem diameter variations. *J Exp Bot* 56, 135-144.

Debat V, David P (2001) Mapping phenotypes: canalization, plasticity and developmental stability. Trends Ecol Evol 16, 555-561.

Deslauriers A, Beaulieu M, Balducci L, Giovannelli A, Gagnon MJ, Rossi S (2014) Impact of warming and drought on carbon balance related to wood formation in black spruce. *Annals Bot* 114, 335-345.

Desprez-Loustau ML, Marçais B, Nageleisen LM, Piou D, Vanini A (2006) Interactive effects of drought and pathogens in forest trees. *Ann. For. Sci*. 63, 595-610.

Earles JM *et al*. (2016) Bark water uptake promotes localized hydraulic recovery in coastal redwood crown. *Plant Cell Environ* 39, 320-328.

Ellenberg H (1996) Vegetation Mitteleuropas mit den Alpen, 5th edn. Ulmer, Stuttgart, Germany, p 1095.

Eschrich W, Burchardt R, Essiamach S (1989) The induction of sun and shade leaves of the European beech (*Fagus sylvatica* L.): anatomical studies. *Trees* 3, 1-10.

Flexas J, Badger M, Chow WS, Medrano H, Osmond CB (1999) Analysis of the relative increase in photosynthetic O_2 uptake when photosynthesis in grapevine leaves is inhibited following low night temperatures and/or water stress. *Plant Physiol 121*, 675-684.

Fuhrer J et al. (2006) Climate risks and their impact on agriculture and forests in Switzerland. Climatic Change 79, 79-102.

Galvez DA, Landhäusser SM, Tyree MT (2013) Low root reserve accumulation during drought may lead to winter mortality in poplar seedlings. *New Phytol 198*, 139-148.

Gan JB (2004) Risk and damage of southern pine beetle outbreaks under global climate change. *For Ecol Man* 191, 61-71.

Garcia-Forner N et al. (2016) Responses of two semiarid conifer tree species to reduced precipitation and warming reveal new perspectives for stomatal regulation. *Plant Cell Environ* 39, 38–49.

Giagli K, Gricar J, Vavrcik H, Mensik L, Gryc V (2016) The effects of drought on wood formation in *Fagus sylvatica* during two contrasting years. *IAWA Journal* 37, 332-348

Gitlin AR et al. (2006) Mortality gradients within and among dominant plant populations as barometers of ecosystem change during extreme drought. *Conservation Biology* 20, 1477-1486.

Goisser M et al. (2016) Does belowground interaction with *Fagus sylvatica* increase drought susceptibility of photosynthesis and stem growth in *Picea abies*? *For Ecol Man* 375, 268-278.

Goisser M, Kallenbach C, Haeberle K-H, Matyssek R, Grams TEE (in prep.) European beech and Norway spruce, an unequal couple. Anisohydric versus isohydric control of transpiration at the single leaf and the whole canopy level.

Goldstein G, Bucci SJ, Scholz FG (2013) Why do trees adjust water relations and hydraulic architecture in response to nutrient availability? *Tree Physiol* 33, 238-240.

Guérard N et al. (2007) Do trees use reserve or newly assimilated carbon for their defence reactions? A ^{13}C labelling approach with young Scots pines inoculated with bark-beetle-associated fungus (*Ophiostoma brunneo ciliatum*). *Ann For Sci* 64, 601-608.

Gutschick VP, BassiriRad H (2003) Extreme events as shaping physiology, ecology and evolution of plants: toward a unified definition and evaluation of their consequences. *New Phytol* 160, 21-42.

Hacke UG, Jansen S (2009) Embolism resistance of three boreal conifer species varies with pit structure. *New Phytol* 182, 675-686.

Hacke UG, Sperry JS, Pockmann WT, Davis SD, McCulloh KA (2001a) Trends in wood density and structure are linked to prevention of xylem implosion by negative pressure. *Oecologia* 126, 457-461.

Hacke UG, Stiller V, Sperry JS, Pittermann J, McCulloh KA (2001b) Cavitation fatigue: Embolism and refilling cycles can weaken the cavitation resistance of xylem. *Plant Physiol* 125, 779-786.

Hacke UG et al. (2015) The standard centrifuge method accurately measures vulnerability curves of long-vesselled olive stems. *New Phytol* 205, 116-127.

Hajek P, Kurjak D, von Wuehlisch G, Delzon S, Schuldt B (2016) Intraspecific variation in wood anatomical, hydraulic, and foliar traits in ten European beech provenances differing in growth yield. *Front Plant Sci* 7, 791.

Hartmann H, Ziegler W, Trumbore S (2013a) Lethal drought leads to reduction in non-structural carbohydrates in Norway spruce tree roots but not in the canopy. *Funct Ecol* 27, 413-427.

Hartmann H, Ziegler W, Kolle O, Trumbore S. (2013b) Thirst beats hunger – declining hydration during drought prevents carbon starvation in Norway spruce saplings. *New Phytol* 200, 340-349.

Heinen RB, Ye Q, Chaumont FO (2009) Role of aquaporins in leaf physiology. *J Exp Bot* 60, 2971–2985.

Hera U et al. (2011) Klima en dètail-Neue hochaufgelöste Klimakarten zur klimatischen Regionalisierung Bayerns. *LWF aktuell* 19 (86), 34-37.

Herbette S et al. (2010) Insights into xylem vulnerability to cavitation in *Fagus sylvatica* L.: phenotypic plasticity and environmental sources of variability. *Tree Physiol* 30, 1448-1455.

Hlásny T et al. (2011) Climate change impacts on growth and carbon balance of forests in Central Europe. *Clim Res* 47, 219-236.

Hoch G, Richter A, Körner C (2013) Non-structural carbon compounds in temperate forest trees. *Plant Cell Environ* 26, 1067-1081.

Hölttä T, Mencuccini M, Nikinmaa E (2009). Linking phloem function to structure: analysis with a coupled xylem-phloem transport model. *J Theor Biol* 259, 325-337.

IPCC (2014) Climate change 2014: synthesis report. Contribution of working groups I, II and III to the fifth assessment report of the intergovernmental panel on climate change (core writing team, R.K. Pachauri and L.A. Meyer (eds.)). IPCC, Geneva, Switzerland, 151 pp.

Ishida A, Toma T, Marjenah M (1999) Limitation of leaf carbon gain by stomatal and photochemical processes in the top canopy of *Macaranga conifera*, a tropical pioneer tree. *Tree Physiol* 19, 467-473.

Jacobsen AL, Pratt RB, Davis SD, Ewers FW (2007) Cavitation resistance and seasonal hydraulics differ among three arid Californian plant communities. *Plant Cell Environ* 30, 1599-1609.

Jansen S et al. (2012) Plasmodesmatal pores in the torus of bordered pit membranes affect cavitation resistance of conifer xylem. *Plant Cell Environ* 35, 1109-1120.

Johnson DM, McCulloh KA, Meinzer FC, Woodruff DR, Eissenstat DM (2011) Hydraulic patterns and safety margins, from stem to stomata, in three eastern US tree species. *Tree Physiol* 31, 659-668.

Johnson DM, McCulloh KA, Woodruff DR, Meinzer FC (2012a) Hydraulic safety margins and embolism reversal in stems and leaves: why are conifers and angiosperms so different? *Plant Sci* 195, 48-53.

Johnson DM, McCulloh KA, Woodruff DR, Meinzer FC (2012b) Evidence for xylem embolism as primary factor in dehydration-induced declines in leaf hydraulic conductance. *Plant Cell Environ* 35, 760-769.

Johnson DM, Meinzer FC, Woodruff DR, McCulloh KA (2009) Leaf xylem embolism, detected acoustically and by cryo-SEM, corresponds to decreases in leaf hydraulic conductance in four evergreen species. *Plant Cell Environ* 32, 828-836.

Johnson DM et al. (2016) A test of the hydraulic vulnerability segmentation hypothesis in angiosperm and conifer tree species. *Tree Physiol* 36, 983-993.

Jump AS, Hunt JM, Peñuelas J (2006) Rapid climate change-related growth decline at the southern range edge of *Fagus sylvatica*. *Global Change Biol* 12, 2163-2174.

Katz C, Oren R, Schulze ED, Milburn JA (1989) Uptake of water and solutes through twigs of *Picea abies* (L.) Karst. *Trees* 3, 33-37.

Klein T, Hoch G (2015) Tree carbon allocation dynamics determined using a carbon mass balance approach. *New Phytol* 205, 147-159.

Klein T et. al. (2016) Diurnal dynamics of water transport, storage and hydraulic conductivity in pine trees under seasonal drought. *iForest* 9, 710-719; 10.3032/ifor2046.009.

Knipfer T, Cuneo IF, Brodersen CR, McElrone AJ (2016) In situ visualization of the dynamics in xylem embolism formation and removal in the absence of root pressure: a study on excised grapevine stems. *Plant Physiol* 171, 1024-1036.

Kozlovsky TT (1992) Carbohydrate sources and sinks in woody-plants. *The Botanical Review* 58, 107-222.

Kozlovsky TT, Pallardy S.G. (2002) Acclimation and adaptive responses of woody plants to environmental stresses. *The Botanical Review* 68, 270-334.

Lamy JB et al. (2014) Limited genetic variability and phenotypic plasticity detected for cavitation resistance in a Mediterranean pine. *New Phytol* 201, 874-886.

Laur J, Hacke U (2014) Exploring *Picea glauca* aquaporins in the context of needle water uptake and xylem refilling. *New Phytol* 203, 388-400.

Lemoine D, Jacquemin S, Granier A (2002) Beech (*Fagus sylvatica* L.) branches show acclimation of xylem anatomy and hydraulic properties to increased light after thinning. *Ann For Sci* 59, 761-766.

Lens F et al. (2011) Testing hypothesis that link wood anatomy to cavitation resistance and hydraulic conductivity in the genus Acer. *New Phytol* 190, 709-723.

Lenz TI, Wright IJ, Westboy M (2006) Interrelations among pressure-volume curve traits across species and water availability gradients. *Physiol Plant* 127, 423-433.

Leuschner C, Meier IC, Hertel D (2006) On the niche breadth of *Fagus sylvatica*: soil nutrient status in 50 Central European beech stands on a broad range of bedrock types. Ann. For. Sci. 63, 355-368.

Liu Z, Dickmann DI (1993) Responses of two hybrid *Populus* clones to flooding, drought, and nitrogen availability. II. Gas exchange and water relations. *Can J Bot* 71, 927-938.

Lobell DB, Field CB, Cahill KN, Bonfils C (2006). Impacts of future climate change on California perennial crop yields: model projections with climate and crop uncertainties. Agricultural and Forest Meteorology 141, 208-218.

Logan JA, Regniere J, Powell JA (2003) Assessing the impacts of global warming on forest pest dynamics. *Front Ecol Environ* 1, 130-137.

Lyr H, Fiedler HJ, Tranquillini W (1992) Physiologie und Ökologie der Gehölze. Jena, G. Fisher Verlag.

Magnani F, Borghetti M (1995) Interpretation of seasonal changes of xylem embolism and plant hydraulic resistance in Fagus sylvatica. *Plant Cell Environ* 18, 689-696.

Maherali H, Pockman WT, Jackson RB (2004) Adaptive variation in the vulnerability of woody plants to xylem cavitation. *Ecology* 85, 2184-2199.

Martinez-Vilalta J et al. (2009) Hydraulic adjustment of Scots pine across Europe. *New Phytol* 184, 353-364.

Martin-StPaul N et al. (2013) The temporal response to drought in a Mediterranean evergreen tree: comparing a regional precipitation gradient and a throughfall exclusion experiment. *Global Change Biol* 19, 2413-2426.

Martorell S et al. (2015) Plasticity of vulnerability to leaf hydraulic dysfunction during acclimation to drought in grapevines: an osmotic-mediated process. *Physiol. Plant.* 153: 381-391.

Mayr S et al. (2014) Uptake of water via branches helps timberline conifers refill embolized xylem in late winter. *Plant Physiol* 164, 1731-1740.

Mayr S, Wolfschwenger M, Bauer H (2002) Winter-drought induced embolism in Norway spruce (*Picea abies*) at the alpine timberline. *Physiol Plant* 115, 74-80.

McCulloh KA, Johnson DM, Meinzer FC, Lachenbruch B (2011) An annual pattern of native embolism in upper branches of four tall conifer species. *Am J Bot* 98, 1007-1015.

McDowell N, Pockman WT, Allen CD (2008) Mechanisms of plant survival and mortality during drought: why do some plants survive while others succumb to drought? *New Phytol* 178, 719-739.

McDowell NG et al. (2011) The interdependence of mechanisms underlying climate-driven vegetation mortality. *Trends Ecol Evol* 26, 523-532.

McDowell NG et al. (2013) Evaluating theories of drought-induced vegetation mortality using a multimodel-experiment framework. *New Phytol* 200, 304-312.

Mencuccini M (2014) Temporal scales for the coordination of tree carbon and water economies during droughts. *Tree Physiol* 34, 439-442.

Millennium Ecosystem Assessment (2005) Ecosystems and human well-being: general synthesis. Island press, Washington, DC. 137 pp.

Mitchell PJ et al. (2013) Drought response strategies define the relative contributions of hydraulic dysfunction and carbohydrate depletion during tree mortality. *New Phytol* 197, 862-872.

Montwé D, Spiecker H, Hamann A (2014) An experimentally controlled extreme drought in a Norway spruce forest reveals fast hydraulic response and subsequent recovery of growth rates. *Trees* 28, 891-900.

Morris H et al. (2016) A global analysis of parenchyma tissue fractions in secondary xylem of seed plants. *New Phytol* 209, 1553-1535.

Müller B et al. (2011). Water deficits uncouple growth from photosynthesis, increase C content, and modify the relationships between C and growth in sink organs. *J Exp Bot* 62, 1715-1729.

Nardini A, Battistuzzo M, Savi T (2013) Shoot desiccation and hydraulic failure in temperate woody angiosperms during an extreme summer drought. *New Phytol* 200, 322-329.

Nardini A, Lo Gullo MA, Salleo S (2011) Refilling of embolized conduits: is it a matter of phloem unloading? *Plant Sci* 180, 604-611.

Nardini A, Luglio J (2014) Leaf hydraulic capacity and drought vulnerability: possible trade-offs and correlations with climate across three major biomes. *Funct Ecol* 28, 810-818.

Nardini A, Tyree M, Salleo S (2001) Xylem cavitation in the leaf of *Prunus laurocerasus* and its impact on leaf hydraulics. *Plant Physiol* 125, 1700-1709.

Nardini A et al. (2016) Rooting depth, water relations and non-structural carbohydrate dynamics in three woody angiosperms differentially affected by an extreme summer drought. *Plant Cell Environ* 39, 618-627.

Nardini A et al. (2017a) X-ray micro-tomography observations of xylem embolism in stems of Laurus *nobilis* L. are consistent with hydraulic measurements of percent loss of conductance. *New Phytol.* 213, 1068-1075.

Nardini A, Gascò A, Trifilò P, Lo Gullo MA, Salleo S (2007) Ion-mediated enhancement of xylem hydraulic conductivity is not always suppressed by the presence of Ca^{2+} in the sap. *J Exp Bot* 58, 2609-2615.

Nardini A, Savi T, Trifilò P, Lo Gullo MA (2017b) Drought stress and the recovery from xylem embolism in woody plants in *Progress in Botany Vol. 78* (ed. Canovas, F.M., Luettge, U., Matyssek, R.) (Springer).

Niinemets U (2010) Responses of forest trees to single and multiple environmental stresses from seedlings to mature plants: past stress history, stress interactions, tolerance and acclimation. *For Ecol Man* 260, 1623-1639.

Nolf M et al. (2015) Stem and leaf hydraulic properties are finely coordinated in three tropical rain forest tree species. *Plant Cell Environ* 38, 2652-2661.

Nolf M et al. (2017) Visualization of xylem embolism by X-ray microtomography: a direct test against hydraulic measurements. *New Phytol* 214, 890-898.

O'Brien MJ, Leuzinger S, Philipson CD, Tay J, Hector A (2014) Drought survival of tropical tree seedlings enhanced by non-structural carbohydrate levels. *Nature Climate Change* 4, 710-714.

Pammenter NW, Vander Willingen C (1998) A mathematical and statistical analysis of the curves illustrating vulnerability of xylem cavitation. *Tree Physiol* 18, 589-593.

Perterer J, Koerner C (1990) Das Problem der Bezugsgroesse bei physiologisch-oekologischen Untersuchungen an Koniferennadeln. *Forstwissenschaftliches Centralblatt* 109, 220 – 241.

Petrucco L, Nardini A, von Arx G, Saurer M, Cherubini P (2017) Isotope signals and anatomical features in tree rings suggest a role for hydraulic strategies in diffuse drought-induced die-back of *Pinus nigra*. *Tree Physiol* 37, 523-535.

Pittermann J, Sperry JS, Hacke UG, Wheeler JK, Sikkema EH (2005) Torus-margo pits help conifers compete with angiosperms. *Science* 310, 1924.

Pivovaroff AL, Sack L, Santiago LS (2014) Coordination of stem and leaf hydraulic conductance in southern California shrubs: a test of the hydraulics segmentation hypothesis. *New Phytol* 203, 842-850.

Poorter H, Bühler J, van Dusschoten D, Climent J, Postma JA (2012) Pot size matters: a meta analysis of the effects of rooting volume on plant growth. Funct Plant Biol 39, 839-850.

Power SA (1994) Temporal trends in twig growth of *Fagus sylvatica* L. and their relationships with environmental factors. Forestry 67, 13-30.

Pretzsch H et al. (2016) Tree diameter growth after root trenching in a mature mixed stand of Norway spruce (*Picea abies* (L.) Karst) and European beech (*Fagus sylvatica* (L.)). Trees 30, 1761-1773.

Pretzsch H et al. (2014) Mixed Norway spruce (*Picea abies* (L.) Karst) and European beech (*Fagus sylvatica* (L.)) stands under drought: from reaction pattern to mechanism. Trees 28, 1305-1321.

Rita A, Cherubini P, Leonardi S, Todaro l, Borghetti M (2015) Functional adjustments of xylem anatomy to climatic variability: insights from long-term *Ilex aquifolium* tree-rings series. Tree Physiol 35, 817-828.

Sack L, Pasquet-Kok J (2011) Leaf pressure-volume curve parameters. http://prometheuswiki.publish.csiro.au/tikicitation.php?page=Leaf%20pressurevolume%20curve%20parameters#sthash.1KxZH2vQ.dpuf (31 October 2017, last accessed date)

Sala A, Piper F, Hoch G (2010) Physiological mechanisms of drought-induced tree mortality are far from being resolved. *New Phytologist* 186, 274-281.

Salleo S, Trifilò P, Esposito S, Nardini A, Lo Gullo AM (2009) Starch-to-sugar conversion in wood parenchyma of field-growing *Laurus nobilis* plants: a component of the signal pathway for embolism repair? *Funct Plant Biol* 36, 815-825.

Savi T et al. (2016) Species-specific reversal of stem xylem embolism after a prolonged drought correlates to endpoint concentration of soluble sugars. *Plant Physiol Biochem* 106, 198-207.

Savi T et al. (2017) Drought-induced embolism in stems of sunflower: a comparison of in vivo micro-CT observations and destructive hydraulic measurements. *Plant Physiol Biochem* 120, 24-29.

Schloter M et al. Short term effects of ozone on the plant-rhizosphere-bulk soil system of young beech trees. *Plant Biol* 7, 728-736 (2005).

Schlyter P, Stjernquist I, Bärring L, Joensson AM, Nilsson C (2006) Assessment of the impacts of climate change and weather extremes on boreal forests in northern Europe, focusing on Norway spruce. *Climate Research* 31, 75-84.

Scholander P, Bradstreet E, Hemmingsen E, Hammel H (1965). Sap pressure in vascular plants: negative hydrostatic pressure can be measured in plants. *Science* 148, 339-346.

Scholz A, Klepsch M, Karimi Z, Jansen S (2013) How to quantify conduits in wood? *Front Plant Sci* 4, 53;

Scholz FG, Bucci SJ, Goldstein G (2014) Strong hydraulic segmentation and leaf senescence due to dehydration may trigger die-back in *Nothofagus dombeyi* under severe droughts: a comparison with the co-occurring *Austrocedrus chilensis*. *Trees* 28, 1475-1487.

Schuldt B et al. (2016) How adaptable is the hydraulic system of European beech in the face of climate change-related precipitation reduction? *New Phytol* 210, 443-458.

Scoffoni C, Vuong C, Diep S, Cochard H, Sack L (2014) Leaf shrinkage with dehydration: coordination with hydraulic vulnerability and drought tolerance. *Plant Physiol* 164, 1772-1788.

Secchi F, Pagliarani C, Zwieniecki MA (2017) The functional role of xylem parenchyma cells and aquaporins during recovery from severe water stress. *Plant Cell Environ* 40, 858-871.

Secchi F, Zwieniecki MA (2011) Sensing embolism in xylem vessels: the role of sucrose as a trigger for refilling. *Plant Cell Environ* 34, 514-524.

Secchi F, Zwieniecki MA (2016) Accumulation of sugars in the xylem apoplast observed under water stress conditions is controlled by xylem pH. *Plant Cell Environ* 39, 2350–2360.

Sellin A (2000) Estimating the needle area from geometric measurements: application of different calculation methods to Norway spruce. *Trees* 14, 215-222.

Sevanto S, McDowell NG, Dickman IT, Pangle R, Pockman WT (2014) How do trees die? A test of the hydraulic pailure and carbon starvation hypotheses. *Plant Cell Environ.* 37, 153-161.

Sevanto S (2014) Phloem transport and drought. *J Exp Bot* 65, 1751-1759.

Silva EN, Ferreira-Silva SL, Viegas RA, Silveira JAG (2010) The role of organic and inorganic solutes in the osmotic adjustment of drought-stressed *Jatropha curcas* plants. *Env Exp Bot* 69, 279-285.

Soudzilovskaia NA *et al.* (2013) Functional traits predict relationships between plant abundance dynamic and long-term climate warming. *Proceedings of the National Academy of Sciences, USA* 110, 18180-18184.

Sperry JS, Donnelly JR, Tyree MT (1988) A method for measuring hydraulic conductivity and embolism in xylem. *Plant Cell Environ* 11, 35-40.

Sperry JS, Hacke UG, Oren R, Comstock JP (2002) Water deficits and hydraulic limits to leaf water supply. *Plant Cell Environ* 25, 251-263.

Sperry JS, Hacke UG (2004) Analysis of circular bordered pit function. I Angiosperm vessels with homogeneous pit membranes. *Am J Bot* 91, 369-385.

Spiecker H, Hansen J, Klimo E, Skovsgaard JP, Sterba H, von Teuffel K (eds) (2004) Norway spruce conversion – options and consequences. Brill, Leiden.

Srichuwong S, Jane JL (2007) Physicochemical properties of starch affected by molecular composition and structures: a review. *Food Sci Technol* 16, 663-674.

Stewart JD, Zine El-Abidine A, Bernier PY (1995). Stomatal and mesophyll limitations of photosynthesis in black spruce seedlings during multiple cycles of drought. *Tree Physiol* 15, 57-64.

Strati S, Patiño S, Slidders C, Cundall EP, Mencuccini M (2003) Developement and recovery from winter embolism in silver birch: seasonal patterns and relationships with the phenological cycle in oceanic Scotland. *Tree Physiol* 23, 663-673.

Stribley GH, Ashmore MR (2002) Quantitative changes in growth pattern of young woodland beech (Fagus sylvatica L.) in relation to climate and ozone pollution over 10 years. *For Ecol Man* 157, 191-204.

Sultan SE (2000) Phenotypic plasticity for plant development, function and life history. *Trends Plant Sci* 5, 537-542.

Taiz L, Zeiger E (2010) Plant physiology (5th ed.). Sunderland MA: Sinauer Associates Inc.

Tardieau F, Simonneau T (1998) Variability among species of stomatal control under fluctuating soil water status and evaporative demand: modelling isohydric and anisohydric behaviours. *J Exp Bot* 49, 419-432.

Tokumoto I et al. (2014) Small-scale variability in water storage and plant available water in shallow, rocky soils. *Plant and Soil* 385, 193-204.

Torres-Ruiz JM et al. (2015) Direct X-ray microtomography observation confirms the induction of embolism upon xylem cutting under tension. *Plant Physiol* 167, 40-43.

Trifilò P et al. (2014) Relax and refill: xylem rehydration prior to hydraulic measurements favours embolism repair in stems and generates artificially low PLC values. *Plant Cell Environ* 37, 2491-2499.

Tyree MT, Hammel HT (1972) The measurement of the turgor pressure and the water relations of plants by the pressure-bomb technique. *J Exp Bot* 23, 267-282.

Tyree MT, Ewers FW (1991) The hydraulic architecture of trees and other woody plants. *New Phytol* 119, 345-360.

Tyree MT, Zimmermann MH (2002) Xylem structure and the ascent of sap. 2nd Edn. Berlin: Spriger Verlag, 283 p.

Ulri M et al. (2013) Xylem embolism threshold for catastrophic hydraulic failure in angiosperm trees. *Tree Physiol* 33, 672-683.

Umebayashi T et al. (2016) Spatial distribution of xylem embolisms in the stems of *Pinus thunbergii* at the threshold of fatal drought stress. *Tree Physiol* 36, 1210-1218.

Van der Werf GW, Sass-Klaassen UGW, Mohren GMJ (2007) The impact of the 2003 summer drought on the intra-annual growth pattern of beech (*Fagus sylvatica* L.) and oak (*Quercus robur* L.) on a dry site in the Netherlands. *Dendrochronologia* 25, 103-112.

Vandegehuchte MW, Bloemen J, Vergeynst LL, Steppe K (2015) Woody tissue photosynthesis: salve on the wounds of drought? *New Phytol* 208, 998-1002.

Venturas MD, MacKinnon ED, Jacobsen AL, Pratt RB (2015) Excising stem samples under water at native tension does not induce xylem cavitation. *Plant Cell Environ* 38, 1060-1068.

Voicu MC, Cooke JEK, Zwiazek JJ (2009) Aquaporin gene expression and apoplastic water flow in bur oak (*Quercus macrocarpa*) leaves in relation to the light response of leaf hydraulic conductance. *J Exp Bot* 60: 4063–4075.

Wheeler JK, Huggert BA, Tofte AN, Rockwell FE, Holbrook NM (2013) Cutting xylem under tension or supersaturated with gas can generate PLC and the appearance of rapid recovery from embolism. *Plant Cell Environ* 36, 1938-1949.

Wiley E, Rogers BJ, Hodgkinson R, Landhäusser SM (2016) Nonstructural carbohydrate dynamics of lodgepole pine dying from mountain pine beetle attack. *New Phytol* 209, 550-562.

Williams AP et al. (2013) Temperature as a potent driver of regional forest drought stress and tree mortality. *Nature Clim Change* 3, 292-297.

Wortemann R et al. *(*2011) Genotypic variability and phenotypic plasticity of cavitation resistance in *Fagus sylvatica* L. across Europe. *Tree Physiol* 31, 1175-1182.

Yang Q, Zhang W, Li R, Xu M, Wang S (2016) Different responses of non-structural carbohydrates in above-ground tissues/organs and root to extreme drought and re-watering in Chinese fir (*Cunninghamia lanceolata*) saplings. *Trees* 30, 1863-1871.

Yang SJ, Zhang YJ, Sun M, Goldstein G, Cao KF (2012) Recovery of diurnal depression of leaf hydraulic conductance in a subtropical woody bamboo species: embolism refilling by nocturnal root pressure. *Tree Physiol* 32, 414-422.

Yazaki K et al. (2015) Recovery of physiological traits in saplings of invasive *Bischofia* tree compared with three species native to the Bonin Islands under successive drought and irrigation cycles. *Plos One* 10, e0135117; 10.1371/journal.pone.0135117.

Yazaki K, Sano Y, Fujikawa S, Nakano T, Ishida A (2010) Response to dehydration and irrigation in invasive and native saplings: osmotic adjustment versus leaf shedding. *Tree Physiol* 30, 597-607.

Yoshimura K et al. (2016) The dynamics of carbon stored in xylem sapwood to drought-induced hydraulic stress in mature trees. *Sci Rep* 6, 24513; 10.1038/srep24513.

Zwieniecki MA, Holbrook NM (2009) Confronting Maxwell's demon: biophysics of xylem embolism repair. *Trends Plant Sci* 14, 530-534.

Zwieniecki MA, Melcher P, Ahrens ET (2013) Analysis of spatial and temporal dynamics of xylem refilling in Acer rubrum L. using magnetic resonance imaging. Front Plant Sci 4, 265; 10.3389/fpls.2013.00265.

Appendix A – Supplementary data and material

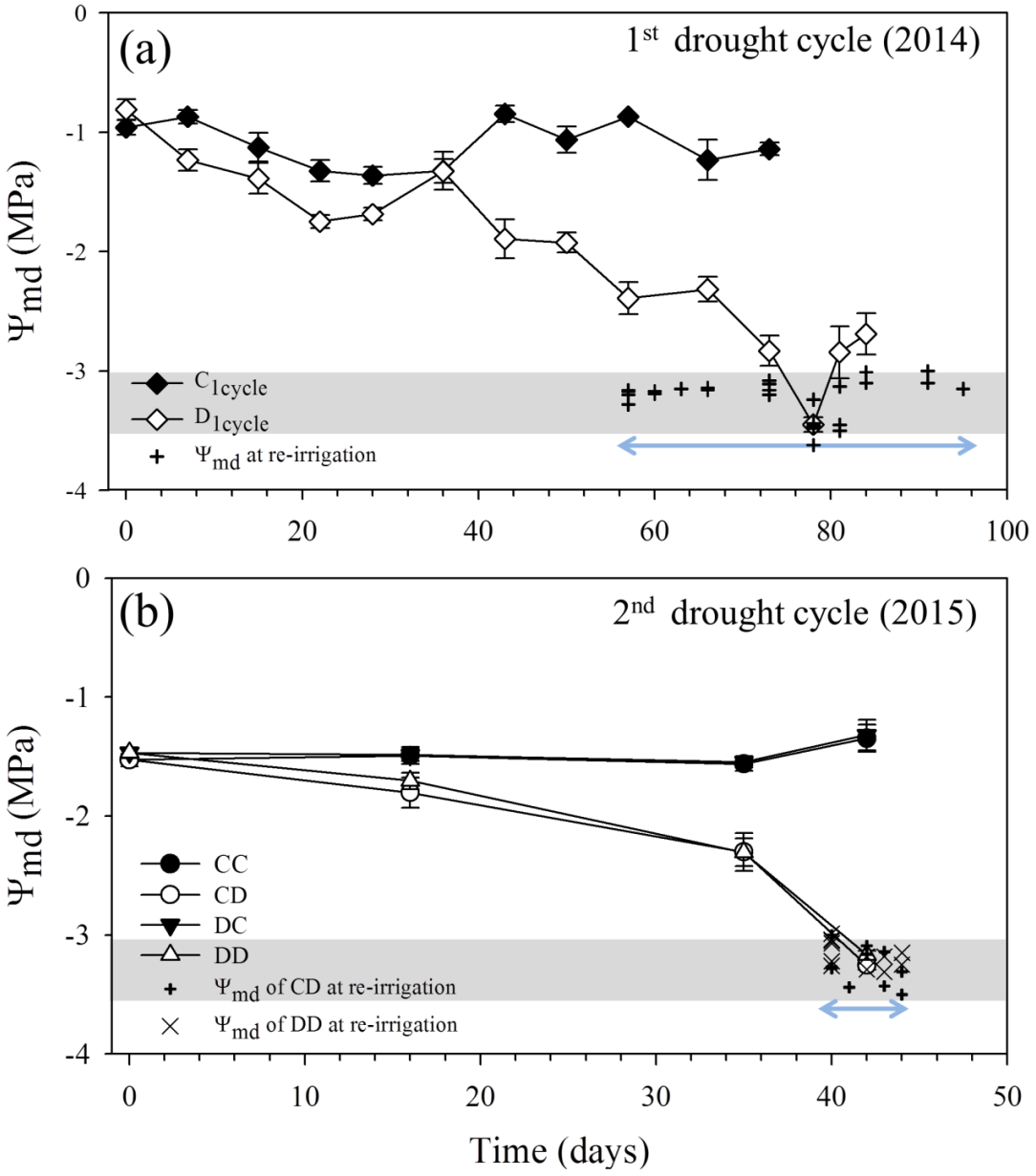

Figure S1. Changes in midday leaf water potentials (Ψ_{md}) over the first and second drought cycles in Norway spruce seedlings. (a) Ψ_{md} monitored over the first drought cycle (summer 2014) in well-irrigated (control, C_{1cycle}, closed symbols) and drought stressed (D_{1cycle}, open symbols) trees, from the time when irrigation was withheld (Day 0). **(b)** Ψ_{md} monitored over the second drought cycle (summer 2015) in CC (control in 2014 and 2015), CD (control in 2014, drought in 2015), DC (drought in 2014, control in 2015) and DD (drought in 2014 and 2015) trees, from the time when irrigation was reduced (Day 0). Note the different time scales in (a) and (b). Symbols denote means and bars are standard errors, while crosses indicate for each D_{1cycle} individual the Ψ_{md} at re-irrigation. The shaded horizontal area highlights the target range of Ψ_{md} for re-irrigation of drought-stressed trees and the blue arrow indicates the time period when plants were re-irrigated.

Table S 1. Parameters measured under well-watered conditions before the beginning of the second drought cycle (summer 2015). Percentage loss of xylem hydraulic conductance (PLC), maximum specific hydraulic conductivity (k_s), Pre-dawn (Ψ_{pd}), xylem (Ψ_{xyl}) and midday (Ψ_{md}) water potential, CO_2 assimilation rate (A), stomatal conductance (g_s), leaf transpiration rate (E), water potential at turgor loss point (Ψ_{tlp}), osmotic potential at full turgor (π_0), bulk modulus of elasticity (ε), leaf mass per area (LMA), evapotranspiration (ET) and stem non-structural carbohydrates measured at the end of June 2015 in control (C_{1cycle}) and drought (D_{1cycle}) treatments from the first drought cycle. NSC specimens were measured separately in wood and bark. "Total soluble" is the sum of all soluble NSCs. Values are means ± standard error. Number of replicates (n) and P-value from Welch's t-tests are given.

Parameter		C_{1cycle}	D_{1cycle}	n	P-value
PLC (%)		2.6 ± 2.6	0.62 ± 0.62	4	1.00
k_s (kg MPa^{-1} s^{-1} m^{-1})		0.74 ± 0.11	0.55 ± 0.11	4	0.27
Ψ_{pd} (MPa)		-0.41 ± 0.08	-0.40 ± 0.06	7	0.99
Ψ_{xyl} (MPa)		-1.11 ± 0.07	-0.86 ± 0.04	7	0.01
Ψ_{md} (MPa)		-1.53 ±0.05	-1.47 ± 0.04	7	0.40
A (µmol m^{-2} s^{-1})		1.71 ± 0.32	2.18 ± 0.34	7	0.34
g_s (mmol m^{-2} s^{-1})		14.5 ± 2.9	19.5 ± 3.0	7	0.26
E (mmol m^{-2} s^{-1})		0.82 ± 0.15	0.96 ± 0.12	7	0.46
Ψ_{tlp} (MPa)		-1.57 ± 0.10	-1.58 ± 0.15	5	0.94
π_0 (MPa)		-1.39 ± 0.11	-1.42 ± 0.14	5	0.90
ε (MPa)		26.8 ± 5.9	32.4 ± 9.6	5	0.63
LMA (g m^{-2})		146 ± 10	165 ± 15	5	0.32
ET (g day^{-1})		383 ± 58	353 ± 61		0.19
Starch (mg g^{-1})	wood	2.14 ± 0.42	1.29 ± 0.43	4	0.21
	bark	17.85 ± 2.93	18.37 ± 7.13	4	0.95
Sucrose (mg g^{-1})	wood	3.50 ± 1.05	4.20 ± 0.51	4	0.58
	bark	35.75 ± 2.21	36.8 ± 2.21	4	0.75
Fructose (mg g^{-1})	wood	3.35 ± 0.58	2.50 ± 0.47	4	0.30
	bark	14.07 ± 1.51	16.20 ± 2.02	4	0.43
Glucose (mg g^{-1})	wood	2.75 ± 0.57	2.00 ± 0.13	4	0.28
	bark	11.77 ± 2.11	12.82 ± 2.33	4	0.75
Pinitol (mg g^{-1})	wood	3.82 ± 0.99	4.55 ± 0.86	4	0.60
	bark	20.62 ± 1.89	22.40 ± 2.20	4	0.56
Stachyose (mg g^{-1})	wood	0.20 ± 0.20	0.57 ± 0.25	4	0.28
	bark	1.87 ± 0.64	2.75 ± 0.27	4	0.28
Raffinose (mg g^{-1})	wood	0.75 ± 0.13	0.75 ± 0.18	4	1.00
	bark	0.00 ± 0.00	0.75 ± 0.75	4	0.39
Galactose (mg g^{-1})	wood	1.95 ± 0.25	1.52 ± 0.62	4	0.56
	bark	8.82 ± 0.82	5.57 ± 2.01	4	0.21
Total soluble (mg g^{-1})	wood	16.32 ± 3.32	16.10 ± 2.16	4	0.96
	bark	92.92 ± 2.85	97.30 ± 10.89	4	0.80
Total NSCs (mg g^{-1})	wood	18.46 ± 3.73	17.39 ± 1.75	4	0.81
	bark	110.77 ± 4.32	115.67 ± 11.95	4	0.72

Leaf water potential isotherm parameters measured in Norway spruce saplings at re-irrigation in the second drought cycle (summer 2015). Water potential at turgor loss point (Ψ_{tlp}), osmotic potential at full turgor (π_0), bulk modulus of elasticity (ε) and leaf mass per area (LMA) measured the week after re-irrigation, in the second drought cycle, in twigs of control (i.e. well-irrigated, CC and DC) and drought (CD and DD) plants. Values are means ± SE and *P*-values from Welch's t-test are given.

	CC & DC	CD & DD	*P*-value
Ψ_{tlp} (MPa)	-1.79 ± 0.03	-1.99 ± 0.11	0.16
π_0 (MPa)	-1.56 ± 0.01	-1.72 ± 0.11	0.21
ε (MPa)	30.0 ± 18.8	21.2 ± 3.2	0.82
LMA (g m^{-2})	154 ± 14	169 ± 6	0.42

Table S2. Effect of the two drought cycles on stem non-structural carbohydrate (NSC) content in Norway spruce saplings. *P*-values from two-way ANOVA examining the effect of the first drought cycle (first), the second drought cycle (second) on non-structural carbohydrate (NSC) content (measured separately in stem wood and bark) in the "end-drought" and "re-irrigation" campaigns performed in the second drought cycle. "Total soluble" is the sum of all soluble NSCs. *P* <0.05 indicate significant effects and are formatted in bold.

		End-drought (2015)		Re-irrigation (2015)	
		first	second	first	second
Starch	wood	0.13	0.12	0.58	0.11
	bark	0.60	**<0.001**	0.51	0.67
Sucrose	wood	0.73	0.28	0.83	**0.02**
	bark	**0.03**	0.16	0.48	0.69
Fructose	wood	0.67	0.56	0.54	0.33
	bark	0.44	**0.04**	0.24	0.06
Glucose	wood	0.90	0.89	0.50	**0.01**
	bark	0.53	0.24	0.74	0.98
Pinitol	wood	0.67	**<0.001**	0.05	0.10
	bark	0.38	0.88	0.24	0.09
Stachyose	wood	0.61	**0.02**	0.76	0.34
	bark	0.35	0.76	0.35	**0.04**
Raffinose	wood	0.96	0.27	0.49	0.90
	bark	0.11	0.87	0.78	**0.003**
Galactose	wood	0.42	0.07	0.07	0.08
	bark	0.74	**0.03**	0.97	**<0.001**
Total soluble	wood	0.75	0.15	0.10	**0.01**
	bark	0.10	0.95	0.69	0.66
Total NSCs	wood	0.99	0.16	0.07	**0.005**
	bark	0.28	0.26	0.80	0.64

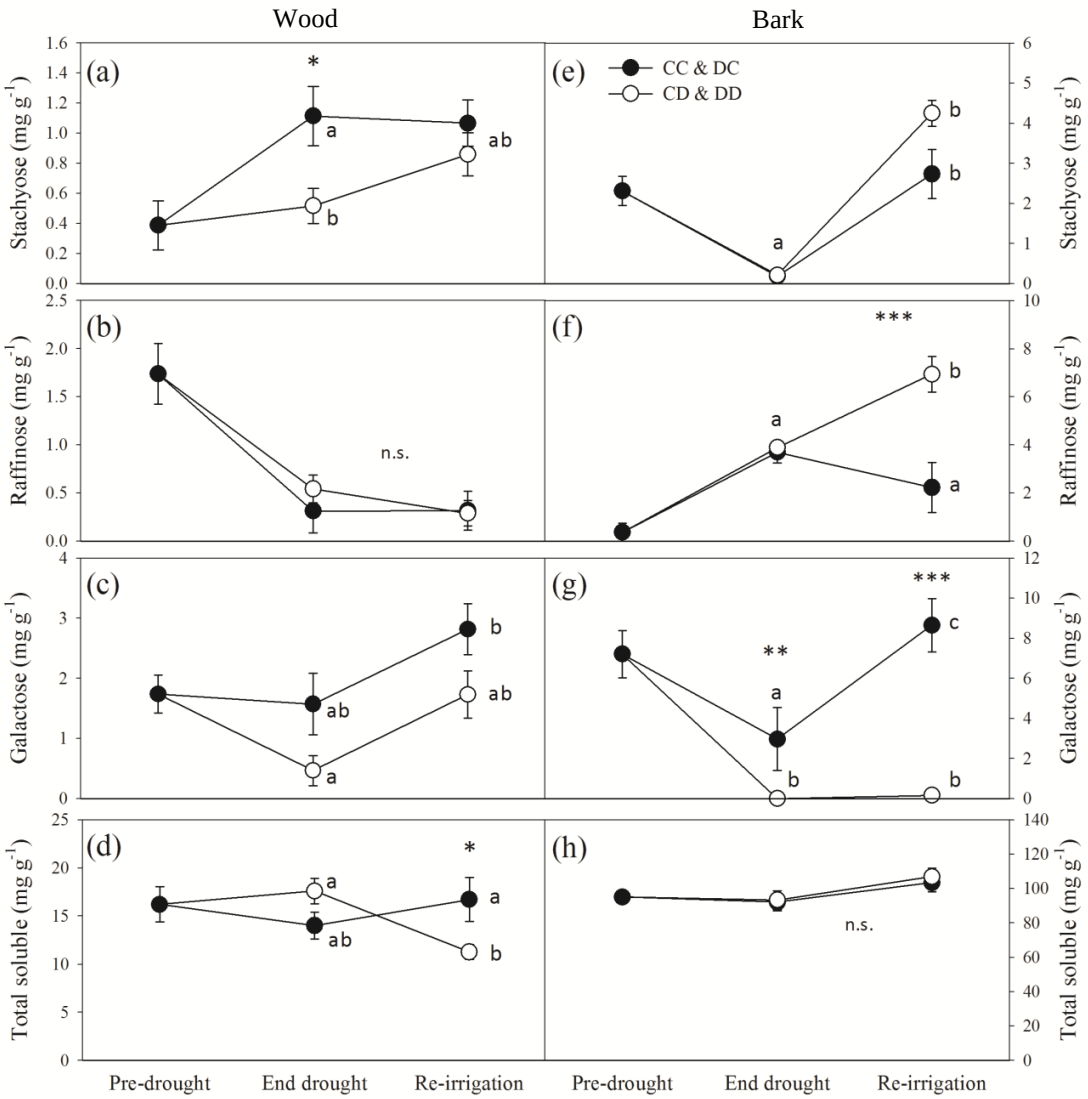

Figure S2. Additional non-structural carbohydrates (NSC) measured in Norway spruce stems during the second drought cycle (2015). (a-c) NSC concentration (in mg g^{-1} of dry mass) in stem wood and **(d-f)** bark, measured in "pre-drought", "end drought" and "re-irrigation" campaigns. "Total soluble" is the sum of all soluble sugars measured (sucrose, fructose, glucose, pinitol, stachyose, raffinose and galactose). In the "pre-drought" campaign, data were pooled in one single group. In the "end drought" and "re-irrigation" campaigns, well-watered (CC and DC) as well as drought (CD and DD) treatments were pooled, resulting in one control (CC & DC) and one drought (CD & DD) group. Please note the different scales between wood and bark NSCs content. Bars are means ± standard error (n = 6-12). Different letters indicate significant differences between treatments and campaigns (two-way ANOVA and Tukey-HSD, only data of "end drought" and "re-irrigation" are compared). n.s. = no significant difference. Asterisks denote the significance of differences among treatments within a given campaign (*0.01<P<0.05, **0.001<P<0.01, ***P<0.001).

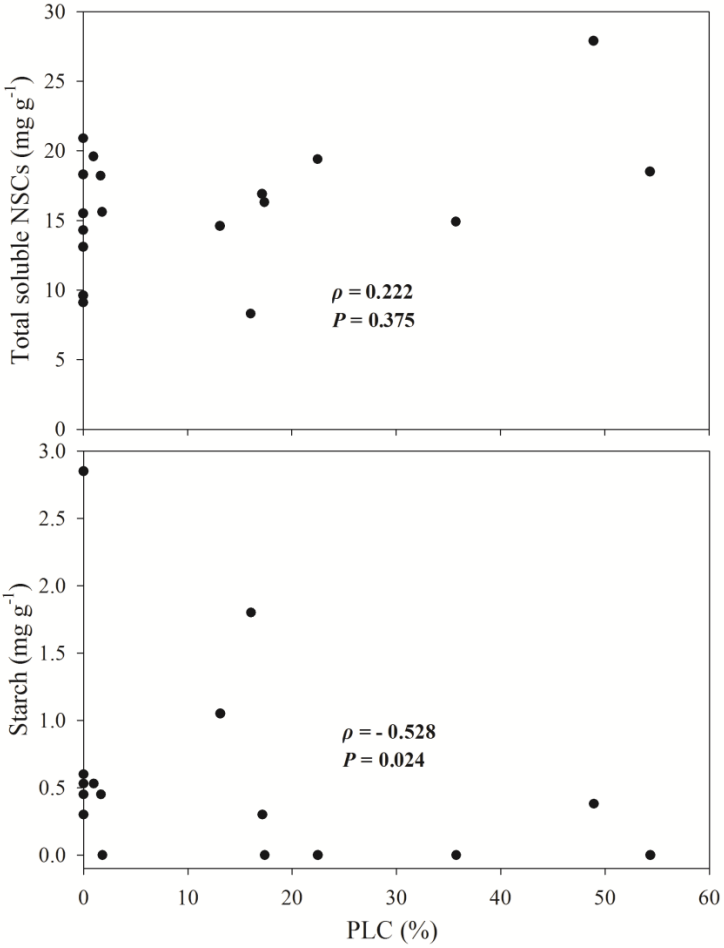

Figure S3. The relationship between stem wood non-structural carbohydrates (NSCs) and PLC at the end of the second drought cycle ("end drought" campaign) in Norway spruce seedlings. The correlation between percentage loss of xylem hydraulic conductance (PLC) and total soluble NSCs **(a)** or starch content **(b)** measured in the stem wood in the "end-drought" campaign (summer 2015). The Spearman correlation coefficient (ρ) and *P*-value (*P*) are reported.

Calculation of theoretical minimum glucose concentration necessary to generate enough osmotic pressure for refilling of embolized tracheids in the measured Norway spruce samples

Percentage loss of xylem conductivity (PLC) before re-irrigation = 20%

Percentage loss of xylem conductivity (PLC) after recovery = 0%

Ψ_{xylem} after refilling = -0.62 MPa; assumed required osmotic pressure ~ -0.7 MPa

Assumed a sample of d = 0.8 cm and length (L) 4 cm (volume = 2 cm^{-3}). Wood density = 0.51 g cm^{-3}.

Area cross section (A_{tot}) = πr^2 = 50.2 mm^2

Area pith (A_{pith}) = πr^2= 1.1 mm^2

Area $_{wood}$ = A_{tot} - A_{pith}= 49.1 mm^2

Volume wood = Area $_{wood}$ x L = 49.1 x 40 = 1964 mm^3 = 1.964 cm^3= 1.964 ml

The sapwood area occupied by tracheids in spruce samples (from anatomical analysis) is about 25% and PLC recovered was 20%, therefore the volume of gas filled tracheids (V_{trach}) to be refilled was:

V_{trach} = 1.964 X 0.25 x 0.20= 0.0982 ml

Assuming a temperature (T) of 293 K:

Solute concentration (C_s) = π/(R*T) = 0.7 /(8.314x10^{-3} x 293)= 0.287 mol l^{-1}

Therefore in 0.0982 ml there are 2.82 x 10^{-5} mol of solutes

2.82 x 10^{-5} * 180 = 5.08 mg= mass of glucose in the sample

The wood density of spruce samples was 0.51 g cm^{-3} (DW of the 2 cm^{-3} sample is 1.02 g), therefore:

Glucose concentration required = 5.08/1.02= 5.0 mg g^{-1} DW

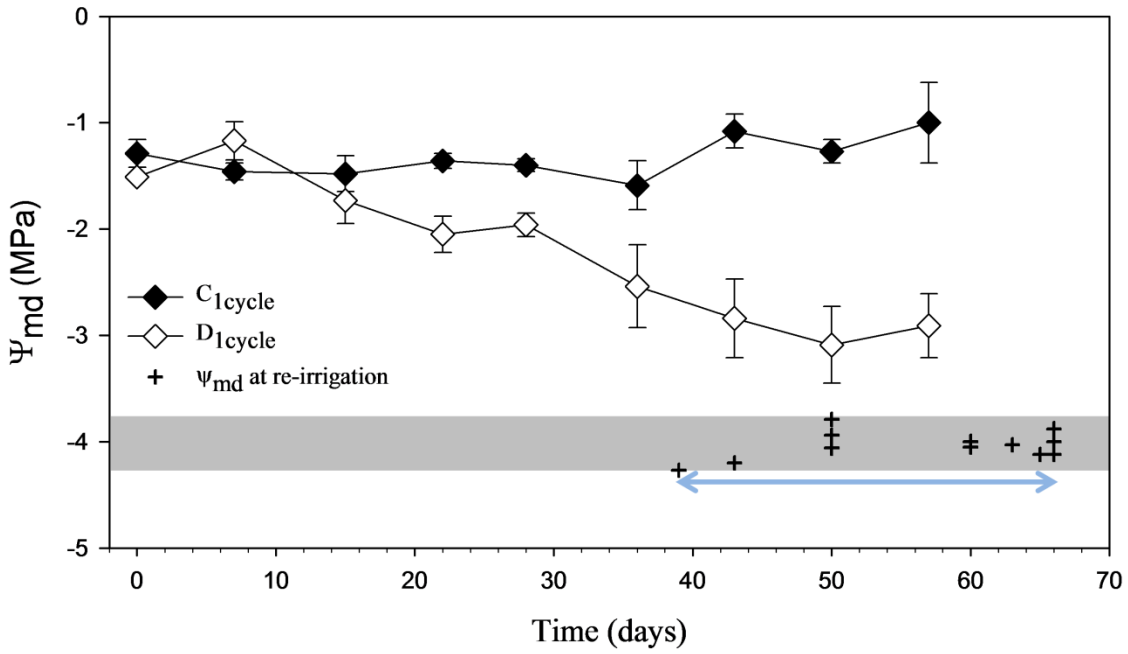

Figure S4. Changes in midday leaf water potentials (Ψ_{md}) over the first drought cycle in European beech seedlings. Ψ_{md} was monitored over the first drought cycle (summer 2014) in well-irrigated (control, C_{1cycle}, closed symbols) and drought stressed (D_{1cycle}, open symbols) trees, from the time when irrigation was withheld (Day 0). Symbols denote means and bars are standard errors, while crosses indicate for each D_{1cycle} individual the Ψ_{md} at re-irrigation. The shaded horizontal area highlights the target range of Ψ_{md} for re-irrigation of drought-stressed trees and the blue arrow indicates the time period when plants were re-irrigated.

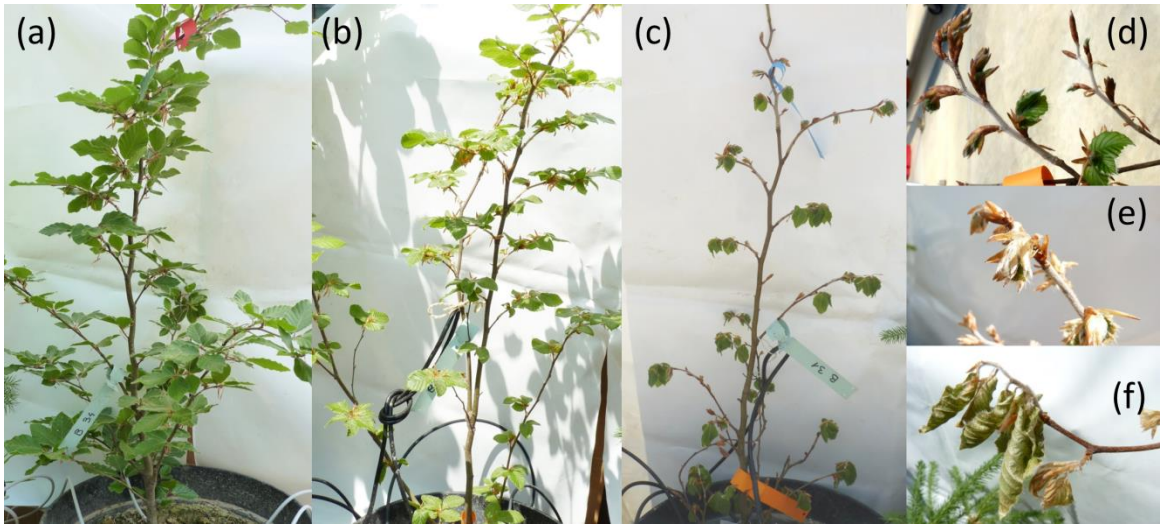

Figure S5. Examples of European beech saplings after the 2015 spring flush (1 June). Control (C_{1cycle}) trees **(a)**, drought (D_{1cycle}) trees which recovered from the previous year drought cycle **(b)** and drought trees which did not complete new shoot formation **(c)**, started to desiccate and then died. Figures **(d)** and **(e)** show examples of incomplete leaf flush and **(f)** shows desiccated newly formed leaves.

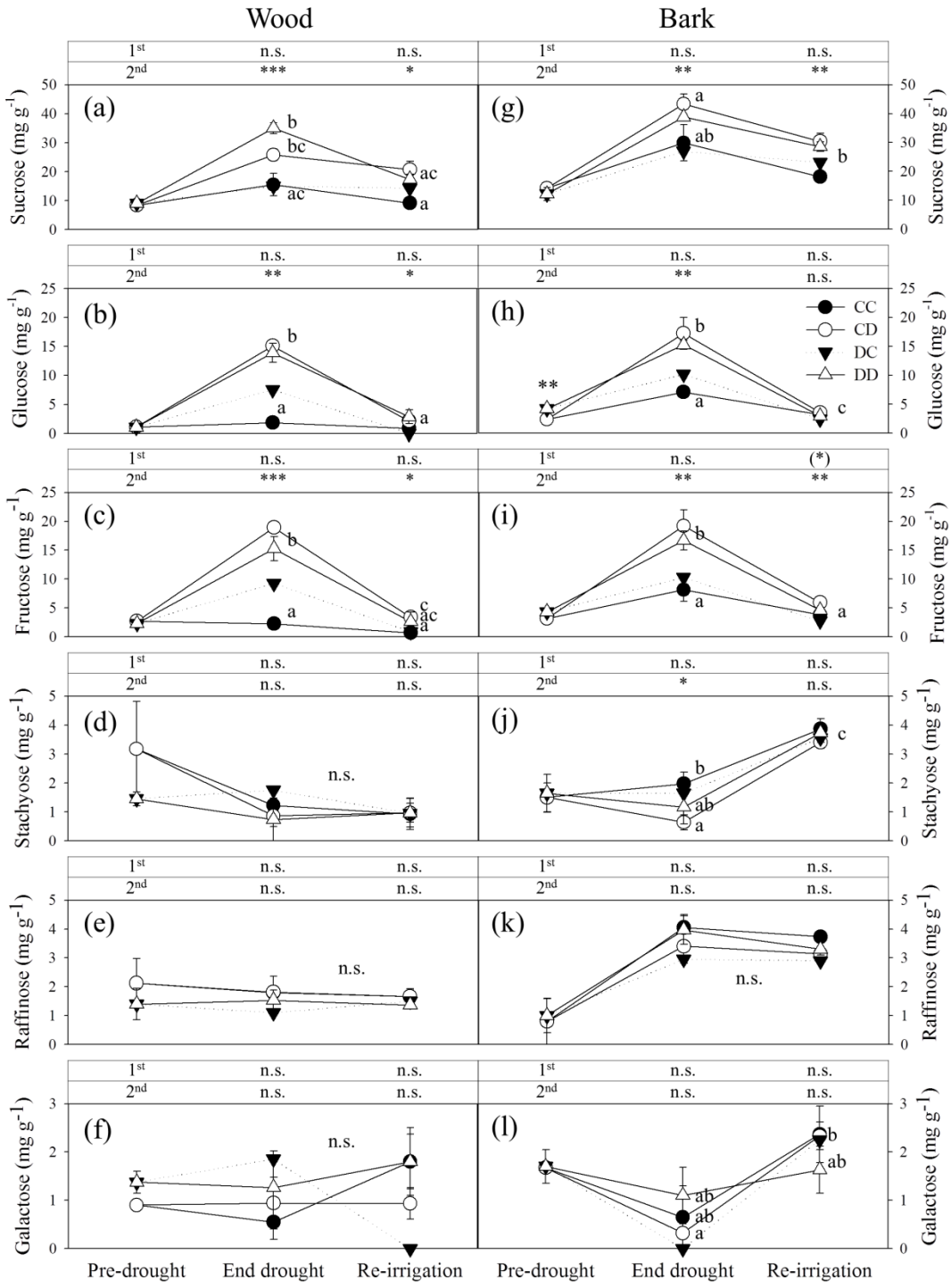

Figure S6. Soluble sugar content dynamics in European beech stems during the second drought cycle (2015). Concentration (in mg g^{-1} of dry mass) of soluble NSC specimens measured in stem wood **(a-f)** and bark **(g-l)**, in the "pre-drought", "end drought" and "re-irrigation" campaigns. In the "pre-drought" campaign, all plants were well irrigated and only two groups were present (control, C_{1cycle}, and drought, C_{1cycle}, treatments of the first drought cycle, *n*=4). In the "end-drought" and "re-irrigation" campaigns, different letters indicate significant differences between treatments and campaigns (*n*=3-6, two-way ANOVA with treatment and campaign as factors, followed by Tukey HSD test). The DC group (*n*=2, error bars omitted) was not included in the statistical analysis. On top of each panel, the results of two-way ANOVA, examining the effect of the first (1^{st}) and second drought cycle (2^{nd}) on NSC content measured in

the "end drought "and "re-irrigation" campaigns, are shown (*0.01<*P*<0.05, **0.001<*P*<0.01, ***P<0.001, n.s. = not significant).

Table S3. Effect of the two drought cycles on non-structural carbohydrate (NSC) content measured in European beech stems. *P*-values from two-way ANOVA examining the effect of the first drought cycle (first) and the second drought cycle (second) on non-structural carbohydrate (NSC) content measured (separately in stem wood and bark) in the "end-drought" and "re-irrigation" campaigns performed in the second drought cycle. "Total NSC" is the sum of all specimens, "Total soluble" is the sum of all soluble NSC. P <0.05 indicate significant effects and are formatted in bold. 0.05 < P < 0.10 are underlined.

		End-drought (2015)		Re-irrigation (2015)	
		first	second	first	second
Starch	wood	0.991	**0.013**	**0.028**	0.254
	bark	0.692	0.057	0.675	0.244
Main soluble	wood	0.571	**<0.001**	0.716	**0.002**
	bark	0.595	**0.002**	0.745	**0.005**
Total NSC	wood	0.610	0.342	**0.026**	0.728
	bark	0.662	**0.008**	0.933	**0.009**
Sucrose	wood	0.207	**<0.001**	0.674	**0.011**
	bark	0.375	**0.008**	0.575	**0.006**
Glucose	wood	0.889	**<0.001**	0.868	**0.023**
	bark	0.934	**0.002**	0.183	0.357
Fructose	wood	0.863	**<0.001**	0.602	**0.015**
	bark	0.809	**0.002**	0.075	**0.005**
Stachyose	wood	0.730	0.168	0.990	0.957
	bark	0.631	**0.015**	0.774	0.466
Raffinose	wood	0.374	0.866	0.358	0.813
	bark	0.958	0.734	0.439	0.432
Galactose	wood	0.275	0.955	0.662	0.668
	bark	0.656	0.830	0.296	0.625
Total soluble	wood	0.498	**<0.001**	0.970	**0.002**
	bark	0.689	**0.002**	0.570	**0.007**

Candidate's contribution to the work and to the related publications

The doctoral candidate developed most of the concepts, research questions and the experimental design of all parts of the present thesis, with contributions from co-authors.

Field and laboratory measurements were in great part (~ 90%) performed by the doctoral candidate, while the rest was done by students, supervised by the candidate. Field water potential and SVWC data from the KROOF experiment were furnished by Christian Kallenbach as part of the accepted paper Tomasella et al. (2017a). In the greenhouse, the doctoral candidate participated in all phases, from planting to the final harvest of saplings and was the main responsible for the plant maintenance over the two years of the experiment. Data analysis and figure preparation have been performed by the candidate.

Regarding the two publications resulting from the doctoral work (Tomasella et al. 2017 a, b) and included as part of the thesis, the candidate wrote the first draft of them and was responsible for submission and correspondence to the journals. Co-authors discussed and contributed to the improvement of the manuscript in all phases of publication.

Acknowledgements

I acknowledge the TUM 'International Graduate School of Science and Engineering' (IGSSE) within the Tree'n'ing project, and the IGSSE-Laura Bassi Fellowship for financial support.

I would like to thank Prof. Rainer Matyssek for having given me the possibility to conduct my Ph.D. project at his chair and Dr. Karl-Heinz Häberle for mentoring, help with experiments and suggestions on manuscripts.

I thank Prof. Thorsten Grams for having accepted to supervise my Ph.D thesis and for important suggestions to ameliorate it.

I thank Prof. Stefan Mayr (University of Innsbruck) and Prof. Andrea Nardini (University of Trieste), who with their expertise in plant hydraulics contributed to the experiments and helped with the preparation of the related articles, being always available for discussions and suggestions. I also thank Prof. Mayr for having hosted me in his labs for three months.

I thank Prof. Urs Schmidhalter of the Chair of Plant Nutrition (WZW, Technische Universität München) for allowing us to use the greenhouse space and facilities for the experiment on saplings, as well as the technical staff of the greenhouse.

I thank the students Benjamin Hesse and Anna Machlet, who helped with the experiments during their thesis and/or as technical assistants (Hiwis).

I would also like to thank Dr. Frank Fleischmann for help with irrigation system setup in the greenhouse and HPLC analysis, and the present and past technicians of the chair (Thomas Feuerbach, Josef Heckmair, Roman Meyer, Peter Kuba and Johanna Lebherz), as well as Christian Kallenbach and Dr. Michael Goisser for help given during the Ph.D.

A special thank goes to my family that, albeit the physical distance, has always supported and encouraged me in these years.

Curriculum vitae

Personal information

Name	Martina Tomasella
Date and place of birth	18.10.1988 Sacile (Italy)
Contact	martina.tomasella@tum.de

Education and training

Since 1.02.2014	Ph.D. student at the Chair of Ecophysiology of Plants (WZW, Technische Universität München), Freising (Germany). Research project: "Mechanisms of tree vulnerability to drought", acronym "Tree'n'ing" (Tree Ecophysiology and Engineering"). Ph.D. funded by: - International School of Science and Engineering, IGSSE (1.02.2014-31.03.2017) - IGSSE-Laura Bassi Fellowship (1.04.2017-30.09.2017)
February - April 2016	Research stay at the Institut für Botanik – University of Innsbruck (Austria) – Prof. Dr. Stefan Mayr Measurements of vulnerability to xylem embolism and wood anatomy of European beech and Norway spruce branches
November - December2013	Internship at the Department of Agricultural and Environmental Sciences (DISA), section of Plant Biology, University of Udine (Italy) Biochemical laboratory analysis
2011-2013	Master's degree in "Scienze e tecnologie per l'ambiente e il territorio" (Environmental Sciences) – University of Udine and Trieste (Inter-University Degree) – Italy
2007-2011	Bachelor's degree in "Scienze e tecnologie per l'ambiente e la natura" (Environmental and natural sciences) – University of Udine (Italy)
July – September 2009	Internship at the Alpine Botanical Garden "Giangio Lorenzoni" - Veneto Agricoltura (Regional Agency for Agriculture, Forestry and Food Farming), Pian del Cansiglio (Italy)
2002-2007	Secondary school diploma: scientific certificate – Licei "G.A. Pujati" Sacile (Italy)

Scientific presentations at conferences

7.10.2016	ISHS Symposium – Sensing plant water status – Potsdam (Germany) Title of presentation: "Drought induced cavitation in juvenile beech and spruce trees: which are their water use strategies and margins for embolism repair?".
26-30.06.2016	Plant Biology Europe EPSO/FESPB 2016 Congress - Prague (Czech Republic) Title of poster: "Water use strategies and vulnerability to cavitation of beech and spruce under drought: the KROOF (Kranzberg Roof) experiment".
14.05.2014	Xylem-Group meeting – Besse (France) Title of presentation: "Water relations of an invasive halophyte (*Spartina patens*): osmoregulation and ionic effects on xylem hydraulics".

Scientific projects

Since February 2014	"Tree'n'ing" (Tree Ecophysiology and Engineering") Project – International Graduate School of Science and Engineering (IGSSE)
Since February 2014	Kranzberg – Roof experiment (acronym KROOF)

Publications

- Tomasella M., Beikircher B., Häberle K.-H., Hesse B., Kallenbach C., Matyssek R., Mayr S. (2017a) Acclimation of branch and leaf hydraulics in adult *Fagus sylvatica* and *Picea abies* in a forest through-fall exclusion experiment. Tree Physiology 38, 198-211; DOI: 10.1093/treephys/tpx140.
- Tomasella M., Häberle K.-H., Nardini A., Hesse B., Machlet A., Matyssek R. (2017b) Post-drought hydraulic recovery is accompanied by non-structural carbohydrate depletion in the stem wood of Norway spruce saplings. Scientific reports 7, 14308; 10.1038/s41598-017-14645-w.
- Hafner B.D., Tomasella M., Häberle K.-H., Goebel M., Matyssek R., Grams T.E.E. (2017) Hydraulic redistribution under moderate drought among English oak, European beech and Norway spruce determined by deuterium isotope labeling in a split-root experiment. Tree Physiology 37, 950-960.
- Casolo V., Tomasella M., De Col V., Braidot E., Savi T., Nardini A. (2015) Water relations of an invasive halophyte (*Spartina patens*): osmoregulation and ionic effects on xylem hydraulics. Functional Plant Biology 42, 264-273.
- Tomasella M., Tomasella Mi., Roffare G., Casolo V. (2014) Flora and vegetation of two wetlands of Pian del Cansiglio (Belluno): Lamaraz and Lama Lissandri. *Gortania-Atti del Museo Friulano di Storia Naturale Botanica Zoologia* 36, 15-32.